2016-02-23

Eosinophils as Drivers of the IL-23/IL-17 Axis: Implications for Acute Aspergillosis and Allergic Asthma: A Dissertation

Evelyn V. Santos Guerra
University of Massachusetts Medical School

EOSINOPHILS AS DRIVERS OF THE IL-23/IL-17 AXIS: IMPLICATIONS FOR ACUTE ASPERGILLOSIS AND ALLERGIC ASTHMA

A Dissertation Presented

By

Evelyn Vieira Santos Guerra

Submitted to the Faculty of the

University of Massachusetts Graduate School of Biomedical Sciences, Worcester

in partial fulfillment of the requirements for the degree of

DOCTOR OF PHILOSOPHY

February 23, 2016

Immunology and Microbiology

EOSINOPHILS AS DRIVERS OF THE IL-23/IL-17 AXIS: IMPLICATIONS FOR ACUTE ASPERGILLOSIS AND ALLERGIC ASTHMA

A Dissertation Presented
By

Evelyn Vieira Santos Guerra

The signatures of the Dissertation Defense Committee signify completion and approval as to style and content of the Dissertation

_____
Stuart M. Levitz, M.D., Thesis Advisor

_____
Sanjay Ram, M.D., Member of Committee

_____
Jennifer Wang, M.D., Member of Committee

_____
Jun Huh, Ph.D., Member of Committee

_____
Robert A. Cramer, Jr., Ph.D., Member of Committee

The signature of the Chair of the Committee signifies that the written dissertation meets the requirements of the Dissertation Committee

_____
Leslie Berg, Ph.D., Chair of Committee

The signature of the Dean of the Graduate School of Biomedical Sciences signifies that the student has met all the graduation requirements of the school

_____
Anthony Carruthers, Ph.D.,
Dean of the Graduate School of Biomedical Sciences

Program
Immunology and Microbiology
February 23, 2016

DEDICATION

I would like to dedicate the following work to my mom, who instilled in me a love of learning and revealed to me the rewards of scholarship.

ACKNOWLEDGMENTS

The past five or so years have been filled with many expected and unexpected challenges. I cannot fathom being able to overcome each challenge without all those who supported and encouraged this project, my vision, career and dreams. I would like to thank first and foremost, my advisor, Stu Levitz, who never waivered in his support for my work. He made me feel welcome in an environment I was not sure I belonged in, while also pushing me to develop as a scientist. His trust afforded me the privilege to test my own ideas in the laboratory, and I count myself very fortunate to have had him as a mentor.

The community I found within the Levitz lab has been indispensible in completing this project. Thanks to Charles Specht for the all crucial feedback and expertise provided, as well as offering me a friendly ear for my ideas and frustrations. I am particularly thankful for all the ways in which Chrono Lee helped me perform all my experiments. He was instrumental in getting all of my animal studies done, and providing me with instruction on various techniques. Chrono is probably one of the most patient teachers I have ever had. Thanks to Haibin Huang for his expertise, essential feedback on my work, and assistance in getting me started in the lab. I am also very thankful for Chelsea Bueter's advice and awesome friendship, and Gary Ostroff's expertise and feedback in lab meetings. All the kindness I experienced from each lab member will not be forgotten.

Thanks to Chris Mueller and Cindy Greer for sensitizing and challenging mice for our asthma studies, Jun Huh for generously sharing with us different strains of mice, as

well as Robert Cramer and Tobias Hohl for kindly providing us with different strains of *Aspergillus fumigatus*. I also wish to thank Leslie Berg, Sanjay Ram, Jennifer Wang and John Harris for serving on my TRAC, and all the guidance, feedback, and support I received during the course of my research. Thanks to my fellow MD/PhD students for all the advice and sympathy. I relied on many of my peers for getting through all the hurdles of graduate school, especially for helping me get through my qualifying exam. Thanks to Anouch Matevossian, Abhishek Satischadran, Tia Brodeur, Rachel Buglione-Corbett, Brian Quattrochi, Dmitry Ratner, and Victor Liu. And last but most definitely not least, thanks to Kristina Prachanronarong for being such an amazing friend and roommate for so many years.

I could not have even dreamed of pursuing a PhD if it weren't for those who inspired and encouraged me prior to joining UMMS. Thanks to my previous mentors: Karlie Intlekofer, who still keeps tabs on me, and helped edit my QE proposal and my dissertation, Lyle Craker, who was the first person to open his lab to me, and Sandy Petersen, who served as my undergraduate capstone project mentor. In addition, I would like to thank all my friends outside of UMMS who never let me give up and who are always inspiring me in more ways than I can count. In particular I would like to thank Arlene Pimentel, Clara do Nascimento, Magaly Rojas, Dana Sun, and Amelia Alibozek.

I cannot be more grateful to my parents, Marcia Shaffer and Jair Santos, for fostering in me an enthusiasm for learning and an interest in science. They made enormous sacrifices for me to have the opportunities I have now. My sister, Natalyn Santos, and my parents are the most fearless people I know, and have always dared me to

dream big. Even when the odds were razor thin, they never doubted my potential. I am extremely grateful for all the examples of strength they have provided me throughout the years.

Finally, I would like to thank my husband, Patrick Guerra. I like to joke that I am his first graduate student because of all the mentoring I received from him. Throughout graduate school, Patrick has experienced with me every triumph and failure, and has always encouraged me to reach for the stars. He has edited manuscripts, listened to practice talks, helped me analyze data, helped troubleshoot, and given me advice on every aspect of navigating graduate school. I am filled with gratitude for his role in my life, as I certainly would not have made it this far without him.

Abstract

Aspergillus fumigatus is an opportunistic fungal pathogen that causes lethal invasive pulmonary disease in immunocompromised hosts and allergic asthma in sensitized individuals. This dissertation explores how eosinophils may protect hosts from acute infection while driving asthma pathogenesis by co-producing IL-23 and IL-17 in both contexts. In an acute model of pulmonary aspergillosis, eosinophils were observed to associate with and kill *A. fumigatus* spores *in vivo*. In addition, eosinopenia was correlated with higher mortality rates, decreased recruitment of inflammatory monocytes to the lungs, and decreased expansion of lung macrophages. As IL-17 signaling must occur on a local level to elicit its stereotypical response, such as the up-regulation of antimicrobial peptides and specific chemokines from stromal cells, eosinophils were discovered to be a significant source of pulmonary IL-17 as well as one of its upstream inducers, IL-23. In the context of asthma, this discovery opens a new paradigm whereby eosinophils might be driving asthma pathogenesis.

TABLE OF CONTENTS

LIST OF TABLES

LIST OF FIGURES

List of Abbreviations

ABPA	Allergic bronchopulmonary aspergillosis
Af cpe	*Aspergillus fumigatus* crude protein extract
AHR	Airway hyperresponsiveness
AIDS	Acquired immunodeficiency syndrome
ANOVA	Analysis of variance
APC	Antigen presenting cell
APRIL	A proliferation-inducing ligand
β-ME	β-mercaptoethanol
BALF	Bronchoalveolar lavage fluid
BM	Bone marrow
BM-Eos	Bone marrow-derived eosinophils
BUV	Brilliant ultraviolet
BV	Brilliant violet
CCR	CC chemokine receptor
CD	Cluster of differentiation
cDNA	Copy deoxyribonucleic acid
CGD	Chronic granulomatous disease
CMC	Chronic mucocutaneous candidiasis
CXCL	Chemokine (C-X-C motif) ligand
CXCR	Chemokine (C-X-C motif) receptor

Cy	Cyanine
dsRed	*Discosoma* spp. red fluorescent protein
EGF	Epidermal growth factor
ELISA	Enzyme-linked immunosorbent assay
ENA-78	Epithelial-derived neutrophil-activating peptide 78
EPX	Eosinophil peroxidase
FBS	Fetal bovine serum
FC	Flow cytometry
FITC	Fluorescein isothiocyanate
FLARE	Fluorescent *Aspergillus* Reporter
FMO	Fluorescence minus one
FSC-A/H	Forward scatter area/height
G-CSF	Granulocyte-colony stimulating factor
GFP	Green fluorescent protein
GM-CSF	Granulocyte macrophage-colony stimulating factor
Hprt	Hypoxanthine-guanine phosphoribosyltransferase
H&E	Hematoxylin and eosin
IACUC	Institutional Animal Care and Use Committee
ICS	Intracellular cytokine staining
IFN	Interferon
Ig	Immunoglobulin
IL	Interleukin

IL-17R	Interleukin-17 receptor
IL-23R	Interleukin-23 receptor
ILC	Innate lymphoid cell
IMDM	Isocove's modified Dulbecco's medium
iNKT	Invariant natural killer T cells
ip	Intraperitoneal
KC	Keratinocyte chemoattractant
KO	Knock-out
LBDM	Low-density bone marrow (cells)
LPS	Lipopolysaccharide
Ly6C/Ly6G	Lymphocyte antigen 6 complex, locus C/G
M1	Classically activated macrophages
M2a/c	Alternatively activated macrophages type A/C
mAb	Monoclonal antibody
MBP	Major basic protein
MFI	Median fluorescence intensity
mFLT3L	Murine FMS-like tyrosine kinase 3 ligand
MIP-2	Macrophage inflammatory protein-2
moDC	Monocyte-derived dendritic cell
mRNA	Messenger RNA
mSCF	Murine stem cell factor
NADPH	Nicotinamide adenine dinucleotide phosphate

NGF	Nerve growth factor
OT	Oro-tracheal
OVA	Ovalbumin
PBMC	Peripheral blood mononuclear cells
PBS	Phosphate buffered saline
PCR	Polymerase chain reaction
PDGF	Platelet-derived growth factor
PE	Phycoerythrin
Pen	Penicillin
PerCP	Peridinin chlorophyll protein complex
PGE_2	Prostaglandin E_2
PHOX	Phagocytic oxidase
PRR	Pattern recognition receptor
qPCR	Quantitative polymerase chain reaction
RNA	Ribonucleic acid
RAR	Retinoic acid receptor
ROR	Retinoic acid receptor-related orphan receptor
RPM	Revolutions per minute
rRNA	Ribosomal RNA
RT	Reverse transcription
SAFS	Severe asthma with fungal sensitization
SCF	Stem cell factor

SD	Standard deviation
SEM	Standard error of the mean
Siglec-F	Sialic acid-binding immunoglobulin-type lectin F
SSC-A	Side scatter area
STAT	Signal transducer and activator of transcription
Strep	Streptomycin
TCR	T cell receptor
T_C	Cytotoxic T lymphocyte
TGF-β	Transforming growth factor-β
T_H	Helper T lymphocyte
TLR	Toll-like receptor
TNF-α	Tumor necrosis factor-α
TSLP	Thymic stromal lympohoietin
VEGF	Vascular endothelial growth factor
WT	Wild-type

Chapter I: Introduction

Aspergillus is a genus of highly successful saprophytic fungi found worldwide (1) at densities often reaching 12 – 17 spores per cubic meter of air (2,3). *Aspergillus* spp. begin their lifecycle as conidia (i.e., spores) that are produced asexually by conidiophores, and range from 2 to 10 μm in diameter depending on the species (4-6). The conidia are covered by a layer of hydrophobic proteins that enhance their buoyancy in air and ability to be dispersed (1,7,8). Once resting conidia find adequate sources of water, carbon and nitrogen, they swell and germinate into multinucleated hyphal structures (9). Germination triggers the release of hydrolytic enzymes that digest organic polymers into units for import into the cell (1,5,7). Air interfaces allow hyphae to sprout conidiophores, thus completing their lifecycle (9) (**Figure 1.1**).

Aspergillus and human health. The same qualities that make *Aspergillus* conidia so easily dispersible in air also give them access to the human airway. Conidia can be small enough to reach the alveolar space, where they frequently interact with epithelial and innate immune cells. Despite their ubiquity and abundance, very few people suffer from this interaction because the mucociliary apparatus in conducting airways and professional phagocytes in alveolar spaces efficiently clear conidia. However, when a defect in the epithelial barrier, immune regulation, or phagocytic capacity is present, hosts become susceptible to colonization or invasion by *Aspergillus* spp. (10).

Out of the 40 species of *Aspergillus* that can cause disease in humans (11), *A. fumigatus* is the most prevalent (5). It is still unclear why this species outnumber other *Aspergillus* spp. in cases of invasive aspergillosis (12), allergic bronchopulmonary

aspergillosis (ABPA) (13), and aspergilloma (5). Instead of harboring virulence factors that are specialized to the human host, a convergence of attributes make *A. fumigatus* successful in both its natural habitats (e.g., compost heaps) and in predisposed hosts (5,7,14). Some of these attributes include: their relative abundance in air, small spore size (2.5 – 3 μm in diameter), preference for germinating at body temperature (37^{o}C), ability to grow at a wide pH range (2.1 – 8.8), resistance to oxidative stress, and production of toxic secondary metabolites (7).

Protection from *A. fumigatus* is conferred from all arms of the immune system including the epithelial barrier, and innate and adaptive immune cells. For example, disruption of the pulmonary epithelial barrier (e.g., cavitary lesions caused by tuberculosis) become potential spaces for conidia to germinate, proliferate and form aspergillomas (5).

The most severe illness caused by *A. fumigatus* occurs when the fungus invades pulmonary tissue sometimes disseminating to other organs, including the brain. This type of infection, called invasive aspergillosis is most prevalent when there is a breach in the innate immune system. This is exemplified by chronic granulomatous disease (CGD), one of the few primary immunodeficiencies where *Aspergillus* spp. acts as a pathogen. CGD is characterized by mutations in the NADPH oxidase (PHOX) complex, the enzyme responsible for the respiratory burst in phagocytes (15,16). Invasive aspergillosis can occur anywhere along the respiratory tract affecting alveolar spaces, bronchial tree, and nasal passages (5).

Other risk factors for invasive aspergillosis include iatrogenic immunosuppression following the transplant of hematopoietic stem cells or solid organs. Patients with hematologic malignancies are also susceptible to infection, as well as those who suffer from natural or acquired immunodeficiencies such as various types of aplastic anemias and advanced AIDS. Severe and prolonged neutropenia is the most common risk factor for incidence and mortality with invasive aspergillosis in this heterogeneous group of patients (5,12,17).

Molds such as *A. fumigatus* can also elicit an allergic response from atopic patients that can lead to either mild or severe asthma. Mild allergic asthma is typically controlled with standard treatments such as corticosteroids and β_2-adrenergic receptor agonists (18). In contrast, severe asthma with fungal sensitization (SAFS) is often poorly controlled with standard therapies leading to higher mortality rates (19). Sensitization to *A. fumigatus* can be determined by challenge with fungal antigens using a skin prick test, where the development of a 3 mm wheal reveals an atopic individual, or by assessment of specific antibodies. Sensitized individuals with high levels of IgE specific to *A. fumigatus* have been reported to have higher incidences of colonization by the fungus and worse respiratory function (20). Some of these patients respond well to antifungal treatment, suggesting that colonization plays a significant role in the pathogenesis of this disease (13).

A subset of *A. fumigatus* sensitized individuals suffers from a level of symptom severity exceeding that of SAFS patients. In such cases individuals are evaluated for ABPA. Criteria for ABPA diagnosis includes a history of asthma or cystic fibrosis (CF),

very high levels of serum IgE, specific antibodies against *A. fumigatus*, and marked leukocyte infiltration into the lungs observed by chest radiography (13). ABPA patients produce copious amounts of mucus, and often develop bronchial outpouchings called bronchiectasis, respectively providing *A. fumigatus* with a rich medium and potential space to grow. Therefore, ABPA patients are chronically or intermittently colonized with *A. fumigatus* and often benefit from antifungal treatment (13).

Although ABPA is marked by high eosinophilia, inflammation driven by continual exposure to *A. fumigatus* antigens induces high levels of interleukin (IL)-8 and neutrophils in the lungs (21). IL-8 is a pleiotropic cytokine that can bind chemokine (C-X-C) motif receptor (CXCR)-1 and -2 on the surface of neutrophils and stromal cells to induce neutrophil chemotaxis, increase mucus production, collagen deposition, and angiogenesis (22). All of these functions are associated with asthma pathogenesis. In fact, in an ovalbumin (OVA) sensitization model of asthma, CXCR-$2^{-/-}$ mice were protected from developing airway hyperresponsiveness (AHR), a hallmark symptom of asthma (23). These findings were confirmed in an *A. fumigatus* sensitization model of asthma (24), however, lack of CXCR-2 signaling is lethal in primary infection models (25). The incongruent outcomes observed in CXCR-$2^{-/-}$ mice in an acute infection model compared to an asthma model highlight how specific immune responses to *A. fumigatus* can be beneficial or harmful to a host depending on the context of the interaction with the pathogen.

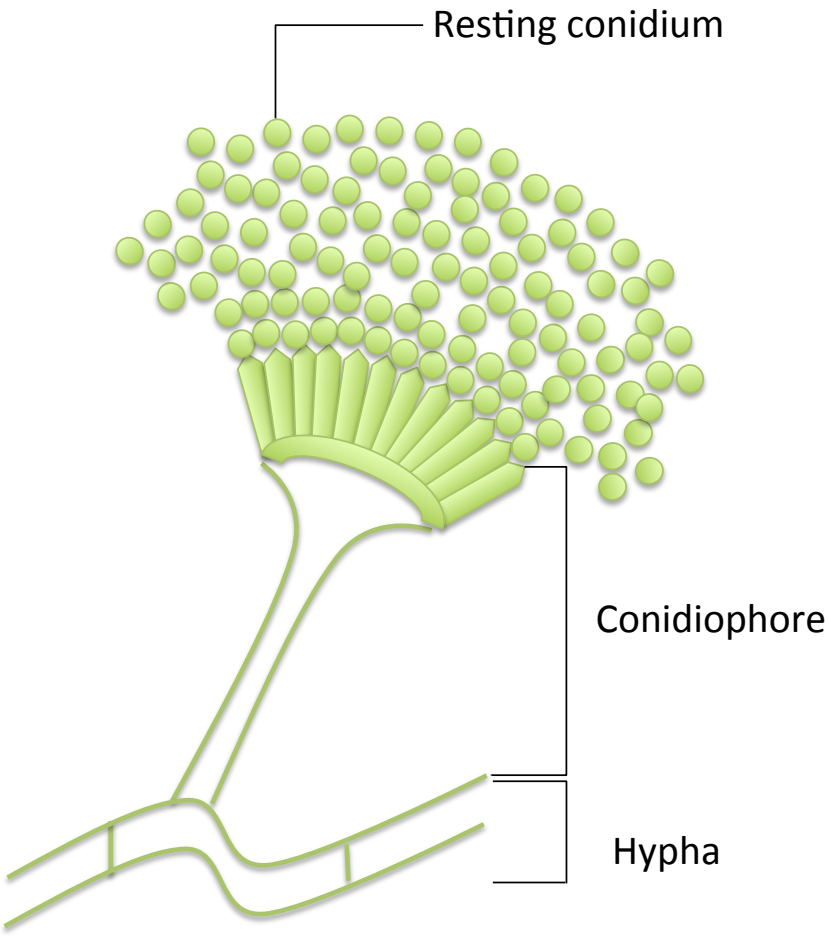

Figure 1.1: The lifecycle of *Aspergillus fumigatus.* Conidiophores asexually produce resting conidia that are easily dispersible due to their small size and hydrophobicity. A conidium will swell and grow into hyphae upon encountering an environment that is conducive to germination. Access to an air interface will induce conidiophore formation.

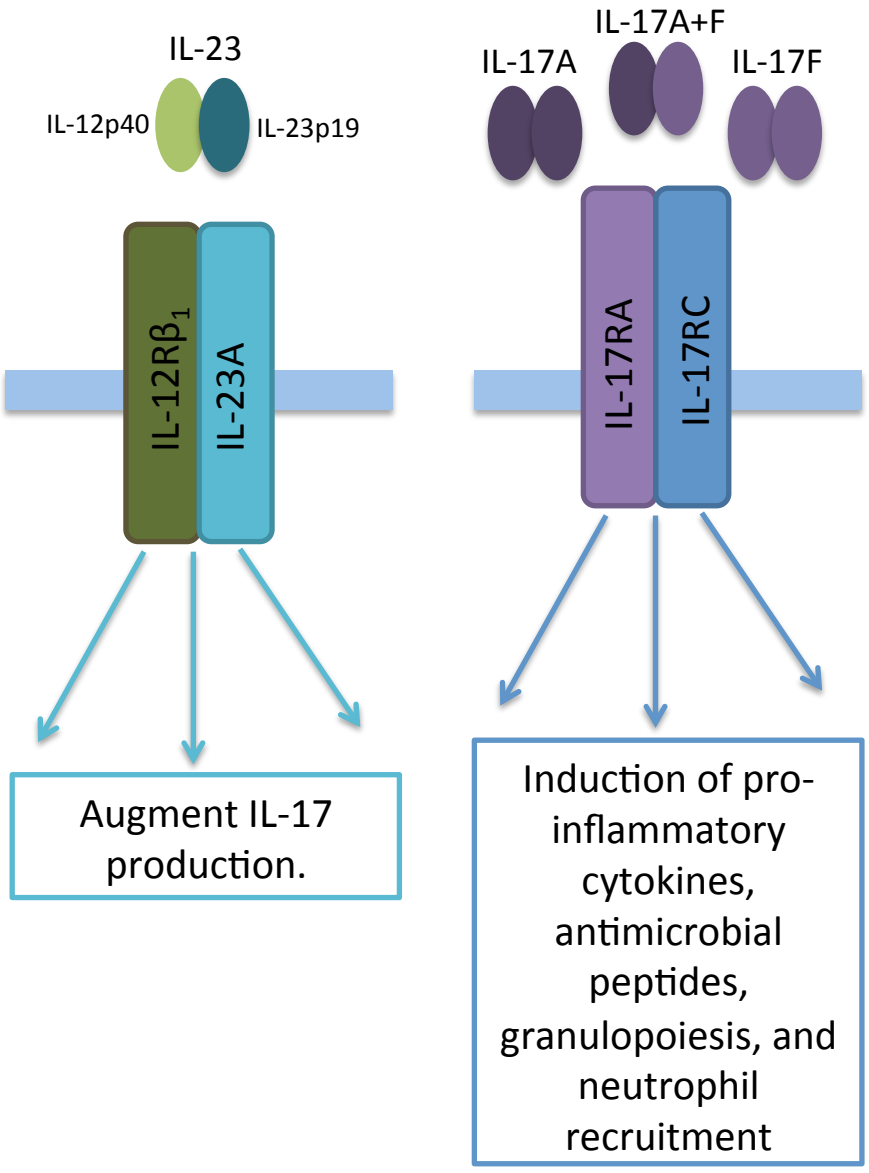

Figure 1.2: The IL-23/IL-17 Axis. IL-23 is a heterodimeric cytokine made up of an IL-12p40 subunit and an IL-23p19 subunit. Upon binding its receptor (IL-23R), IL-23 signaling can either augment or induce IL-17 production depending on the cell expressing the receptor. The IL-17RA/RC receptor binds to the three configurations formed by IL-17A and IL-17F as these subunits can either homo- or heterodimerize. Ligation with the IL-17RA/RC receptor triggers the production of antimicrobial peptides, pro-inflammatory cytokines and chemokines including IL-6, G-CSF, GM-CSF, CXCL-1, -2, and -5.

The IL-23/IL-17 Axis. The IL-17 family of cytokines is composed of six members ranging from IL-17A through F. IL-17A exists as a disulfide-linked homodimer and binds with high affinity to IL-17RA, IL-17RC is then recruited to form a fully functional signaling receptor. IL-17A also forms a disulfide-linked heterodimer with IL-17F. IL-17F can exist as a homodimer as well, binding the same IL-17R heterodimer as IL-17A. Cells of the innate and adaptive immune system can produce different configurations of the IL-17A and F dimers. These cells include: γδ T cells, invariant natural killer T cells (iNKT), lymphoid-tissue inducer like cells, neutrophils, $CD8^+$ T cells (T_C17) and $CD4^+$ T cells (T_H17) (26,27). For clarity, the IL-17RA/RC ligands will be referred to as IL-17. IL-17 up-regulates the expression of CXCR-2 ligands (i.e., CXCL-1, CXCL-2 and CXCL-5) as well as several pro-inflammatory cytokines, metalloproteases and antimicrobial peptides (27).

IL-23 can either induce or augment IL-17 release depending on the cell type expressing IL-23 receptor (IL-23R). IL-23 is a member of the IL-12 cytokine family, sharing with the cognate cytokine the IL-12p40 chain, and dimerizing with the IL-23p19 chain to form a functional signaling molecule. IL-23R is also a heterodimeric receptor composed of the IL-12Rβ_1 and IL-23A subunits. The relationship between IL-23 and IL-17 is known as IL-23/IL-17 axis (29) (**Figure 1.2**). *A. fumigatus* readily elicits IL-23 and IL-17 production from the lungs after exposure (30). Although recognized primarily for the induction of neutrophilia, IL-17 also recruits eosinophils in a model of chronic aspergillosis (31). However, the exact mechanism underlying IL-17-driven eosinophil

recruitment is still unclear. Recently, high levels of IL-17 have been correlated with symptom severity in both non-atopic and atopic asthma (28).

One other IL-17 family member that is associated with *A. fumigatus* exposure is IL-17E. Often referred to as IL-25, this cytokine signals through the IL-17RA/RB receptor complex. IL-17E is an epithelial-derived cytokine that has been shown to enhance IgE production in ABPA (32,33). There is evidence that contact between chitin, an *A. fumigatus* cell wall component, and airway epithelial cells induce the production of IL-17E, IL-33 and thymic stromal lymphopoietin (TSLP). IL-17E, IL-33 and TSLP activate resident innate lymphoid type 2 cells (ILC2s) to produce IL-5 and IL-13. This cascade of events ultimately leads to the recruitment of eosinophils to the lungs (34).

Eosinophils in allergic asthma. The role eosinophils play in allergen sensitization, inflammatory exacerbations, and airway remodeling in asthma is highly complex. This may be partially due to the fact that asthma is a heterogeneous disease with numerous etiologies and presentations (35,36). In addition, eosinophils are equipped with a vast number of immune mediators within their granules and have been associated with several different functions that are sometimes redundant and contradictory. For example, eosinophils play a role in sensitization by both instructing dendritic cells to elicit a T_H2 response in asthma models, and acting as antigen presenting cells (APCs) in draining lymph nodes (37,38). Eosinophils also drive active inflammation and tissue destruction by recruiting T_H2 cells to the lungs and releasing several cytolytic proteins. In contrast,

they also promote inflammation resolution by producing protectins and resolvins to inhibit granulocyte migration and elicit efferocytosis in macrophages (39).

Some of the contradictory functions performed by eosinophils might be accounted for by the specific context they encounter (40). For example, in the context of acute infection with *A. fumigatus,* eosinophils play a protective role and prevent mice from succumbing to infection. This has been demonstrated with a strain of *A. fumigatus* that overexposes chitin on its surface (Af5517) (41), and is also presented in this dissertation with a different fungal strain (CEA10). O'Dea et al. (41) have shown that eosinopenic mice are just as susceptible to acute infection with Af5517 as mice that are deficient in $Ly6G^+$ cells, a myeloid cell population that includes neutrophils. However, if mice are exposed repeatedly with *A. fumigatus,* eosinopenic mice succumb to infection at higher rates than mice depleted of $Ly6G^+$ cells. The authors attribute the discrepancy in mortality between the two models to enhanced T_H2 responses, which they claim is beneficial in acute infection but detrimental in chronic exposure (41).

In the following chapters, I detail how eosinophils also directly contribute to the production of IL-23 and IL-17 in both acute aspergillosis and in asthma models where mice were sensitized to either *A. fumigatus* or OVA. In producing both IL-23 and IL-17, eosinophils do not seem to affect the recruitment of neutrophils, instead the recruitment of inflammatory monocytes and the expansion of macrophages are hampered in eosinopenic mice. This dissertation explores a novel eosinophil function that might be both protecting hosts from an acute pulmonary infection with *Aspergillus* spp. while also driving asthma pathogenesis in atopic patients.

Preface to Chapter II

Evelyn Guerra performed the experiments.

Evelyn Guerra and Stuart Levitz designed experiments.

CHAPTER II: Innate IL-23/IL-17 Axis Kinetics in Acute Aspergillosis

Abstract

Although frequently inhaled, *Aspergillus fumigatus* conidia rarely cause disease. The inhalation of these infective particles by an immunocompromised host, however, can cause severe infections that are difficult to diagnose and are often lethal. Neutrophils play an important function in protecting hosts from infection. The role of the IL-23/IL-17 axis, which promotes the development and recruitment of these phagocytes, is largely unknown in pulmonary aspergillosis. This chapter characterizes the innate IL-23/IL-17 axis in response to a pulmonary challenge with *A. fumigatus*. Genes involved in the axis, namely *Il23p19*, *Il17a* and *Il17f,* were rapidly expressed in response to acute aspergillosis. *Il17a* showed a biphasic pattern of mRNA production that was consistent with the temporal pattern of IL-17AF release in the lungs. *Cxcl5*, a gene that encodes a neutrophil chemokine downstream of the IL-23/IL-17 axis, displayed mRNA expression kinetics that matched the pattern of IL-17AF release in the lungs, suggesting that *Cxcl5* might be regulated by this IL-17 dimer in our model. Finally, the model revealed that IL-23p19 and IL-17A are co-produced within a few hours of infection and again on the second day of infection.

Introduction

Aspergillus fumigatus is a ubiquitous, saprophytic mold generally found in decaying matter. It reproduces mainly through asexual sporulation, a process that produces small (2.5 - 3 μm), hydrophobic conidia (5). Its ability to disperse through air means humans are continuously exposed to these spores through the lungs. In most healthy individuals, conidia are promptly cleared either by the mucociliary apparatus of major conducting airways or by resident phagocyte activity. In immunocompromised and atopic individuals, however, these mold spores can cause invasive aspergillosis and allergic bronchopulmonary aspergillosis (ABPA) respectively (5).

Although uncommon, invasive aspergillosis is a highly lethal disease that is often misdiagnosed. Prolonged neutropenia is major risk factor for acquiring it, particularly in patients who have undergone hematopoietic stem cell transplant or solid organ transplant. Non-neutropenic patients at risk for developing invasive aspergillosis are generally pharmacologically immunosuppressed and/or suffer from chronic obstructive pulmonary disease (42).

As neutropenia is a major risk factor for developing invasive aspergillosis, this chapter aims to characterize the innate IL-23/IL-17 axis that plays a significant role in neutrophil development, recruitment and function. IL-23 is a heterodimeric cytokine consisting of IL-23p19 and IL-12p40 subunits (43). IL-23 receptor (IL-23A/IL-12Rβ_1) ligation activates signal transducer and activator of transcription (STAT)-3, which then augments or induces IL-17 production depending on the cell type stimulated (15). IL-17 is a family of cytokines, consisting of members ranging from A through F. These

cytokines bind distinct receptors and form homodimers, although IL-17A and IL-17F can heterodimerize. IL-17AA, IL-17FF, and IL-17AF all bind the same heterodimeric receptor, IL-17RA/RC, albeit with different affinities. IL-17AA has the highest affinity for IL-17RA/RC, while IL-17FF binds with the least affinity and IL-17AF exhibits an intermediary affinity (44). In fact, these dimers are the IL-17 family members involved in the IL-23/IL-17 axis (29). For the remainder of this dissertation, IL-17 will refer to IL-17RA/RC ligands.

IL-17RA/RC is generally expressed on some leukocytes and the surface of stromal cells (i.e., fibroblasts, epithelial and endothelial cells). IL-17 signaling up-regulates the expression of antimicrobial peptides, granulopoeitic cytokines (e.g., granulocyte-colony stimulating factor [G-CSF]) (26), pro-inflammatory cytokines (e.g., IL-1, Tumor necrosis factor [TNF-] α, and IL-6) (45), and chemokines, including neutrophil chemokines (CXCL-1, CXCL-2, and CXCL-5) (46).

In this chapter, the murine innate IL-23/IL-17 axis is characterized by assessing the temporal pattern of mRNA levels for *Il23p19, Il17a* and *Il17f* in response to *A. fumigatus*. To determine which IL-17 dimers are involved in this innate response, I also characterized the release kinetics of IL-17AA, IL-17FF and IL-17AF in the bronchoalveolar lavage fluid (BALF) of C57Bl/6 mice infected with *A. fumigatus* conidia. In addition, the temporal pattern of mRNA production was assessed for the three neutrophil chemokines previously shown to be regulated by the IL-23/IL-17 axis (26). Finally, these experimental approaches revealed that IL-17A and IL-23p19 are co-produced at specific time points after infection.

Materials and Methods

Mice. Six- to eight-week old C57Bl/6 mice were obtained either from Jackson Laboratories or bred in pathogen-free conditions at the University of Massachusetts in accordance with guidelines approved by the Institutional Animal Care and Use Committee (IACUC).

Reagents. Flow cytometry (FC) buffer used in staining was composed of phosphate buffered saline (PBS; Corning) supplemented with 2% fetal bovine serum (FBS; Tissue Culture Biologicals).

Aspergillus fumigatus culture and murine acute pulmonary aspergillosis model. Wild-type (WT) *A. fumigatus* from the AF293 strain was obtained from the Fungal Genetics Stock Center in Kansas. AF293 was grown from frozen stocks on Sabouraud-dextrose agar (Remel™) slants. Conidia were harvested by vortexing slants with PBS containing 0.01% Tween-20 (Thermo-Fisher) and filtering the suspension twice through a 30 μm nylon mesh folded over a 15 mL conical tube. Suspensions were then washed three times with 0.01% Tween-PBS, and re-suspended in the same solution at a concentration of $6.67x10^8$ conidia/mL. C57Bl/6 mice were infected via the oro-tracheal (OT) route with 75 μL of conidial suspension, with each mouse receiving $5x10^7$ conidia. Control mice received 75 μL of vehicle (0.01% Tween-PBS). OT infection was facilitated by anesthetizing mice with isoflurane (Piramal Healthcare).

Whole lung RNA isolation and qPCR reaction. Infected and sham-infected mice were euthanized in carbon dioxide chambers. Lung tissue was harvested and homogenized in 1 mL of TRIzol® (Life Technologies) using a PowerGen 700 homogenizer (Fisher; Model GLH-115). Total RNA was extracted according to the manufacturer's protocol and purified using the NucleoSpin® RNA kit (Macherey-Nagel). RNA concentration and purity were measured using NanoDrop 2000 spectrophotometer (Thermo-Fisher). One microgram of each sample was converted to cDNA using iScript™ Reverse Transcription Supermix for RT-qPCR (Bio-Rad). Each target was amplified in triplicate using iQ SYBR Green Supermix (Bio-Rad) in a CFX96 Touch™ Real-Time PCR Detection System (Bio-Rad). Sequences for primers used are listed in **Table 2.1** (Life Technologies). Data were analyzed as described previously with Hypoxanthine-guanine phosphoribosyltransferase (*Hprt*) message serving as the internal control (47).

Table 2.1: Primer sequences used in qPCR reactions.

Target Gene	Forward Primer (5'-3')	Reverse Primer (5'-3')	References
Cxcl-1 (*Kc*)	CGCTTCTCTGTGCAGCGCTGCT	CAAGCCTCGCGACCATTCTTGA	(48)
Cxcl-2 (*Mip-2*)	TCCAGAGCTTGAGTGTGACG	TCCAGGTCAGTTAGCCTTGC	(48)
Cxcl-5 (*Ena78*)	GGTCCACAGTGCCCTACG	GCGAGTGCATTCCGCTTA	(48)
Hprt	AGCGTTTCTGAGCCATTGCT	GCTACCGCTCCGGAAAGC	(49)
Il17a	TTTAACTCCCTTGGCGCAAAA	CTTTCCCTCCGCATTGACAC	(48)
Il17f	TGCTACTGTTGATGTTGGGAC	AATGCCCTGGTTTTGGTTGAA	(48)
Il23p19	TGTGCCCCGTATCCAGTGT	CGGATCCTTTGCAAGCAGAA	(50)

In vivo intracellular cytokine staining. At 2, 24 and 48 h post-infection with $5x10^7$ conidia, C57Bl/6 mice were treated with 500 μg of monensin (Sigma-Aldrich) by intraperitoneal (ip) injection as has been previously described (51). Six hours after monensin treatment, lungs were harvested and dissociated using a lung dissociation kit (Miltenyi Biotec) in combination with the gentleMACS™ Dissociator. Lung single-cell suspensions were enriched for leukocytes by a Percoll™ (BD Pharmingen) gradient as

described by Wiesner et al. (52). Briefly, lung single cell suspensions were pelleted and re-suspended in 40% Percoll™ PBS solution, then overlaid onto 67% Percoll™ PBS. Leukocytes were enriched in the interphase layer after a 20-minute centrifugation step at 650 x g without brake. Interphase cells were washed twice with FC buffer, then Fc receptors were blocked with rat anti-mouse CD16/CD32 monoclonal antibody (mAb) 2.4G2 (BD Pharmingen) as described by the manufacturer. Lung leukocytes were fixed in 2% paraformaldehyde (Electron Microscopy Sciences) PBS solution overnight at 4°C. Fixed cells were permeabilized using Perm/Wash Buffer (BD) according to manufacturer instructions, then stained with rat anti-mouse IL-17A-PE or PE-Cy7 mAb TC11-18H10 (BD Pharmingen or Biolegend) and rat anti-mouse IL-23p19-eFluor 660 mAb fc23cpg (eBioscience). FC data were acquired with a BD LSR II cytometer and analyzed using FlowJo X software (Tree Star Inc.). Quadrant gates were established using fluorescence minus one (FMO) controls. Gating strategy is shown in **Figure 2.1**.

Cytokine quantification in BALF after infection. BALF from C57Bl/6 mice infected as described above was collected after euthanasia at regular time intervals. Briefly, an 18 or 20 gauge plastic catheter (Temuro) was inserted into the tracheas of three mice per time point and lungs were flushed three times with 1 mL of PBS supplemented with cOmplete™ protease inhibitor cocktail (Sigma-Aldrich). BALF samples were flash frozen in dry ice and subsequently stored at -80°C. IL-17AA, IL-17AF and IL-17FF were quantified in each sample using Ready-SET-Go! ELISA sets (eBioscience).

Statistics. Statistical analyses were performed using GraphPad Prism 6 software. One-way ANOVA was used to test differences across time points in qPCR and ELISA experiments.

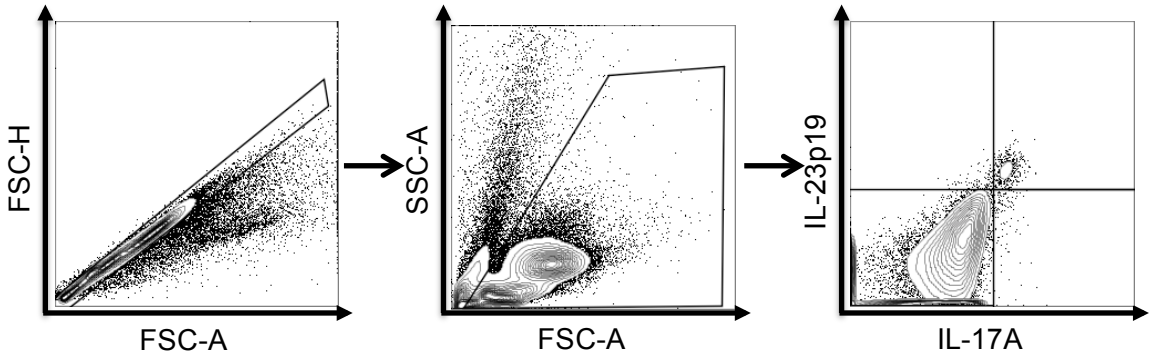

Figure 2.1: Gating strategy for *in vivo* intracellular cytokine staining. Singlet events were gated using the FSC-H/FSC-A window, and then debris was gated out in the SSC-A/FSC-A window. Quadrant gates were determined using FMO controls (not shown).

Results

The transcriptional kinetics of the components of the innate IL-23/IL-17 axis in response to acute aspergillosis. To assess the temporal pattern of mRNA expression of the major components of the IL-23/IL-17 axis, C57Bl/6 mice were either infected with $5x10^7$ *A. fumigatus* conidia (AF293 strain; green) or vehicle (0.01% Tween-PBS; blue) (**Figure 2.2**). At 0, 3, 6, 12, 24, 36, 48, 60 and 72 hours post-infection, the relative mRNA expression of *Il23p19*, *Il17a* and *Il17f* in the lung tissue from three mice per time point were assessed by quantitative PCR (qPCR). *Il23p19* mRNA levels peaked at 36 h post-infection, returning to baseline by 72 h post-infection. *Il17a* showed a biphasic pattern of mRNA production, peaking at 6 h and then again at 48 h post-infection, before returning to baseline at 72 h post-infection. *Il17f* peaked at 12 h post-infection, although the variability at this time point might denote a turning point for its transcription.

The role of IL-23 in the induction and augmentation of IL-17 production differs depending on the source of the latter. For example, in T_H17 development, IL-23 serves to augment cytokine production (53). However, in γδ-T cells, signaling from IL-23 receptor alone induces IL-17 production and release (54). In our model, *Il23p19* mRNA production is congruent with *Il17a* and *Il17f* mRNA levels within the first 12 h of infection, however, as *Il23p19* mRNA levels rise from 12 to 36 h post-infection, *Il17a* and *Il17f* levels return to baseline (**Figure 2.2**). At these time points, the IL-17 sources may not be sensitive to IL-23 signaling or IL-23 may be post-transcriptionally silenced.

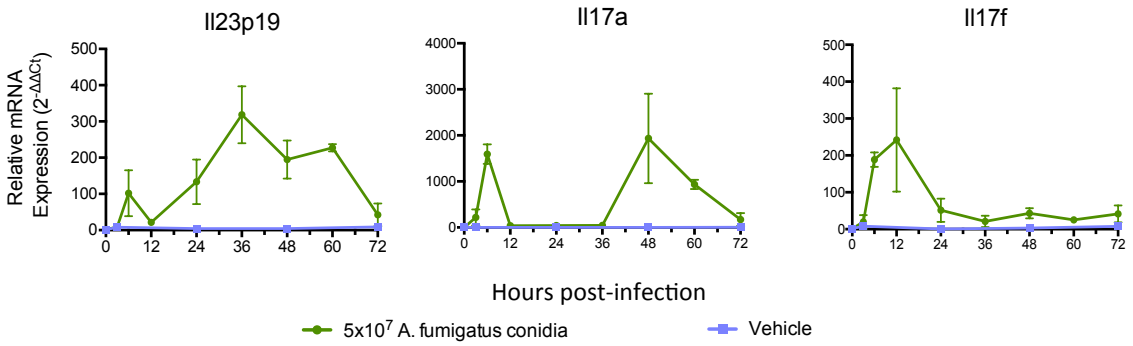

Figure 2.2: The temporal mRNA transcription pattern of the IL-23/IL-17 axis components in acute aspergillosis. *Il23p19*, *Il17a* and *Il17f* transcript levels were assessed at regular time intervals from whole lungs of C57Bl/6 mice infected with 5x10^7 *A. fumigatus* (AF293) conidia or vehicle (n=3 per time point). Relative mRNA expression was calculated using the $2^{-\Delta\Delta Ct}$ analysis method, with *Hprt* amplification used as the internal control. Each point denotes arithmetic mean from three experiments and error bars denote standard error of the mean (SEM). *Il23p19* levels appear to peak at 36 h post-infection ($p < 0.001$). *Il17a* levels appear to peak at 6 h and then again at 48 h post-infection ($p < 0.005$). *Il17f* levels appear to peak at 12 h post-infection ($p < 0.05$).

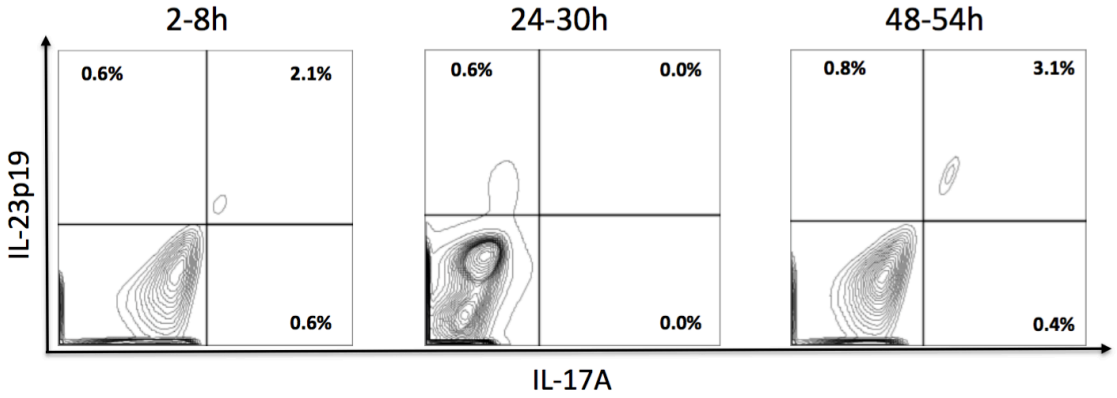

Figure 2.3: Co-production of IL-23p19 and IL-17A coincide with peaks of *Il17a* message. Representative plots from *in vivo* intracellular cytokine staining performed in C57Bl/6 mice infected with $5x10^7$ *A. fumigatus* conidia (AF293) treated with 500 µg of monensin 2, 24 and 48 h post-infection. Six hours after monensin treatment, lung single cell suspensions were fixed and permeabilized, then stained with antibodies against IL-23p19 and IL-17A.

IL-23p19 and IL-17A are co-produced. To assess whether IL-23p19 and IL-17A protein production also diverged around 24 h post-infection, *in vivo* intracellular cytokine staining (ICS) was performed using lung leukocytes from C57Bl/6 mice infected with $5x10^7$ *A. fumigatus* conidia (AF293 strain). At time points that coincided with the peaks of *Il17a* mRNA transcription and at 24 h post-infection, mice were treated with 500 μg of monensin by ip injection. Monensin inhibits cytokine release, thereby allowing for their detection by antibody staining (55). Six hours after monensin treatment, lung leukocytes were assessed for intracellular IL-17A and IL-23p19 by flow cytometry (**Figure 2.3**). At time points that coincided with *Il17a* peak transcription, IL-17A and IL-23p19 were found within the same cells, suggesting that these cytokines are co-produced in response to *A. fumigatus*. Between 24 and 30 h post-infection, only IL-23p19 protein was detected, suggesting that although *Il23p19* message is translated, at this time point it was insufficient to induce enough IL-17A production to be detected by this method. It is important to note that IL-23p19 detection by ICS does not necessarily mean that a fully functional IL-23 heterodimer (IL-23p19/IL-12p40) is produced or released.

IL-17AA, IL-17FF and IL-17AF pattern of release in the airways. Given that IL-17A and IL-17F can homodimerize and heterodimerize, forming IL-17AA, IL-17FF or IL-17AF, the concentration of each dimer in the BALF of infected C57Bl/6 mice was assessed (**Figure 2.4**). IL-17AF was the predominant dimer released over the course of the first three days of infection. In fact, this dimer also followed the biphasic pattern seen in *Il17a* transcription, albeit with a delayed rise and a shorter pause.

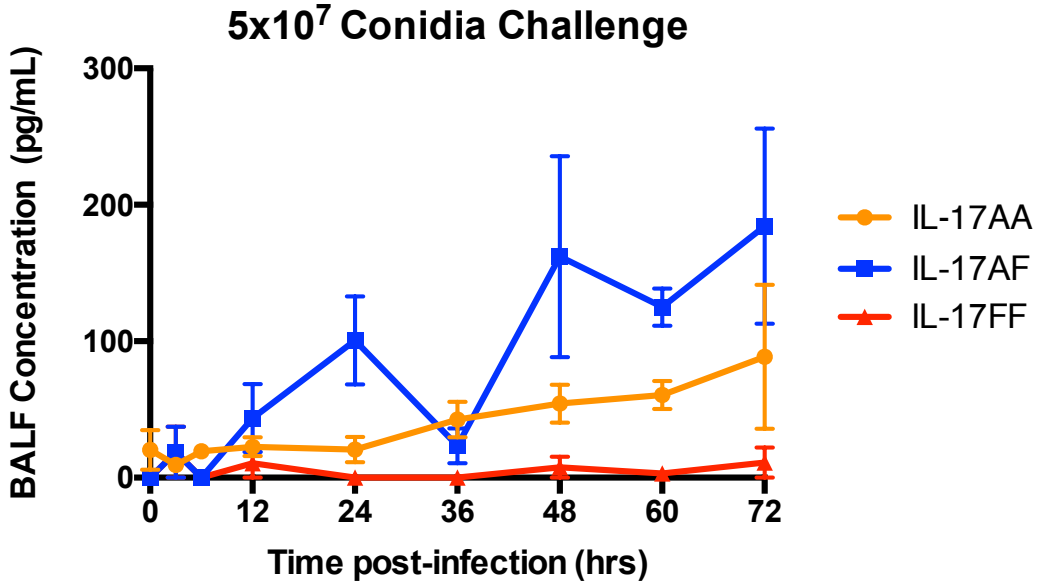

Figure 2.4: Temporal pattern of IL-17 dimer production in acute aspergillosis. BALF were collected from C57Bl/6 mice infected with $5x10^7$ conidia (AF293) at regular time intervals (n=3 per time point) and assessed for the different IL-17 dimers, namely IL-17AA (orange), IL-17AF (blue), and IL-17FF (red). Each point denotes arithmetic mean from three experiments and error bars denote SEM. IL-17AA and IL-17FF showed no difference over a 72 h period ($p > 0.05$), whereas IL-17AF differed across sampling period ($p < 0.05$).

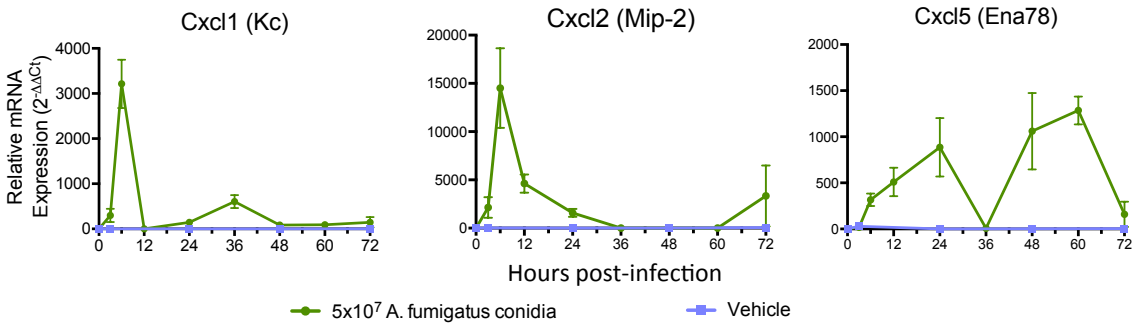

Figure 2.5: Temporal transcriptional pattern of neutrophil chemokines downstream of the IL-23/IL-17 axis in response to acute aspergillosis. *Cxcl1, Cxcl2* and *Cxcl5* relative transcript levels were assessed from whole lungs of C57Bl/6 mice infected with $5x10^7$ conidia (AF293) or vehicle by qPCR (n=3 per time point). Relative gene transcription was calculated using the $2^{-\Delta\Delta Ct}$ analysis method, with amplification of *Hprt* as the internal control. Each point denotes arithmetic mean from three experiments and error bars denote SEM. *Cxcl1* levels appear to peak at 6 h post-infection ($p < 0.0001$). *Cxcl2* levels also appear to peak at 6 h post-infection ($p < 0.001$). *Cxcl5* levels appear to peak at 24 h and then again between 48 and 60 h post-infection ($p < 0.001$).

Temporal transcriptional pattern of neutrophil chemokines downstream of the IL-23/IL-17 axis. One of the effects of IL-17 is the induction of neutrophil chemokines, particularly CXCL (chemokine [C-X-C motif] ligand)-1, -2, and -5 (46). To determine if CXCR-2 ligand transcription pattern in our acute aspergillosis model was similar to the production of IL-17 as shown in **Figure 2.4**, their temporal transcription patterns were assessed as described previously (**Figure 2.5**). Both *Cxcl-1* and *Cxcl-2* peaked at 6 h post-infection, with *Cxcl-1* showing a smaller peak at 36 h post-infection. *Cxcl-2* mRNA levels returned to baseline by 36 h post-infection and remained low until 72 h post-infection. Their pattern of transcription did not particularly resemble the kinetics of the IL-23/IL-17 axis components. The pattern of transcription for *Cxcl-5*, however, highly resembled the pattern of IL-17AF release, suggesting that IL-17AF may induce *Cxcl-5* transcription.

Discussion

To understand the kinetics of the innate IL-23/IL-17 axis in response to the acute pulmonary aspergillosis, the temporal transcription pattern of the major components was assessed in the first 72 h of infection (**Figure 2.2**). In the lungs of C57Bl/6 mice, *Il23p19*, *Il17a* and *Il17f* were promptly expressed, with *Il17f* peaking 12 h post-infection. Interestingly, *Il17a* showed a biphasic pattern of transcription peaking as early as 6 h post-infection, then returning to baseline, only to peak again at 48 h post-infection. *Il23p19*, however, peaked at 36 h post-infection. The temporal transcription pattern for *Il17a* and *Il17f* did not match suggesting that these genes may be differentially regulated in our model (**Figure 2.2**). Although these gene products signal through the same receptor (IL-17RA/RC), in several mouse models Il17a$^{-/-}$ and Il17f$^{-/-}$ diverge in disease outcomes. For example, in dextran sulfate sodium-induced colitis, Il17f$^{-/-}$ mice show milder symptoms, including decreased weight loss, and lower clinical scores compared to Il17a$^{-/-}$ mice (56). Divergence in *Il17a* and *Il17f* transcription has also been observed at the cellular level. Prostaglandin E_2 (PGE_2) stimulation preferentially induces *Il17a* versus *Il17f* transcription in human memory T_H17 cells (CD161$^+$ CCR-6$^+$), while stimulation with IL-23 and IL-1β induced higher levels of *Il17f* transcription (57). There is evidence that strength of T-cell receptor (TCR) signaling, ROR (RAR-related orphan receptor) α-mediated transcriptional activation, and histone modifications (i.e., triple methylation of histone 3 lysine 4 [H3K4me3]), may account for divergence in *Il17a* and *Il17f* transcription (27,57).

Co-production of IL-23p19 and IL-17A suggests that IL-23 may be regulating IL-17 production in an autocrine manner (**Figure 2.3**). However, divergence in *Il23p19* transcription and production from *Il17a* and *Il17f* transcription between 12 h and 36 h post-infection suggests that IL-17 genes may be alternatively induced at these time points.

The transcription of key downstream effectors of the IL-23/IL-17 axis was also measured. The IL-23/IL-17 axis is a major contributor to neutrophil recruitment by up-regulating CXCL-1, -2, and -5 (27). Based on this notion, the transcription kinetics of each of these chemokines were assessed to determine whether there are similarities between their temporal pattern of transcription to that of *Il23p19*, *Il17a* or *Il17f* (**Figure 2.2**). Both *Cxcl-1* and *Cxcl-2* had their highest peaks of mRNA abundance at 6 h post-infection, coinciding with the first *Il17a* peak. If *Il17a* drove the transcription of these chemokines, a delay in peak transcription would be expected. Furthermore, these chemokines have been shown previously to be up-regulated by TNF-α, a cytokine produced as early as 2 h following challenge with *A. fumigatus* (58-61). Alternatively, *Cxcl-1* and *Cxcl-2* transcription peaks could be hidden between time points. At 36 h post-infection, *Cxcl-1* transcription peaked again, although at a much smaller scale. At this time point *Il17a* and *Il17f* transcription had already returned to baseline for 24 and 12 h respectively. Taken together, available evidence is inconsistent with the notion that up-regulation of *Cxcl-1* at this point is driven by IL-17.

Cxcl-5 transcriptional kinetics do not follow the same pattern as *Cxcl-1*, or *Cxcl-2* transcription. In fact, it closely follows the pattern of IL-17AF release, as measured by its

concentration in BALF after infection (**Figure 2.4-2.5**). Although a causative relationship has yet to be established, this may be one way IL-17 regulates CXCR-2 signaling. If that is the case, IL-17-mediated *Cxcl-5* transcription might be a major contributor to lung neutrophilia for days 2 and 3 after infection, as this chemokine is the only CXCR-2 ligand expressed those days. Neutrophils play a significant role in protecting hosts from invasive aspergillosis, as neutropenia is a major risk factor in developing disease. Furthermore, loss of CXCR-2 signaling in mice delays neutrophil recruitment to the lungs after infection with *A. fumigatus* conidia, and renders them susceptible to mortality after infection (25,62).

In this chapter, I have established the temporal pattern of transcription of the main components of the IL-23/IL-17 axis, and some key downstream effectors. In our model of acute aspergillosis, *Cxcl-5* transcription is correlated with IL-17AF release. Additionally, I have discovered that IL-23p19 and IL-17A are co-produced at specific time points after infection with *A. fumigatus*. To my knowledge this is the first report of co-production of these cytokines by a single cell population.

Preface to Chapter III

Chrono Lee performed bone marrow isolations.

Cindy Greer and Chris Mueller sensitized and challenged mice in asthma models.

The UMMS Flow Cytometry Core performed the sorting experiment.

Evelyn Guerra performed remaining experiments.

Evelyn Guerra, Stuart Levitz and Chris Mueller designed the asthma experiments.

Evelyn Guerra and Stuart Levitz designed the remaining experiments.

CHAPTER III: Eosinophils as a Source of IL-23 and IL-17

Abstract

Although the role of the IL-23/IL-17 axis in the primary response to *Aspergillus fumigatus* remains unclear, modeling the infection in mice has led to the discovery of a novel source for these cytokines. This chapter identifies how eosinophils, as first responders to a pulmonary challenge with *A. fumigatus* conidia, act as sources for both IL-23 and IL-17. In addition, this phenomenon was observed in two asthma models, potentially revealing a new therapeutic target for this highly prevalent disease.

Introduction

The antifungal properties of the IL-23/IL-17 axis have been best described in models of oral candidiasis (63). In this model, IL-23p19$^{-/-}$ and IL-17RA$^{-/-}$ mice suffer from higher fungal burdens and increased weight-loss when compared to WT and IL-12p35$^{-/-}$ mice (63,64). Concordantly, defects in genes involved in the IL-23/IL-17 axis can present as chronic mucocutaneous candidiasis (CMC) in humans (63). CMC is characterized by persistent and recurrent *Candida* spp. infections of the oropharynx and cutaneous intertriginous areas (65).

In addition to increasing CMC susceptibility, patients with a *Stat3* mutation can develop invasive aspergillosis secondary to bronchiectasis (66,67). STAT3 is a transcription factor downstream from several cytokines including IL-23 (67,68). Whether defects in the IL-23/IL-17 axis underlie these patients' increased susceptibility to invasive aspergillosis is still unknown.

A few studies have attempted to define a role for the IL-23/IL-17 axis in response to *A. fumigatus*, but a conclusive narrative has yet to be established (30,69). Two groups have reported disparate fungal burdens two or three days post-infection when either IL-23 or IL-17A is knocked out or neutralized. Werner et al. (30) showed that neutralizing IL-17A or IL-23 increased fungal burden in the lungs of infected mice, as assessed by *A. fumigatus* 18S rRNA transcripts, two days post-infection (30). In contrast, Zelante et al. (69) measured fungal burden by assessing levels of chitin, a fungal cell wall component, in IL-23p19$^{-/-}$, IL-12p40$^{-/-}$, IL-12p35$^{-/-}$ and WT mice three days post-infection (69). The authors found that all knock-out (KO) mice had decreased fungal burden compared to

WT; however, IL-23p19$^{-/-}$ animals had the lowest fungal burden. In addition, IL-23p19$^{-/-}$ mice had fewer lung infiltrates than the other KO mice, leading the authors to conclude that IL-23 hampered fungal clearance (69).

Unlike the findings by Zelante et al. (69), at least one other study has shown that chitin loads increase in IL-12p40$^{-/-}$ mice (70), and several other studies have attributed beneficial roles to IL-12 (71-73). Moreover, measuring chitin levels as a function of fungal load may be misleading because resting conidia must swell in order to be effectively killed by phagocytes (5,16,74). Chitin production necessarily increases during conidial swelling to accommodate increased surface area accompanied by rehydration (75). Therefore, it is possible that the findings reported by Zelante et al. (69) support that IL-23 is beneficial in instructing phagocytes to effectively kill *A. fumigatus* conidia. In fact, the decreased leukocyte infiltration seen in IL-23p19$^{-/-}$ mice might actually delay fungal clearance.

In a model of chronic aspergillosis, similar to an asthma model, mice were repeatedly challenged with *A. fumigatus* conidia, and lung homogenates from Il17a$^{-/-}$ mice grew fewer colony forming units than WT mice (31). In light of the studies described above, it is intriguing to consider that IL-17 might be beneficial in the context of an acute infection, but in the setting of chronic exposure to *A. fumigatus,* IL-17 might debilitate fungal killing.

Although first established as a product of CD4^{+} T cells, IL-17 is produced by several cell types from the innate and adaptive arms of the immune system (44). In the adaptive arm, both CD4^{+} (T_H17) and CD8^{+} (T_c17) lymphocytes produce IL-17 (27). In

the innate arm, a growing list of cell types has been implicated in IL-17 production. These include cells from the lymphoid compartment such as ILC3s (66,76), γδ T-17 cells (26), and iNKT-17 cells (27,54). From the myeloid compartment, IL-17 production by neutrophils (77), macrophages (78,79), monocytes (80) and eosinophils (81,82) have been reported.

The source of IL-23 has primarily been studied in connection to T_H17 development. In the context of this paradigm, APCs such as dendritic cells and macrophages have been identified as its main sources (29). In this chapter I show that the co-producers of IL-23 and IL-17 discovered in Chapter II are eosinophils. By *in vivo* ICS, eosinophils are revealed to be a local source of these cytokines in response to both acute *A. fumigatus* infection and in two different asthma models.

Materials and Methods

Mice. Six- to eight-week old C57Bl/6, Balb/c and ΔdblGATA-1 mice on the Balb/c background were obtained either from Jackson Laboratories or bred in pathogen-free conditions at the University of Massachusetts Medical School. All mouse studies were performed in accordance with protocols approved by the IACUC.

Aspergillus fumigatus culture and murine acute pulmonary aspergillosis model. WT *A. fumigatus* (AF293 strain) was grown and harvested as described in Chapter II. Briefly, conidia were inoculated on Sabouraud-dextrose agar (Remel™) slants and incubated for two days at 37°C. Conidia were harvested in PBS containing 0.01% Tween-20 (Thermo-Fisher). Isoflurane-anesthetized mice were infected via the OT route with $5x10^7$ conidia suspended in 0.01% Tween-PBS.

Murine acute allergic asthma model. C57Bl/6 mice were sensitized two times by ip injection of 20 μg of OVA (Sigma-Aldrich) in 100 μL of Imject® Alum (Thermo Scientific) or 200 μg of *A. fumigatus* crude protein extracts (AF cpe) (Greer Laboratories). Sensitization occurred two weeks apart. Twenty-eight days after the first sensitization, mice were challenged with aerosolized 1% OVA or 0.25% AF cpe in saline respectively for 20 minutes. Challenges were repeated on days 29 and 30 (**Figure 3.8A**).

Intracellular cytokine staining, sorting and flow cytometry. Intracellular cytokine staining (ICS) was performed as described in Chapter II. Briefly, mice were treated with 500 μg

of monensin (Sigma-Aldrich) by ip injection, 2 or 48 h after infection with $5x10^7$ conidia, or 48 h after the last challenge in the allergic asthma models. Six hours after monensin treatment, lung single-cell suspensions were prepared using MACS® lung dissociation kit as described by the manufacturer. Single-cell suspensions were enriched for leukocytes using a Percoll™ (GE Healthcare) gradient (52). Interphase cells were collected, counted with the aid of a hemocytometer, and then co-incubated with rat anti-mouse CD16/CD32 monoclonal antibody (mAb) 2.4G2 (BD Pharmingen) to block F_c receptors in accordance with manufacturer's directions. Surface antigens were then stained with antibodies listed in **Table 3.1** and with Fixable Viability Dye eFluor® 780 (eBioscience) or Live/Dead Blue (Life Technologies) for 30 minutes at 4^o C. After two successive wash steps, lung leukocytes were fixed in 2% paraformaldehyde (Electron Microscopy Sciences) PBS solution for at least 15 minutes or overnight at 4^o C. Fixed cells were permeabilized using Perm/Wash Buffer (BD Pharmingen) according to manufacturer instructions and then stained with antibodies listed in **Table 3.1**.

For sorting IL-23p19$^+$ IL-17A$^+$ cells, fixed lung leukocytes were only stained for intracellular cytokines, and then sorted with BD FACSVantage DV-1 Cell Sorter (UMass Medical School Flow Cytometry Core). FC data were acquired with a BD LSR II cytometer and analyzed using FlowJo X software (Tree Star Inc.). Gating was established using FMO controls containing isotype control mAb conjugated with the fluorophore corresponding to the missing antibody as previously described (83).

Table 3.1: Antibodies used in flow cytometry.

Surface Markers			
mAb	**Clone**	**Manufacturer**	**Isotype**
Ly6C-PE-Cy7	HK1.4	Biolegend	Rat IgG2c
Ly6G-PE-CF594	1A8	BD Biosciences	Rat IgG2a
CCR-2-FITC	475301	R&D Systems	Rat IgG2b
CD11c-BV™ 570	N418	Biolegend	Armenian Hamster IgG
Siglec-F-BV™ 421	E50-2440	BD Biosciences	Rat IgG2a
CD11b-BUV™ 395	M1/70	BD Biosciences	Rat IgG2b
F4/80-APC-Cy7	BM8	Biolegend	Rat IgG2a
CD45-PerCP-Cy5.5	30-F11	BD Biosciences	Rat IgG2b
Intracellular Markers			
mAb	**Clone**	**Manufacturer**	**Isotype**
IL-23p19-eFluor® 660	Fc23cpg	eBiosciences	Rat IgG1
IL-17A-PE-Cy7	TC11-18H10.1	Biolegend	Rat IgG1
IL-17AF-eFluor® 660	B8KN8R	eBiosciences	Rat IgG2a

Cytological staining. After sorting, cells were adhered to poly-L-Lysine-coated slides (Sigma-Aldrich) by cytospinning 250 µL of cell suspension at 800 rpm for three minutes (Shandon Cytospin 2). Cells were dried on the slide, and then dipped in hematoxylin solution (Thermo-Fisher) for 30 seconds. Slides were washed in water then dipped in eosin (Thermo-Fisher) for one minute. Increasing concentrations of ethanol (95%-100%) were used to dehydrate slides for a total of two minutes. Finally, slides were dipped three times in Clear-Rite (Thermo Scientific) for one minute each time. Slides were mounted using Permount™ (Fisher Scientific).

Cytokine quantification in BALF after infection. BALF from Balb/c and ΔdblGATA-1 mice infected as described above was collected after euthanasia at 60 h post-infection. BALF collection was performed as described in Chapter II. Ready-SET-Go! ELISA sets

(eBioscience) were used to quantify IL-17AA, IL-1AF, and IL-17FF. IL-23 was measured using R&D Quantikine ELISA kit.

Generation of bone marrow-derived eosinophils (BM-Eos). Bone marrow cells were isolated from murine femurs and differentiated as described previously (84). Briefly, BM cells were subjected to a gradient with Histopaque 1083 (Sigma). Interphase cells were washed twice to remove any leftover Histopaque and cultured in Isocove's modified Dulbecco's medium (IMDM; Life Technologies) supplemented with 10% FBS (Tissue Culture Biologicals), 100 U/mL penicillin and 100 U/mL streptomycin, 1X Glutamax (Life Technologies) and 2 μL of β-mercaptoethanol (Life Technologies). The first four days of culture, cells were stimulated with 100 ng/mL of murine stem cell factor (mSCF) (PeproTech) and 100 ng/mL of murine FMS-like tyrosine kinase 3 ligand (mFLT3L) (PeproTech). The following ten days, cells were stimulated with 10 ng/mL IL-5 (R&D). Cells were fed every other day (**Figure 3.11**). Differentiation was confirmed by flow cytometry with rat mAb against murine Siglec-F-BV421 (BD Biosciences).

BM-Eos Stimulation. BM-Eos were stimulated with live or heat-killed *A. fumigatus* AF293 conidia, zymosan (10-100 μg/mL; Sigma), lipopolysaccharide (LPS, 100 ng/mL; Sigma) and several cytokines at different concentrations and combinations for lengths of time ranging from two hours to two days. Cytokines used to stimulate BM-Eos included IL-5 (10 ng/mL), IL-1β (1-10 ng/mL; R&D), GM-CSF (10 ng/mL; PeproTech), IL-23 (10 ng/mL; eBiosciences), IL-17E (0.1-10 ng/mL; R&D), IL-17AA (0.1-10 ng/mL;

R&D), PGE_2 (10^{-5}-10^{-3} M; Cayman Chemicals), transforming growth factor-β (TGF-β) (1-10 ng/mL; eBiosciences), and IL-6 (10-100 ng/mL; eBiosciences). When co-incubated with live *A. fumigatus* conidia, cultures were supplemented with 0.5 μg/mL of voriconazole (Sigma) to prevent fungal overgrowth. Following stimulation, supernatants were collected for ELISA and/or RNA isolation for qPCR.

Quantitative PCR. RNA from BM-Eos was isolated using Qiagen's RNeasy kit according to the manufacturer's instructions. qPCR was performed using KAPA SYBR FAST One-Step qRT-PCR kit according to instructions provided by the manufacturer, in a CFX96 Touch™ Real-Time PCR Detection System (Bio-Rad). Primer sequences for each target are listed in **Table 3.2** and were designed and synthesized by Sigma or previously published and synthesized by Life Technologies. A 2% agarose gel (Acros Organics) was used to confirm PCR amplicon sizes.

Table 3.2: Primer sequences used in qPCR reactions.

Target Gene	Forward Primer (5'-3')	Reverse Primer (5'-3')	References
Epx	CCAGAGATGGAGACAGATTC	GATAAAGAGATTCGCCTCAG	Sigma
Il17ra	AGTGTTTCCTCTACCCAGCAC	GAAAACCGCCACCGCTTAC	(48)
Il17rc	CCTTGGAACCCAGTGGCTGTA	ACACTGGTGTGATCGGAAGTCTTG	(85)
Il23a	TTACAGCAAAATCATCCCAC-	TTGATGATTACCTGAAGCAG	Sigma

Statistical analysis. Statistical analyses were performed using GraphPad Prism 6 software. T-tests were used to compare means between groups of two. Comparisons between more than two groups were made using one- or two-way ANOVA and Tukey's post-hoc analysis.

Results

Eosinophils co-produce IL-23p19 and IL-17. As discussed in Chapter II, IL-23p19 and IL-17A were co-produced in response to *A. fumigatus* at time points corresponding to *Il17a* transcription. To identify the cell type(s) responsible for their production in acute aspergillosis, the IL-23p19$^+$ IL-17A$^+$ population was sorted 8 h post-infection with 5x10^7 *A. fumigatus* conidia (**Figure 3.1A**). In accordance with eosinophil morphology, the cytoplasm of sorted cells uniformly stained strongly with eosin, and nuclei were characteristically polymorphous (86).

To further confirm that eosinophils were indeed producing IL-23p19 and IL-17A, these double-positive cells were assayed for surface markers characteristic of eosinophils, namely Siglec-F and CD11b (**Figure 3.1B**). In Balb/c mice acutely infected with *A. fumigatus,* the IL-23p19$^+$ IL-17A$^+$ cells were Siglec-F$^+$ CD11b$^+$ and also CD11c$^-$. These markers have been shown to accurately define eosinophils in the murine lungs (86,87). Additionally, in mice where eosinophilopoiesis is disrupted (ΔdblGATA-1), IL-23p19$^+$ IL-17A$^+$ cells were largely absent (**Figure 3.1B**).

In the context of eosinophil deficiency, virtually no IL-23p19$^+$ cells were detected (**Figure 3.2**). As functional IL-23 is comprised of IL-23p19 and IL-12p40 subunits, I confirmed that IL-23 heterodimer was indeed produced in acutely infected lungs of WT mice, and that their levels were significantly diminished in the absence of eosinophils (**Figure 3.3**). In addition, nearly all (96.9%) IL-23p19$^+$ cells were found to be Siglec-F$^+$ CD11c$^-$ (**Figure 3.4A**). The majority (87.1%) of eosinophils recruited to the lungs were

IL-23p19^{+} (**Figure 3.4B**). In conclusion, eosinophils are the predominant local source of IL-23 in our acute aspergillosis model.

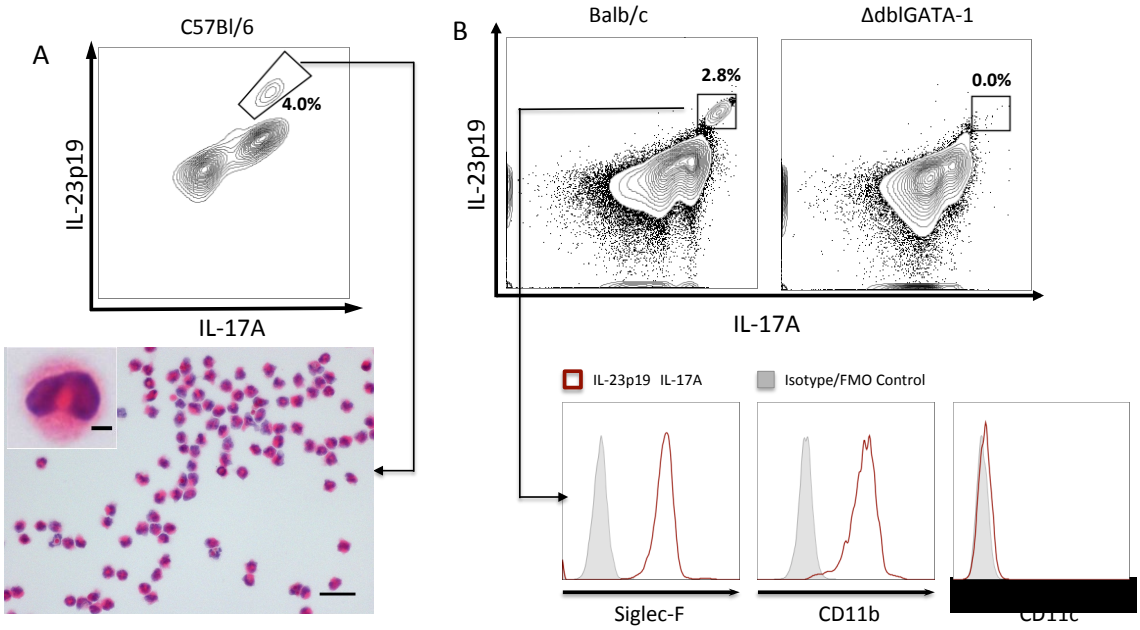

Figure 3.1: Eosinophils co-produce IL-23p19 and IL-17. (**A**) C57Bl/6 mice infected with $5x10^7$ AF293 conidia were treated with 500 µg monensin ip 2 h post-infection, lung single-cell suspensions were made 6 h after monensin treatment. Cells were fixed and permeabilized, then stained with anti-IL-23p19 and anti-IL-17A. FC analysis uncovered a population producing both cytokines. That population was sorted and stained with H&E, revealing cells consistent with eosinophil morphology (i.e., polymorphous nucleus and pink cytoplasm). Scale bar corresponds to 20 µm and 3 µm in figure inset. (**B**) IL-23p19$^+$ IL-17A$^+$ populations were also detected in Balb/c mice infected with $5x10^7$ AF293 conidia, which was absent in ΔdblGATA-1 mice. Further characterization of the IL-23p19$^+$ IL-17A$^+$ population by surface markers confirmed they were eosinophils (Siglec-F$^+$ CD11b$^+$ CD11c$^-$).

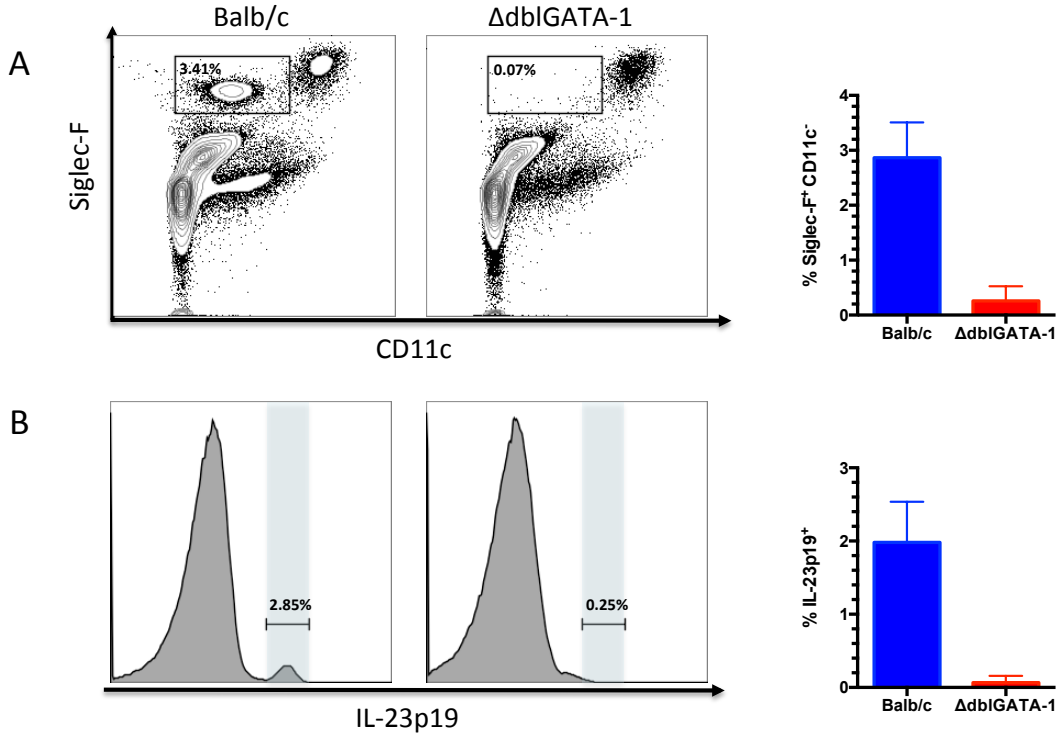

Figure 3.2: Eosinopenic mice lack IL-23p19^{+} cells. (A) ΔdblGATA-1 mice lack lung-recruited eosinophils (Siglec-F^{+} CD11c^{-}) after infection with 5x10^{7} AF293 conidia when compared to Balb/c mice. (**B**) Anti-IL-23p19 staining of lungs from infected Balb/c and ΔdblGATA-1 after treatment with 500 µg of monensin shows nearly complete abrogation of IL-23p19^{+} cells in the absence of eosinophils 8 h post-infection.

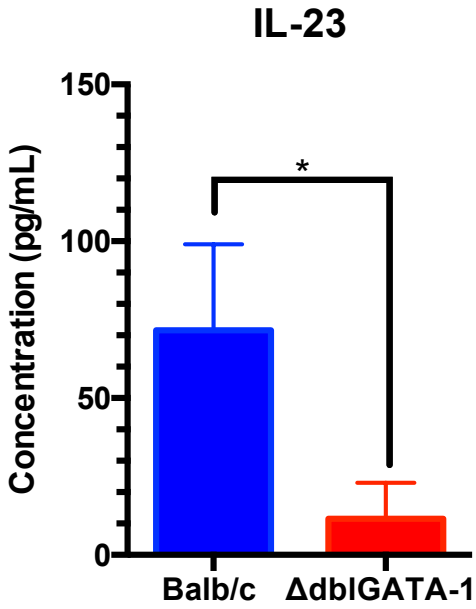

Figure 3.3: Lack of eosinophils correlates with diminished levels of IL-23 in acute aspergillosis. BALF from Balb/c and ΔdblGATA-1 mice were collected 60 h after challenge with $5x10^7$ *A. fumigatus.* IL-23 (IL-23p19/IL-12p40) levels were significantly reduced in eosinopenic mice. Data were statistically analyzed using an unpaired t-test (n = 6); * = $p < 0.05$.

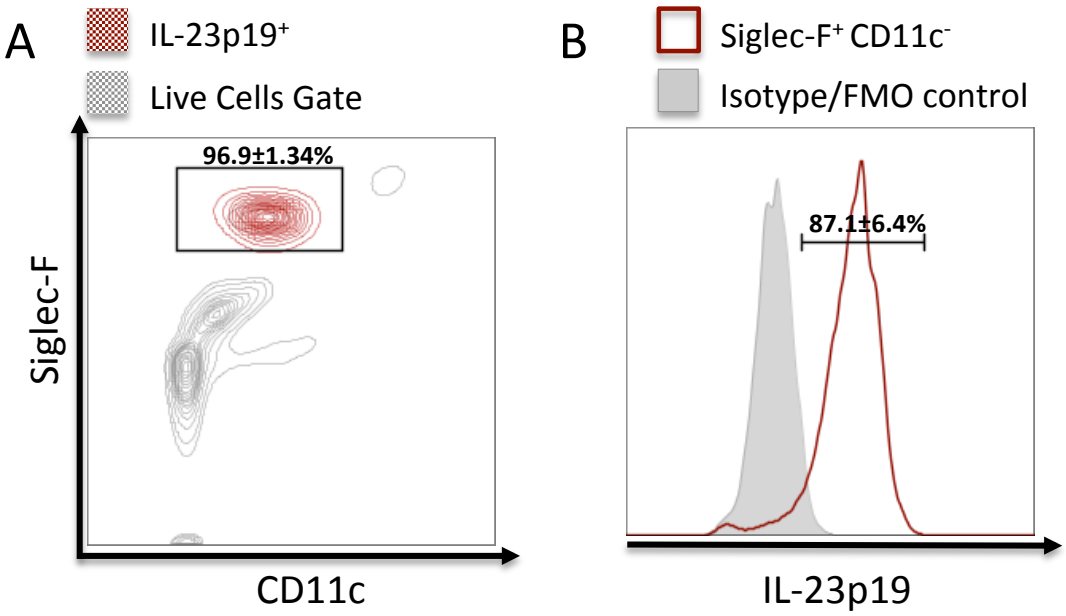

Figure 3.4: Eosinophils are a significant source of local IL-23p19 in acute aspergillosis. (**A**) Overlay of IL-23p19^{+} cells (maroon) onto the live cells gate (gray) in the Siglec-F vs. CD11c window. An average of 96.9±1.34% of IL-23p19^{+} events was found within the eosinophil gate (Siglec-F^{+} CD11c^{-}). (**B**) Representative histogram showing the shift in the IL-23p19 channel of the eosinophil population compared with its FMO/isotype control. A mean of 87.1±6.4% of Siglec-F^{+} CD11c^{-} cells were also IL-23p19^{+}. Arithmetic mean ± standard deviation (SD) shown in each plot (n=5).

Myeloid cells contribute to IL-17 production in acute aspergillosis. To assess whether lack of eosinophils affects IL-17 levels in the lungs of mice acutely infected with *A. fumigatus*, levels of IL-17AA, IL-17FF and IL-17AF were assessed in the BALF of Balb/c and ΔdblGATA-1 mice 60 h post-infection with $5x10^7$ *A. fumigatus* conidia (**Figure 3.5**). Again, IL-17AF was the most abundant IL-17 dimer produced, but in Balb/c mice, IL-17FF is the second most abundant dimer, and IL-17AA the least abundant dimer. In the BALF of infected C57Bl/6 mice, IL-17AA levels were on average higher than IL-17FF, which was barely detected (see Chapter II, **Figure 2.4**).

ΔdblGATA-1 mice (Balb/c background) carry a deletion in the palindromic enhancer sequence of the GATA-1 promoter, which renders them unable to produce eosinophils (88). These mice had lower levels of IL-17AA and IL-17AF than WT mice, but unchanged levels of IL-17FF (**Figure 3.5**). To assess whether other cells from the myeloid compartment contributed to the levels of IL-17 in the lungs of acutely infected mice, I designed a flow cytometry antibody panel to detect eosinophils, lung macrophages, inflammatory monocytes and neutrophils in the lungs. This panel consisted of antibodies against Siglec-F, CD11c, CD11b, CCR-2 and Ly6G. Before performing *in vivo* intracellular cytokine staining with this panel, I confirmed that the markers listed above sufficiently characterized each population of interest. To this end, antibodies against Ly6C and F4/80 were added to the panel. **Table 3.3** lists how each population has been characterized previously (86). The gating strategy for each myeloid cell population is shown in **Figure 3.6**.

Consistent with markers characteristic of eosinophils, Siglec-F^+ $CD11c^-$ cells were also $Ly6C^+$ $Ly6G^+$ $CCR\text{-}2^-$ $CD11b^+$ and $F4/80^+$, (**Figure 3.6A**) (86). Lung macrophages gated as Siglec-F^+ $CD11c^+$ consist of resident alveolar macrophages and recruited macrophages that have differentiated from inflammatory monocytes (89). A distinction between the two populations was not necessary for the purpose of this experiment. Siglec-F^+ $CD11c^+$ cells were $Ly6C^{Lo}$ $Ly6G^-$ $CCR\text{-}2^-$ $CD11b^{Int}$ $F4/80^+$ confirming their identity as lung macrophages (**Figure 3.6A**) (89). Inflammatory monocytes (Siglec-F^- $CD11b^+$ $CCR\text{-}2^+$) were confirmed to be $Ly6C^{Hi}$ $Ly6G^+$ $CD11c^-$ $F4/80^{Lo}$ (**Figure 3.6B**) (89). Finally, neutrophils were gated as Siglec-F^- $CD11b^+$ $CCR\text{-}2^-$ $Ly6G^{Hi}$. This population was found to be $Ly6C^{Hi}$ and $F4/80^-$ as formerly defined (**Figure 3.6B**).

After confirming the identity of the myeloid cells of interest in the lungs of infected animals, I assessed whether each population produced IL-17. Out of three commercially available antibodies against IL-17, two target either the IL-17A or IL-17F subunit. However, it is unknown whether these antibodies selectively recognize their respective homodimers without cross-reactivity against IL-17AF. Importantly, the third antibody recognizes the IL-17AF heterodimer, without cross-reactivity with IL-17AA or IL-17FF. IL-17AF garnered our interest, as it was the most abundant IL-17 permutation in our acute aspergillosis model (**Figure 2.4, 3.5**). While eosinophils were the only cells found to be producing IL-23p19 (**Figure 3.1B, 3.2, 3.4**), IL-17AF was produced by eosinophils, lung macrophages, inflammatory monocytes and neutrophils in C57Bl/6 and Balb/c mice (**Figure 3.7A**).

To measure cytokine abundance within each cell population, I calculated the shift in median fluorescence intensity (MFI) from the FMO/isotype control to the stained sample (ΔMFI). Of all the myeloid cells, eosinophils had the highest ΔMFI for IL-17AF, which did not significantly differ between C57Bl/6 and Balb/c mice. For the other myeloid cells, ΔMFI in the IL-17AF channel greatly differed between C57Bl/6 mice and mice in the Balb/c background (WT and ΔdblGATA-1), however, there were no significant difference between WT (Balb/c) and ΔdblGATA-1 (**Figure 3.7B**).

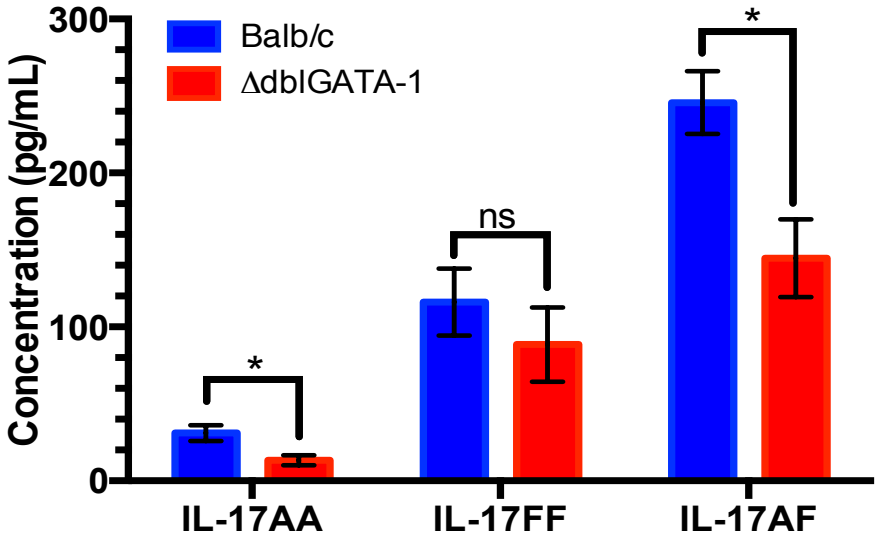

Figure 3.5: Lack of eosinophils correlates with lower levels of certain IL-17 dimers. BALF from Balb/c and ΔdblGATA-1 mice (n=3 per group) infected with $5x10^7$ *A. fumigatus* conidia (AF293 strain) was collected 60 h post-infection. IL-17AA, IL-17FF and IL-17AF levels were assessed by ELISA. IL-17AA and IL-17AF levels were decreased in ΔdblGATA-1 mice, however IL-17FF levels remained unchanged. Data were statistically analyzed using multiple t-tests that were corrected using the Sidak-Bonferroni method * = $p < 0.05$.

Table 3.3: Surface markers characteristic of different myeloid cell populations.

Marker	***Eosinophils***	***Neutrophils***	***Inflammatory Monocytes***	***Lung Macrophages***
Ly6C	+	++	++	Low
Ly6G	+	++	+	-
CCR-2	-	-	+	-
CD11c	-	-	-	+
Siglec-F	+	-	-	+
CD11b	+	+	+	+/-
F4/80	+	-	Low	+

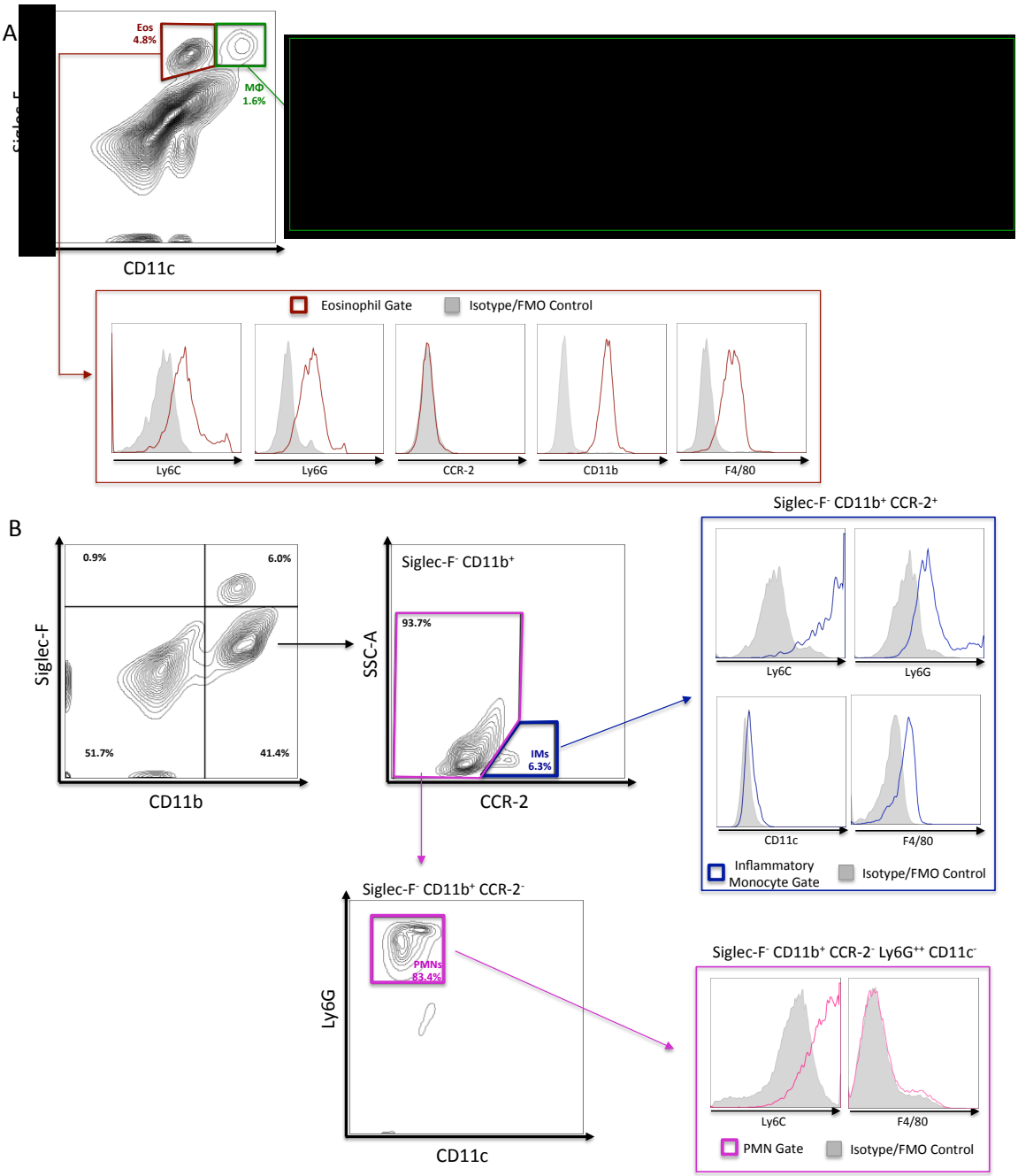

Figure 3.6: Gating strategy for lung myeloid cells elicited in acute aspergillosis. (**A**) Eosinophil gate (Siglec-F^+ $CD11c^-$) was confirmed to be $Ly6C^+$ $Ly6G^+$ $CCR\text{-}2^-$ $CD11b^+$ and $F4/80^+$, in accordance with previous reports. The gate for lung macrophages (Siglec-F^+ $CD11c^+$) was also confirmed with other markers. Lung macrophages were also $Ly6C^{Lo}$ $Ly6G^-$ $CCR\text{-}2^-$, $CD11b^{Int}$ $F4/80^+$. (**B**) Inflammatory monocytes gated as Siglec-F^- $CD11b^+$ $CCR\text{-}2^+$ were found to be $Ly6C^{Hi}$ $Ly6G^+$ $CD11c^-$ $F4/80^{Lo}$. Neutrophils gated as Siglec-F^- $CD11b^+$ $CCR\text{-}2^-$ $Ly6G^{Hi}$ $CD11c^-$ were found to be $Ly6C^{Hi}$ and $F4/80^-$.

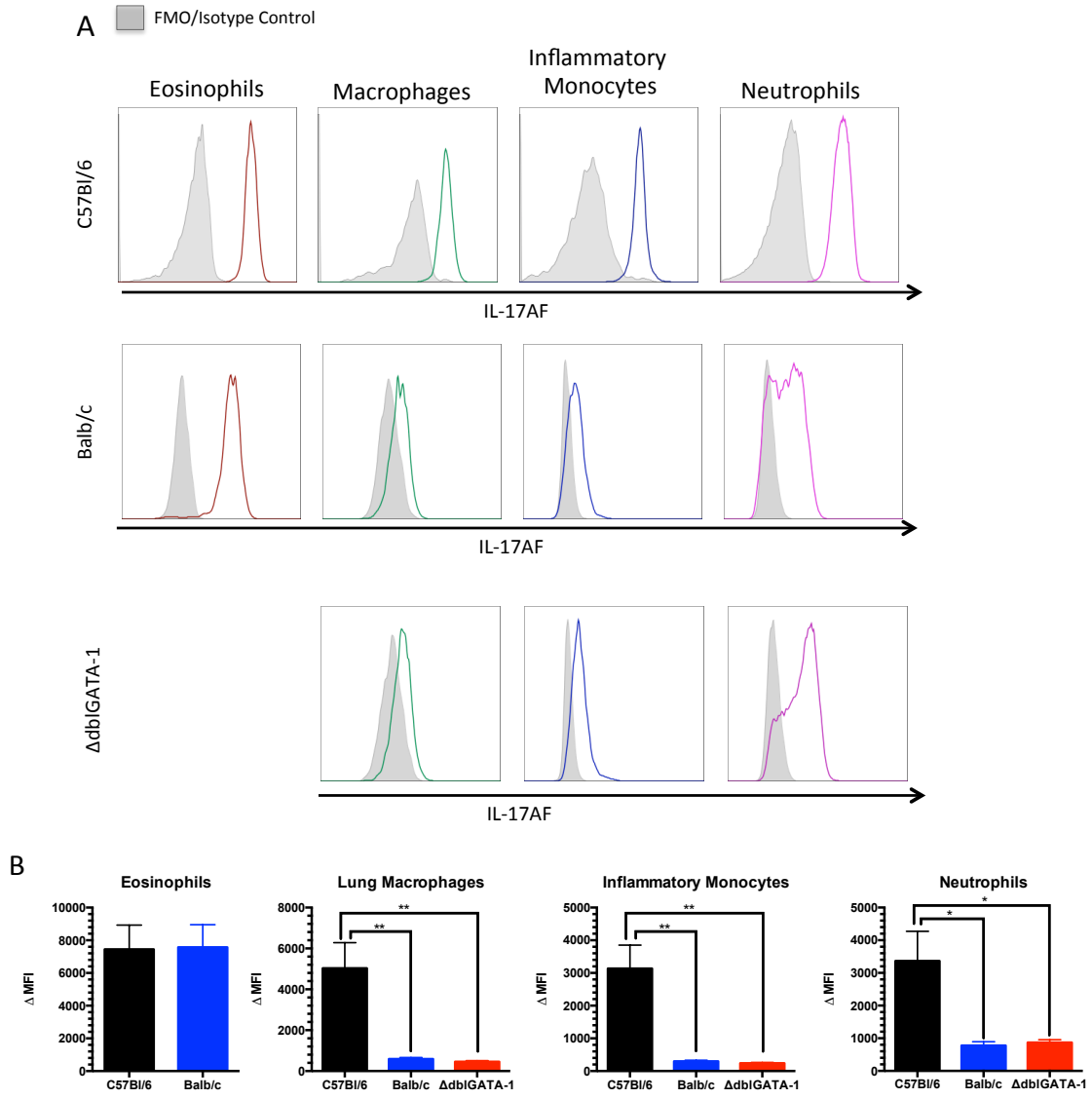

Figure 3.7: Myeloid cells contribute to IL-17AF production in acute aspergillosis. (**A**) Lung myeloid cells isolated from C57Bl/6, Balb/c and ΔdblGATA-1 mice infected with $5x10^7$ *A. fumigatus* conidia (AF293) were assessed for their ability to produce IL-17AF six hours after 500 µg monensin ip injections. IL-17AF was produced by eosinophils, lung macrophages, inflammatory monocytes and neutrophils. (**B**) MFI from FMO/isotype controls was subtracted from MFI of each population to calculate ΔMFI. Data were aggregated from 4-5 mice of each strain, and were analyzed by unpaired t-tests or one-way ANOVA as appropriate. Post-hoc analyses were done using Tukey's multiple comparison tests after one-way ANOVA. * = $p < 0.05$, ** = $p < 0.01$.

Eosinophils co-produce IL-23p19 and IL-17AF in allergic asthma. As eosinophils are thought to drive many of the pathological findings in allergic asthma, and as increased levels of IL-17 have recently been positively correlated with severity of asthma symptoms (90), I wanted to assess whether eosinophils can also produce IL-23p19 and/or IL-17 in murine models of allergic asthma. Two established models of acute allergic asthma were chosen: one where mice were sensitized and challenged with *A. fumigatus* crude protein extracts (*Af* cpe) (33), and another where sensitization was achieved with OVA admixed with aluminum hydroxide then challenged with aerosolized OVA (91) (**Figure 3.8A**). In both allergic asthma models, eosinophils produced both IL-23p19 and IL-17AF (**Figure 3.8B**).

In both asthma models, eosinophils were the most significant producers of local IL-23p19 (**Figure 3.9**). Close to 100% of IL-23p19^{+} cells were found in the eosinophil gate regardless of allergen (**Figure 3.9A**). On average, 35.1% of lung cells produced IL-23p19 in the *A. fumigatus* asthma model, compared to 22.5% in the OVA model (**Figure 3.9A**). Although fewer cells produced IL-23p19 in the OVA model, this difference was not statistically significant (**Figure 3.9B**).

A similar pattern in IL-17AF production was observed in both asthma models as was seen in acute aspergillosis. While IL-17AF is primarily produced by eosinophils, as measured by ΔMFI, lung macrophages, inflammatory monocytes and neutrophils contribute to its production (**Figure 3.10**). Interestingly, eosinophils from the lungs of mice sensitized and challenged with *Af* cpe showed an increased shift in MFI when compared to the OVA sensitized and challenged mice (**Figure 3.10B**).

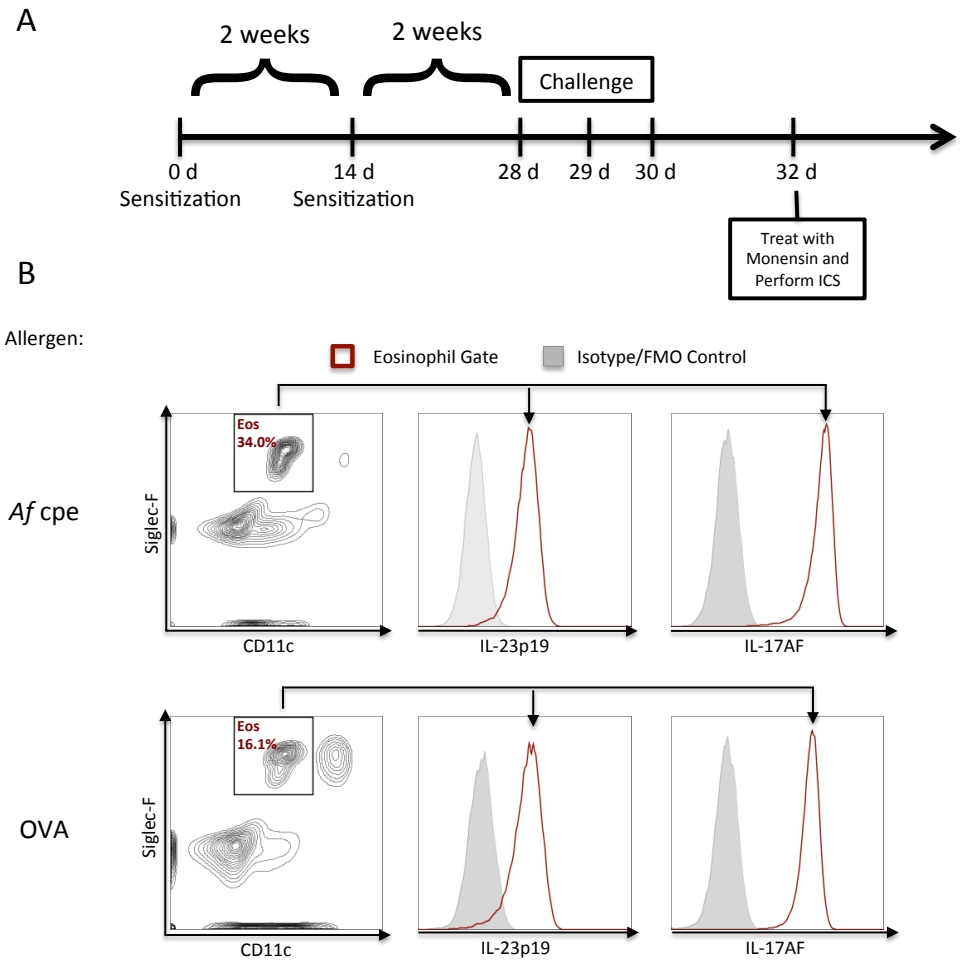

Figure 3.8: Eosinophils co-produce IL-23p19 and IL-17AF in two different models of asthma. (**A**) Schematic of sensitization and challenge timeline for asthma models. C57Bl/6 mice were sensitized with either 20 µg of OVA in 100 µL of alum or 200 µg of *Af* cpe by ip injections twice in two-week intervals. Two weeks after the second sensitization, mice were challenged with either OVA or *Af* cpe by aerosol exposure on days 28, 29, and 30 after the first sensitization. Two days after the last challenge, mice were treated with 500 µg of monensin by ip injection. Six hours after monensin treatment, intracellular cytokine staining was performed in lung single cell suspensions. (**B**) Eosinophils (Siglec-F^+ $CD11c^-$) were found to produce IL-23p19 and IL-17AF.

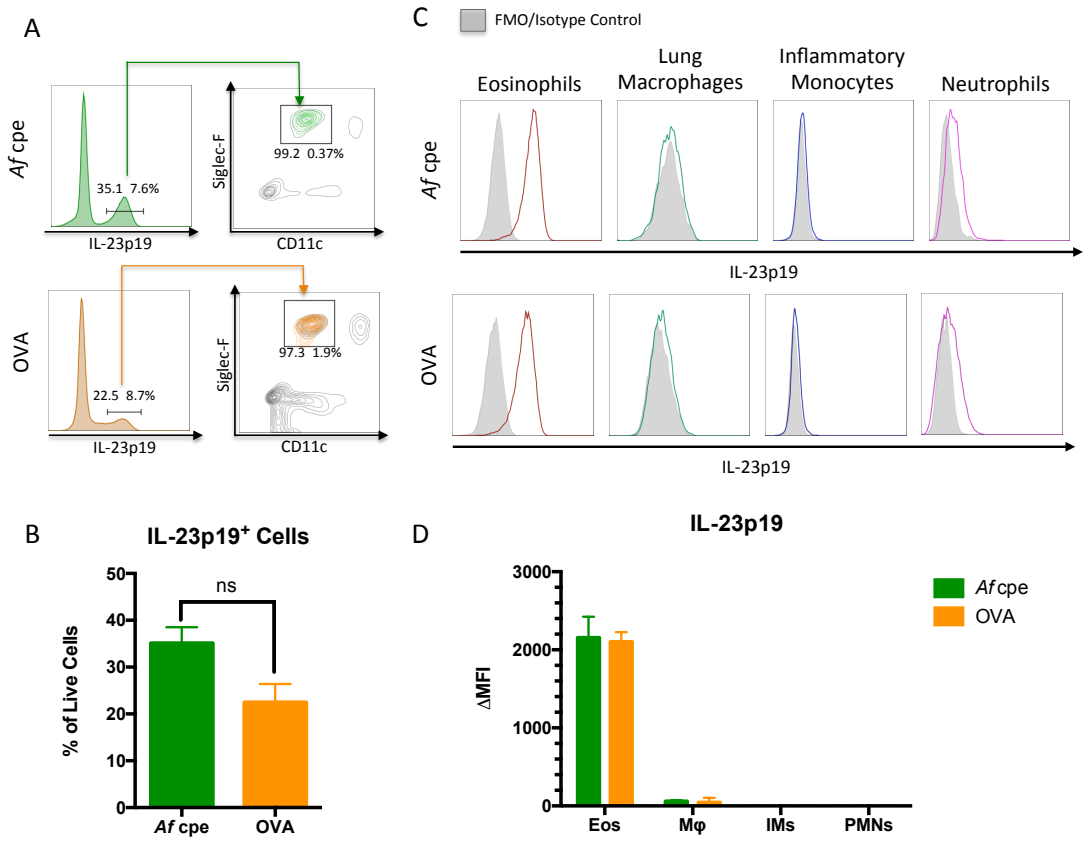

Figure 3.9: Eosinophils are a significant source of local IL-23p19 in asthma. (**A**) In C57Bl/6 mice sensitized and challenged with *A. fumigatus* protein extracts or OVA, eosinophils were the most significant producers of lung IL-23p19. Arithmetic mean ± SD shown in each plot (n=5). (**B**) Although there were fewer IL-23p19^{+} cells in the lungs of the OVA sensitized and challenged mice compared to the *Af* cpe model, the difference was not statistically significant, *ns* = $p > 0.05$. (**C**) Several myeloid cells were assessed for their ability to produce IL-23p19 in *Af* cpe and OVA asthma models. Only eosinophils reliably showed a significant shift in IL-23p19 signal. (**D**) ΔMFIs were calculated for each of the myeloid cell types assessed in (C).

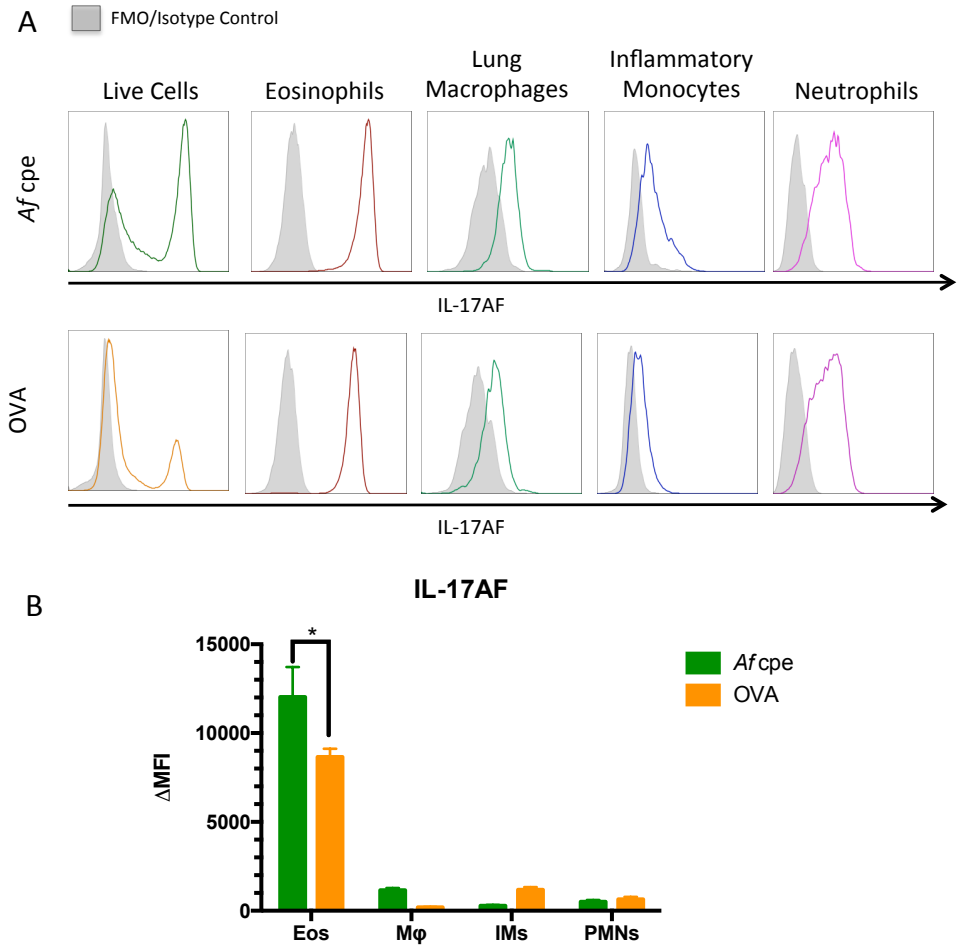

Figure 3.10: Different myeloid cell types contribute to IL-17AF production in asthma. (**A**) In both OVA and *A. fumigatus* asthma models, IL-17AF is produced by eosinophils, lung macrophages, inflammatory monocytes, and neutrophils. (**B**) ΔMFI for each myeloid cell population was calculated as described previously. Eosinophils showed a pronounced shift in signal for IL-17AF compared to the other cell types. The fungal asthma model elicited higher levels of IL-17AF production by eosinophils than the OVA asthma model. Data were analyzed by two-way ANOVA, employing Tukey's multiple comparison test, *=$p<0.05$, n=5 per group.

In vitro stimulation of BM-Eos failed to induce IL-23 or IL-17. BM-Eos were generated as previously described (84) (**Figure 3.11**). To assess whether IL-23 or IL-17 could be induced by *A. fumigatus,* cells and live or heat-killed AF293 conidia were co-incubated for 4, 8 or 24 h. No IL-23, IL-17AA, IL-17AF, or IL-17FF was detected by ELISA in the supernatants of co-cultures. In addition, several combinations of zymosan or LPS, and IL-5, TGF-β, IL-6, GM-CSF, IL-1β, TNF-α, IL-17E (IL-25), PGE_2, IL-23 and IL-17AA were used to stimulate BM-Eos. None of the combinations tried reproducibly induced IL-23 or any of the IL-17 dimers from BM-Eos.

BM-Eos highly express Il17ra, but do not express Il17rc or Il23a. Given that IL-23 induces IL-17 from neutrophils and other innate cell types (54,77), I tested whether BM-Eos express the receptor for IL-23 (IL-23A/IL-12Rβ_1). Freshly differentiated eosinophils expressed eosinophil peroxidase (*Epx*), but no *Il23a* transcript was detected by qPCR (**Figure 3.12**) (27). *Il17ra* and *Il17rc* transcript levels were also assessed in these cells. Although *Il17ra* transcription was detected, its partner in IL-17 signaling, *Il17rc* could not be detected (**Figure 3.12**).

GM-CSF has been shown to activate eosinophils by inducing the transcription of several cytokines, including *Tnf, Il13,* and *Il6*, as well as increasing cell diameter (92). Therefore, I tested whether 18 h activation with GM-CSF induced the transcription of *Il23a* or *Il17rc*, and found that these genes were not induced by this cytokine (**Figure 3.11**).

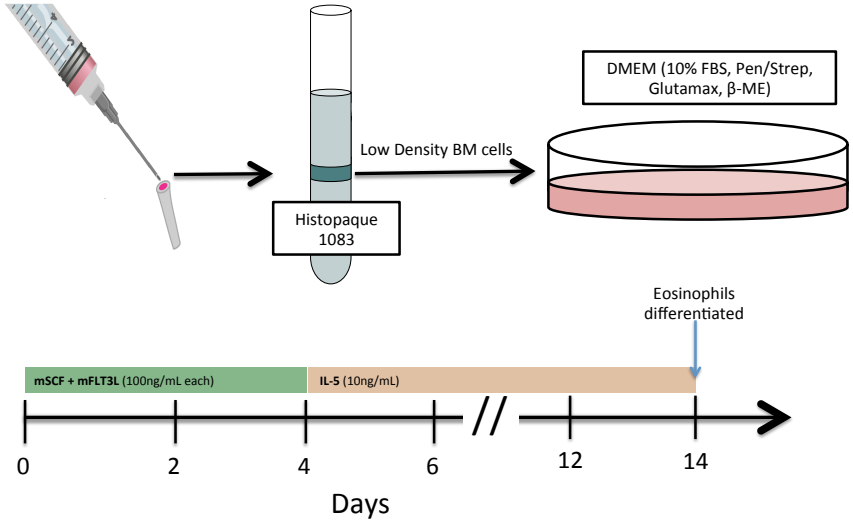

Figure 3.11: Generation of bone marrow-derived eosinophils. BM-Eos were generated by culturing low-density bone marrow (LDBM) cells isolated from the interphase cells generated by a gradient between Histopaque 1083 and Hank's Balanced Salt Solution. LDBM cells were subsequently cultured in mSCF and mFLT3L for 4 days, then IL-5 for 10 days.

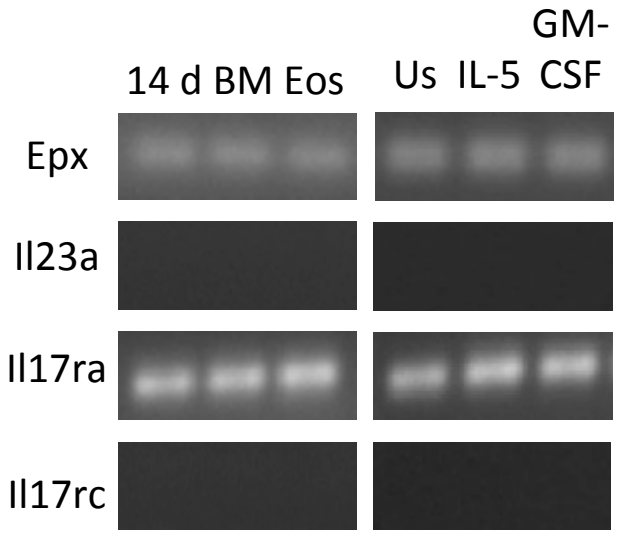

Figure 3.12: Bone marrow-derived eosinophils express *Il17ra*, but not *Il17rc* or *Il23a*. Transcription of eosinophil peroxidase (*Epx*), *Il23a*, *Il17ra* and *Il17rc* was assessed by qPCR from freshly differentiated (14 d) BM-Eos (lanes 1-3 of left panel), as well as BM-Eos left unstimulated (Us; lane 1), or treated with IL-5 (lane 2) or GM-CSF (lane 3) for 18 h (right panel).

Discussion

Since the discovery of T_H17 cells, many other cell types have been recognized to produce IL-17, including: epithelial cells, other lymphocytes (i.e., T_c17, γδ-T cells, iNKT-17 and ILC3s), and myeloid cells (i.e., neutrophils, monocytes, macrophages and eosinophils), (27,54,77-82). IL-23 production, however, is generally thought to be confined to macrophages and dendritic cells (29,43,93). To my knowledge, this is the first report showing that eosinophils are involved in IL-23 production (**Figure 3.1**).

A literature search yielded two other publications describing evidence for eosinophil-derived IL-17. The most recent of which used a reporter IL-17A-EGFP mouse line to show that eosinophils (Siglec-F^+ $CD11b^+$) recruited to the peritoneum produce IL-17 in response to ip LPS injections (82). In our hands, LPS alone does not induce IL-17 production from BM-Eos, even though IL-23 was elicited from bone marrow-derived dendritic cells treated in the same manner within the same experiment (data not shown). In humans, Molet et al. (81) demonstrated that eosinophils from asthmatic patients stained with anti-sense IL-17 cRNA via *in situ* hybridization (81). In our murine models of allergic asthma, eosinophils produced both IL-23p19 and IL-17AF (**Figure 3.8**). Our finding that eosinophils make up a higher proportion of IL-17AF-producing cells in allergic asthma (73.2-% [AF cpe] 65.2% [OVA]) than in acute aspergillosis (14.2%) indicates that eosinophil-derived IL-17 could play a larger role in asthma pathogenesis than in acute aspergillosis.

Research has revealed some overlap in attempting to dissect the role of eosinophils

and IL-17 in asthma pathogenesis. Several asthma mouse models show that absence of eosinophils correlates with decreased AHR, decreased mucus production, and reduced numbers of lung neutrophils (39), findings that were replicated in mouse models that lack IL-17 signaling (94,95). Another example of overlap in roles are the findings that IL-17 signaling and eosinophil co-culture with epithelial cells have separately been shown to up-regulate Mucin 5AC (MUC5AC), a mucin protein produced by bronchial airway goblet cells (95-97).

Given that eosinophils stain with mAbs against IL-17A and IL-17AF (**Figures 3.1, 3.7**), it is unclear whether they are the source of IL-17AA in addition to IL-17AF, as it is unknown whether the mAb clone recognizing the IL-17A subunit also recognizes the heterodimeric cytokine. In ΔdblGATA-1 mice, the BALF of infected animals showed decreased levels of IL-17AA, while IL-17FF levels remained the same (**Figure 3.5**). Although this finding indicates that eosinophils might produce IL-17AA but not IL-17FF, it is also possible that these specific IL-17 dimers are differentially regulated by IL-23, as its levels were significantly diminished in the absence of eosinophils (**Figure 3.3**). In other myeloid cells of ΔdblGATA-1 mice, no decrease in ΔMFI for IL-17AF was detected (**Figure 3.7B**), suggesting that IL-23 does not drive IL-17AF production from these cells. Whether IL-23 is necessary for eosinophil-derived IL-17 is still to be determined.

To assess whether IL-23 provides an autocrine signal that induces eosinophil production of IL-17, an *in vitro* system was established using BM-Eos. Several candidate

stimulants of IL-23 and IL-17 production failed to induce production of these cytokines (data not shown). I found that BM-Eos do not produce IL-23 or IL-17 during *ex vivo* development, or express their cognate receptors *Il23a* or *Il17rc* (**Figure 3.12**). While *Il17ra* mRNA was detected in freshly differentiated BM-Eos, this subunit can also dimerize with IL-17RB and bind IL-17E (IL-25) (44). Concordantly, IL-17RA/RB has previously been found to be expressed by human eosinophils (98). In mice, IL-17E up-regulates IL-5 production from ILC2s, thus inducing eosinophil recruitment (34). However, the direct effect of IL-17E on eosinophils is still unknown. Given that *A. fumigatus* has been reported to induce IL-17E from epithelial cells (34), BM-Eos were treated with varying concentrations of IL-17E, but those attempts failed to induce IL-23 or IL-17 (data not shown).

The discovery that eosinophils play a role in the innate response to acute aspergillosis as producers of IL-23 and IL-17 raises several questions. It has only recently become clear that the IL-23/IL-17 axis plays a significant role in fungal infections (63), as well as in driving asthma pathogenesis (90). The novel findings described in this chapter link asthma, eosinophilia, the IL-23/IL-17 axis, and fungal infections. These connections may lead to an updated model of fungal infection resolution and asthma pathogenesis, as well as indicate new potential therapeutic targets for both diseases.

Preface to Chapter IV

Evelyn Guerra performed experiments.

Evelyn Guerra and Stuart Levitz designed the experiments.

CHAPTER IV: Effects of Eosinopenia in Acute Aspergillosis

Abstract

Prolonged granulocytopenia is among the most well established risk factors for invasive aspergillosis. However, the contribution of granulocytes other than neutrophils in preventing invasive aspergillosis has been largely ignored. The findings described herein demonstrate that eosinophils associate with and kill *A. fumigatus* conidia *in vivo*, in addition to inducing the recruitment of inflammatory monocytes and expansion of macrophages in the lungs. Finally, I show that eosinopenic mice are more susceptible to acute infection with *A. fumigatus* conidia than wild-type mice.

Introduction

Best known for their role in allergic diseases and helminth infections, eosinophils play significant roles against several different pathogens in addition to the resolution of inflammation, tissue repair, and maintaining mucosal integrity (37). They are well equipped for such a diverse array of functions as they are deployed with granules containing pre-formed cytokines, chemokines, and antimicrobial/cytotoxic proteins. Additionally, eosinophils maintain sensitivity to a wide variety of environmental stimuli, expressing receptors for cytokines, chemokines, lipid mediators, danger associated molecular patterns, as well as opsonized and non-opsonized pathogens (37,86,99).

In healthy individuals, eosinophils make up a small percentage of peripheral blood leukocytes; however, eosinophilia is a hallmark of several allergic diseases including ABPA (13). Very little is known about their involvement in acute aspergillosis. In fact, only recently have eosinophils been considered part of the innate immune response to acute aspergillosis (100). Lilly et al. (100) have shown that ΔdblGATA-1 mice infected with the ATCC 13073 strain of *A. fumigatus* conidia suffer from higher fungal burdens than WT mice. In addition, they have found that BM-Eos co-incubated with *A. fumigatus* conidia inhibits fungal growth and release several cytokines and chemokines, including: IL-1β, IL-4, IL-13, IL-9, CCL-2, CCL-4, and CCL-11 (100).

In this chapter, I assess the capacity of eosinophils to associate with and kill conidia *in vivo.* I also investigate their function as immunomodulators in acute aspergillosis by regulating the recruitment of inflammatory monocytes and the expansion

of macrophages in the lungs. Finally, I describe their ability to confer protection against mortality in acute aspergillosis.

Materials and Methods

Mice. Six- to eight-week old C57Bl/6, Balb/c and ΔdblGATA-1 mice were obtained either from Jackson Laboratories or bred in specific pathogen-free conditions at the University of Massachusetts. All mouse studies were performed in accordance with guidelines approved by the IACUC.

Aspergillus fumigatus culture and murine acute pulmonary aspergillosis model. Green fluorescent protein (GFP)- and red fluorescent protein (dsRed)-expressing *A. fumigatus* (AF293 strain) were kindly provided by Tobias Hohl. Each strain was grown and harvested as described in Chapter II. The CEA10 strain was a generous gift from Robert Cramer. They were grown in glucose minimum media (GMM: 10g Dextrose, 15g Agar, 0.52g KCl, 0.52g $MgSO_4 \bullet 7H_2O$, 1.52g KH_2PO_4, 1mL of trace elements [40mg $Na_2B_4O_7 \bullet 10H_2O$, 400mg $CuSO_4 \bullet 5H_2O$, 800mg $FeSO_4 \bullet 7H_2O$, 800mg $MnSO_4 \bullet 4H_2O$, 800mg $Na_2MoO_4 \bullet 2H_2O$, 8g $ZnSO_4 \bullet 7H_2O$ in 1L of distilled H_2O], pH 6.5 in 1L of distilled H_2O) (101). All chemicals for GMM were obtained from Sigma. Conidia were harvested in PBS containing 0.01% Tween-20 (Thermo-Fisher). Isoflurane-anesthetized mice were infected via the OT route with $5x10^7$ conidia suspended in 0.01% Tween-PBS.

Cytological staining. BALF was collected from C57Bl/6 mice infected with GFP-AF293 conidia as described in Chapter II. Cells pelleted from BALF were fixed for 15 minutes with 2% paraformaldehyde in PBS. After washing out fixative, cells were adhered to poly-L-Lysine coated slides (Sigma-Aldrich) by cytospin. Cells were dried on the slide,

and then stained with H&E as described in Chapter III. Slides were examined for eosinophils associating with GFP-expressing conidia using a Nikon Eclipse E400 microscope.

Creating Fluorescent Aspergillus Reporter (FLARE) conidia. FLARE conidia were created as described previously (102). Briefly, $5x10^8$ dsRed conidia (AF293) per mL were incubated with 0.5 mg/mL 6-((6-((Biotinoyl)Amino)Hexanoyl)amino)Hexanoic Acid, Sulfosuccinimidyl Ester, Sodium Salt (Biotin-XX, SSE) (ThermoFisher) in 50 mM carbonate buffer (Sigma), pH 8.3 at 4^{o}C for 2 h in a tube rotator. Excess Biotin-XX, SSE was washed off with 0.1 M Tris-HCl pH 8.0 (Sigma), then conidia were incubated with 0.02 mg/mL Streptavidin, Alexa Fluor® 633 (Life Technologies) away from light at room temperature for 30 minutes. Labeling was confirmed by flow cytometry prior to infecting animals.

Staining for flow cytometry. Lungs from infected mice were collected and dissociated using a MACS® lung dissociation kit as described by the manufacturer. Single-cell suspensions were enriched for leukocytes using a Percoll™ (GE Healthcare) gradient (52). Interphase cells were collected, counted with the aid of a hemocytometer, and co-incubated with rat anti-mouse CD16/CD32 monoclonal antibody (mAb) 2.4G2 (BD Pharmingen) to block F_c receptors in accordance with the manufacturer's directions. Surface antigens were then stained with antibodies listed in **Table 4.1** and with Fixable Viability Dye eFluor® 780 (eBioscience) for 30 minutes at 4^{o}C. After two successive

wash steps, lung leukocytes were fixed in 2% paraformaldehyde (Electron Microscopy Sciences) PBS solution for 15 minutes at 4°C, and re-suspended in FC buffer after two washes. For *ex vivo* ICS, interphase cells collected from a Percoll™ gradient were incubated with Roswell Park Memorial Institute medium (RPMI; Life Technologies) supplemented with 100 U/mL streptomycin, 100 U/mL penicillin, 10% FBS (Tissue Culture Biologicals) and 1 μM monensin (Sigma) in a tissue culture incubator (37°C, 5% CO_2) for 5 h prior to surface staining. After overnight fixation, cells were permeabilized with Perm/Wash Buffer (BD Pharmingen) according to manufacturer instructions and then stained with rat anti-mouse IL-17AF-eFluor 660 mAb B8KN8R (Biolegend) or rat anti-mouse IL-23p19-eFluor 660 mAb fc23cpg (eBioscience). FC data were acquired with a BD LSR II cytometer and analyzed using FlowJo X software (Tree Star Inc.). Gating was established using FMO controls containing isotype control mAb conjugated with the fluorophore corresponding to the missing antibody. Lung myeloid populations were gated as described in **Figure 3.6**. Surface markers identifying each population are reviewed in **Table 4.2**. Number of each lung myeloid cell type was calculated by multiplying the proportion of each cell type by the number of live cells.

Table 4.1: Antibodies used in flow cytometry.

mAb	***Clone***	***Manufacturer***	***Isotype***
Ly6G-PE-Cy7/PE-CF594	1A8	Biolegend/BD	Rat IgG2a
CCR-2-FITC	475301	R&D Systems	Rat IgG2b
CD11c-BV™ 570	N418	Biolegend	Armenian Hamster IgG
Siglec-F-BV™ 421	E50-2440	BD Biosciences	Rat IgG2a
CD11b-BUV™ 395	M1/70	BD Biosciences	Rat IgG2b
F4/80-APC-Cy7	BM8	Biolegend	Rat IgG2a
CD45-PerCP-Cy5.5	30-F11	BD Biosciences	Rat IgG2b

Table 4.2: Surface markers identifying different myeloid cell populations.

Marker	***Eosinophils***	***Neutrophils***	***Inflammatory Monocytes***	***Lung Macrophages***
Ly6G	+	++	+	-
CCR-2	-	-	+	-
CD11c	-	-	-	+
Siglec-F	+	-	-	+
CD11b	+	+	+	+/-

Cytokine quantification in BALF after infection. BALF from Balb/c and ΔdblGATA-1 mice infected with CEA10 conidia was collected after euthanasia at 60 h post-infection. Ready-SET-Go! ELISA sets (eBioscience) were used to quantify IL-17AA, IL-1AF, IL-17FF and CCL-2. CXCL-5 was quantified using R&D Quantikine kit. CXCL-1 and CXCL-2 were measured using a custom Bio-Plex® Multiplex System (Bio-Rad).

Statistical analysis. Statistical tests were performed using Graph Pad Prism 6. T-tests were used to compare the means of two groups. In data sets where the mean of more than two groups was compared, I used 2-way ANOVAs. In comparing Kaplan-Meyer curves, the Mantel-Cox test was used.

Results

Eosinophils associate with and kill A. fumigatus. In conjunction with being recruited to the lungs early in acute aspergillosis (see Chapter III), eosinophils have the capacity to associate with and kill conidia. Association is used here to describe binding with or without phagocytosis. An eosinophil associating with a GFP-expressing conidium is shown in the micrograph in **Figure 4.1**. Here, cells were prepared from BALF of C57Bl/6 mice within the first day of infection. In addition to identifying neutrophils and mononuclear cells in these H&E stained samples, several cells had characteristic eosinophil morphology having taken up eosin within their cytoplasms and displaying polymorphous nuclei (86).

The Fluorescent Aspergillus Reporter (FLARE) assay developed by Hohl et al. (102) was used to quantitatively assess the ability of eosinophils to associate with and kill *A. fumigatus* conidia *in vivo*. This assay exploits the instability of fluorescent proteins (i.e., dsRed) in denaturing environments such as phagolysosomes to assess the viability of conidia associated with a leukocyte of interest. Alexa Fluor® 633 was then used to identify dead conidia (102) (**Figure 4.2**).

The ability of eosinophils to associate with and kill conidia in the lungs of infected Balb/c mice was assessed on days one and three post-infection by using FLARE. Over this time period there was an increase in the number of eosinophils (Siglec-F^+ $CD11c^-$), even though the proportion of total leukocytes in the lungs remained the same (**Figure 4.3A, B**). Association was calculated by adding the proportion of cells associated with live conidia (Gate R1) to the proportion of cells associated with dead conidia (Gate R2).

The majority of eosinophils did not associate with conidia, and the small proportion that did remained constant from day one to day three post-infection (**Figure 4.3C, D**). However, over the same time period, the proportion of eosinophils associated with dead conidia increased, suggesting an increase in conidial killing by these cells (**Figure 4.3C, D**).

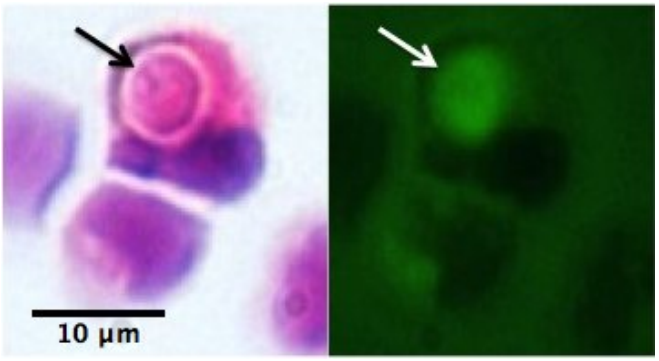

Figure 4.1: Eosinophils associate with *A. fumigatus* conidia. Photomicrograph of H&E preparation of BALF from C57Bl/6 mouse infected with $5x10^7$ GFP-expressing *A. fumigatus* conidia (AF293 strain). Left panel shows brightfield image of an eosinophil with conidium (black arrow), and right panel shows image from GFP channel, where the white arrow indicates a conidium.

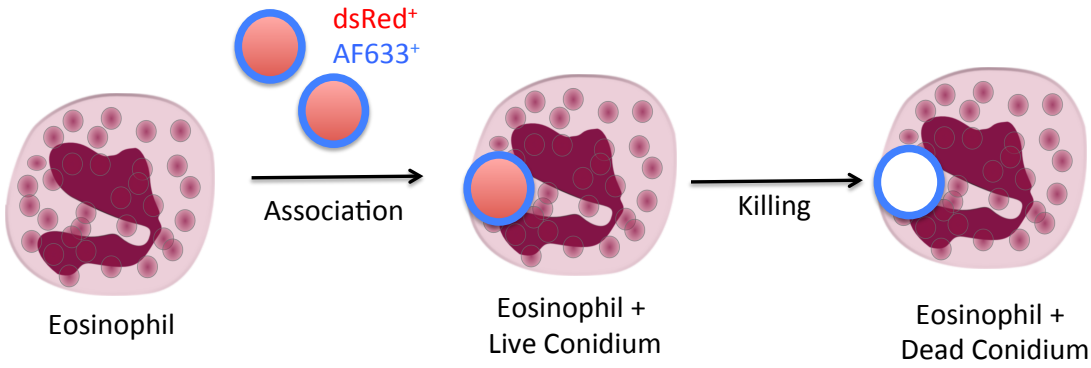

Figure 4.2: Assessing conidial killing *in vivo* using the FLARE method. *A. fumigatus* conidia (AF293 strain) expressing dsRed were labeled with Alexa Fluor 633. Leukocytes associated with live conidia can be identified as being part of a $dsRed^{+}$ $AF633^{+}$ population. Dead conidia will lose dsRed signal as the protein denatures, presumably within the acidic environment of a phagolysososme. This strategy allows cells associated with dead conidia to be identified as a $dsRed^{-}$ $AF633^{+}$ population. Schematic adapted from Jhingran et al. (102).

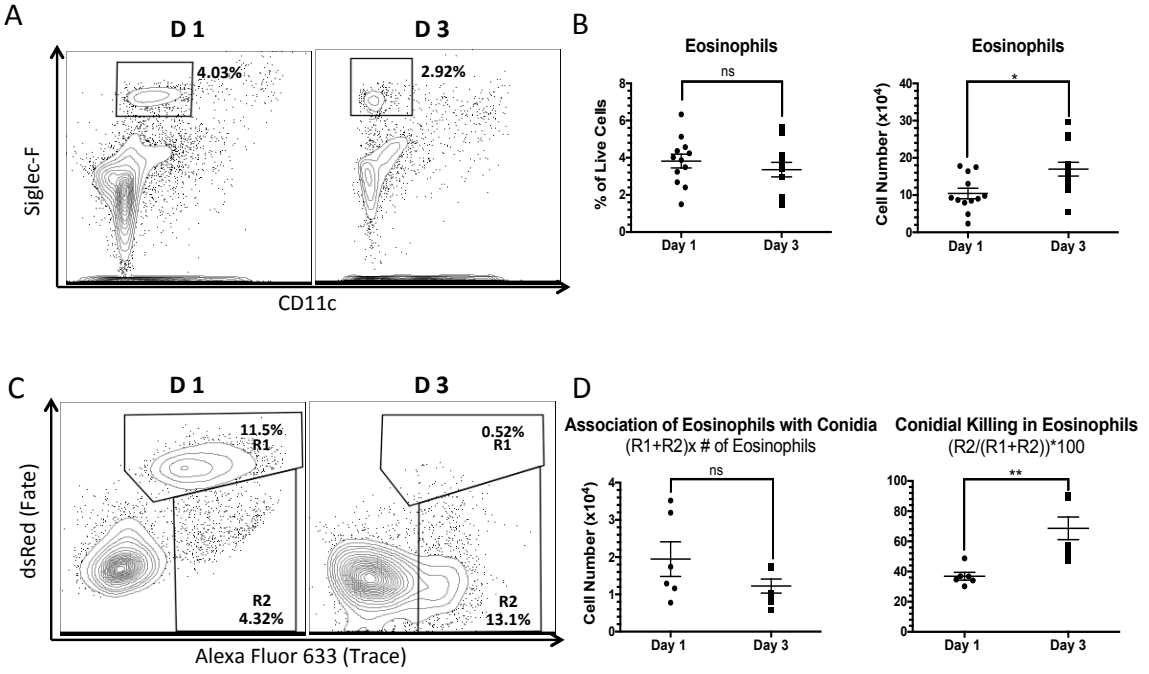

Figure 4.3: Eosinophils associate with and kill *A. fumigatus* conidia. (**A,C**) Balb/c mice were infected with $5x10^7$ FLARE conidia, as described in **Figure 4.2**. One and three days post-infection, lung single cell suspensions were assessed for eosinophils (Siglec-F^+ $CD11c^-$), and their capacity to associate and kill conidia. (**B**) Proportion of eosinophils to total live lung cells at day 1 (•) and day 3 (■) post-infection was not significantly different. However, due to an increase in cell number at day three, the calculated number of eosinophils was found to increase over time. (**D**) The number of eosinophils associated with conidia was not different between day one and day three, which was calculated by multiplying the sum of proportions of events in gates R1 and R2 by the number of eosinophils. An increase in conidial killing was observed from day one (36.9%) to day three (68.6%) post-infection. Percent conidial killing was calculated by the quotient of events in gate R2 and the sum of R1 and R2 multiplied by 100. Data were statistically analyzed using t-tests, * = $p < 0.05$, ** = $p < 0.01$, *ns* = $p > 0.05$.

Eosinophils enhance inflammatory monocyte recruitment and lung macrophage population expansion. As discussed in Chapter II, one of the major effects of the IL-23/IL-17 axis is the induction of factors that enhance granulopoiesis, neutrophil chemotaxis and activation (54). Given that neutrophil function is an important factor in combating *A. fumigatus* (25), the potential that eosinopenia affected lung neutrophilia after infection was investigated. First, I assessed the number of leukocytes ($CD45^+$ cells) three days after infection with $5x10^7$ *A. fumigatus* conidia in the lungs of Balb/c and ΔdblGATA-1 mice. I found that BALB/c mice had approximately $2x10^6$ more $CD45^+$ cells than ΔdblGATA-1 mice (**Figure 4.4A**). This difference could not be accounted for the lack of eosinophils in ΔdblGATA-1 mice, as their numbers averaged $1.7x10^5 \pm 0.2x10^5$ in Balb/c mice at the same time point.

To determine if the decreased abundance of $CD45^+$ cells in ΔdblGATA-1 was due to diminished neutrophil recruitment to the lungs, at 60 h post-infection the levels of neutrophil chemokines regulated by IL-17 was assessed, specifically CXCL-1, -2, and -5 (**Figure 4.4B**). No significant differences were detected for these chemokines in the absence of eosinophils. Finally, the number of neutrophils (Siglec-F^- $CD11b^+$ CCR-2^- $Ly6G^{Hi}$ $CD11c^-$) one and three days post-infection was quantified in Balb/c and ΔdblGATA-1 mice (**Figure 4.4C**). No differences were detected between groups; however, the number of inflammatory monocytes (Siglec-F^- $CD11b^+$ CCR-2^+) and lung macrophages (Siglec-F^+ $CD11c^+$) increased from day one to day three in Balb/c mice but not in ΔdblGATA-1 mice (**Figure 4.5A, B**). In fact, at day three post-infection, ΔdblGATA-1 mice had fewer numbers of inflammatory monocytes and macrophages in

the lungs. These data suggest that lack of eosinophils disrupts inflammatory monocyte recruitment, which then hampers lung macrophage expansion, as inflammatory monocytes can differentiate into macrophages (89).

One chemokine involved in inflammatory monocyte recruitment is CCL-2, which is one out of four ligands that bind CCR-2 (103). CCL-2 has been shown to be produced by eosinophils after stimulation with *A. fumigatus* conidia (100) and to be up-regulated by IL-17 in other inflammatory contexts (46,48,53,104,105). To test whether decreased levels of CCL-2 cause the decreased numbers of inflammatory monocytes in the lungs three days post-infection, levels of CCL-2 in BALF samples were assessed in Balb/c and ΔdblGATA-1 mice 60 h post-infection with $5x10^7$ conidia (**Figure 4.5C**). No differences in the levels of this specific CCR-2 ligand were detected, suggesting that in eosinopenic mice, inflammatory monocyte recruitment is regulated through alternative means.

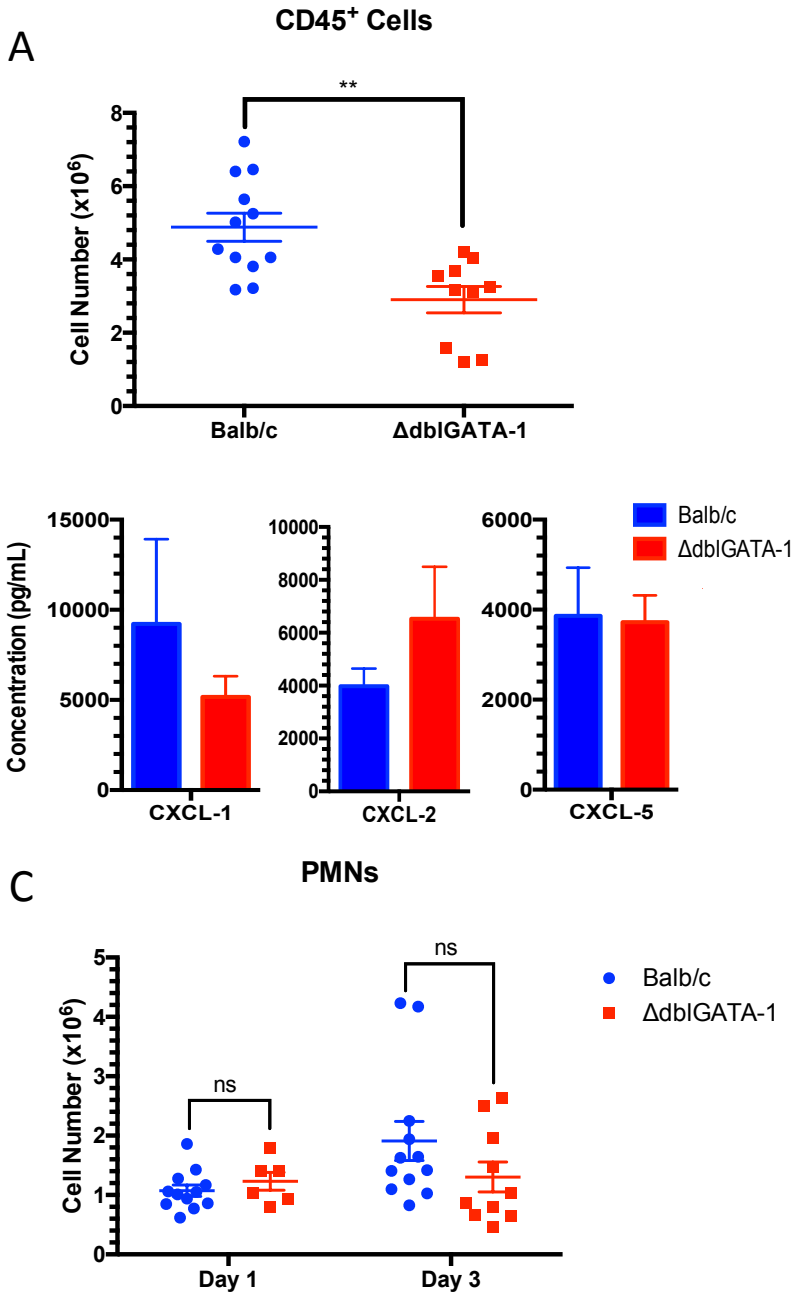

Figure 4.4: Lack of eosinophils does not affect neutrophil chemokine levels or neutrophil numbers in the lungs. (**A**) Lack of eosinophils correlates with lower levels of $CD45^+$ in the lungs three days after infection with $5x10^7$ conidia. Data were statistically analyzed using t-tests, ** = $p < 0.001$. (**B**) CXCR-2 ligand levels are not significantly different in eosinopenic mice compared to WT mice 60 h after challenge. (**C**) From day one to day three post-infection, neutrophil numbers in the lungs do not significantly differ, and the lack of eosinophils do not affect neutrophil recruitment. Data were statistically analyzed by 2-way ANOVA, *ns* = $p > 0.05$.

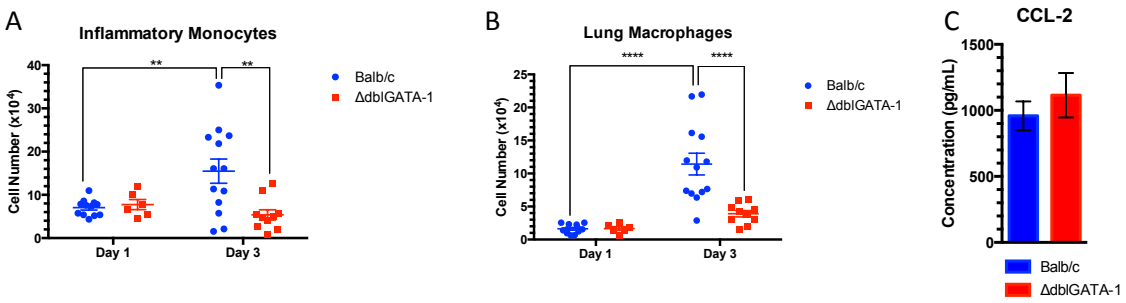

Figure 4.5: Eosinopenic mice show decreased recruitment of inflammatory monocytes to the lungs and reduced expansion of lung macrophages following challenge with *A. fumigatus.* (**A,B**) Lung single-cell suspensions from Balb/c (•) and ΔdblGATA-1 (eosinopenic; ■) mice infected with $5x10^7$ AF293 conidia were made one and three days post-infection and assessed for phagocytes. Inflammatory monocyte and lung macrophage numbers failed to increase in the absence of eosinophils. Data were statistically compared by 2-way ANOVA and post-hoc comparisons between groups were performed using Tukey's multiple comparison test. (**C**) Levels of inflammatory monocyte chemokine CCL-2 in BALF of infected Balb/c and ΔdblGATA-1 60 h post-infection.

Eosinopenia renders mice more susceptible to acute aspergillosis. Infecting Balb/c and ΔdblGATA-1 mice with $5x10^7$ *A. fumigatus* conidia from the AF293 strain rendered no casualties (**Figure 4.6A**). However, after infection with the same inoculum of the CEA10 strain, which has been shown to be a more virulent strain in other mouse models of acute aspergillosis (106-110), ΔdblGATA-1 succumbed to infection at higher rates than Balb/c mice (**Figure 4.6B**).

The increase in mortality observed with the CEA10 strain in ΔdblGATA-1 mice prompted the question of whether eosinophils also produce IL-23 and IL-17 in response to this specific strain. Unfortunately, as mice were more ill after infection with this strain, treatment with monensin precipitated their death before the six-hour incubation ended. Therefore, instead of performing *in vivo* intracellular cytokine staining after infection, I incubated leukocytes with monensin *ex vivo* for cytokine staining. Myeloid cells showed the same pattern of staining with mAbs against IL-23p19 and IL-17AF. Eosinophils were the only cells positive for both cytokines, while inflammatory monocytes, macrophages and neutrophils were positive for IL-17AF (**Figure 4.7**).

Although eosinophils produce IL-23 and IL-17AF in response to infection with CEA10 conidia, when assessing for IL-17AF levels in the BALF of Balb/c and ΔdblGATA-1 mice, eosinopenic mice showed increased production of both this dimer and IL-17FF (**Figure 4.8**). Interestingly, levels of two CXCR-2 ligands, namely CXCL-1 and CXCL-2, were decreased in ΔdblGATA-1 mice compared to Balb/c mice. However, CXCL-5 levels remained unchanged between the two groups (**Figure 4.9**).

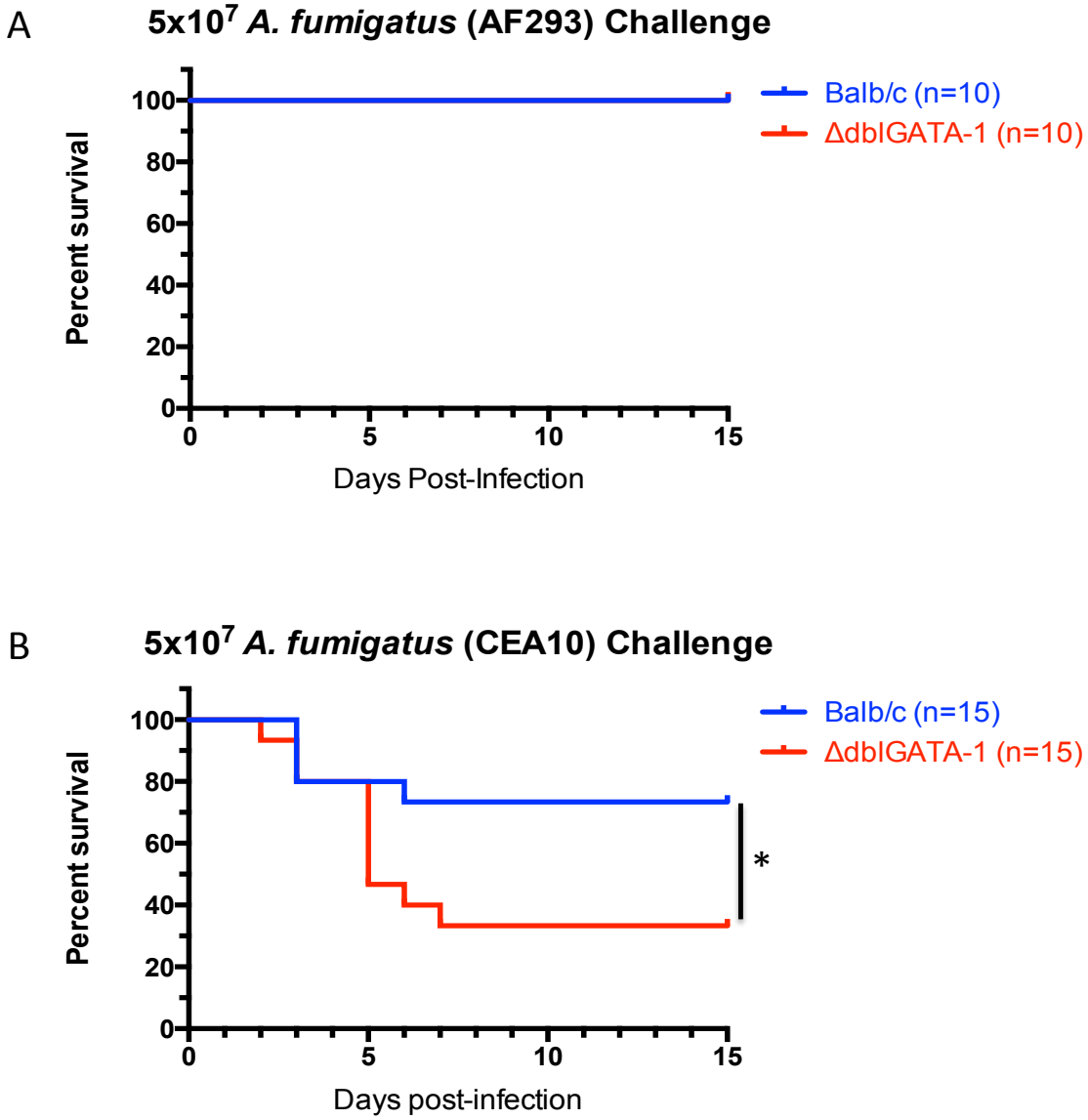

Figure 4.6: Eosinophils play a protective role against mortality in acute infection with the CEA10 strain of *A. fumigatus* but not with the AF293 strain. (**A**) Mortality study of Balb/c (**blue**) and ΔdblGATA-1 (**red**) mice infected with $5x10^7$ AF293 conidia and (**B**) CEA10 conidia. Kaplan-Meyer curve shows combined data from two or three separate experiments. Data were statistically analyzed using the Mantel-Cox test, *=$p<0.05$.

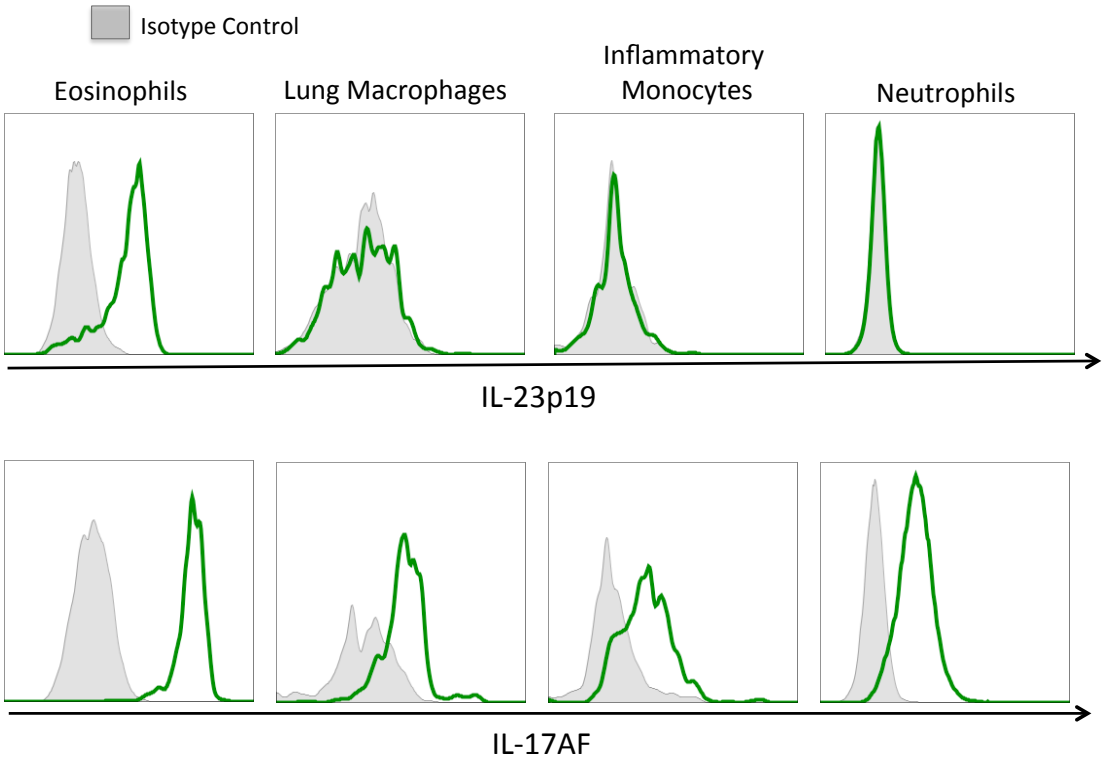

Figure 4.7: Eosinophils co-produce IL-23 and IL-17AF in response to the CEA10 strain of *A. fumigatus* conidia. In C57Bl/6 mice infected with $5x10^7$ CEA10 conidia, eosinophils also co-produce IL-23 and IL-17AF, while macrophages, inflammatory monocytes and neutrophils contributed to IL-17AF production.

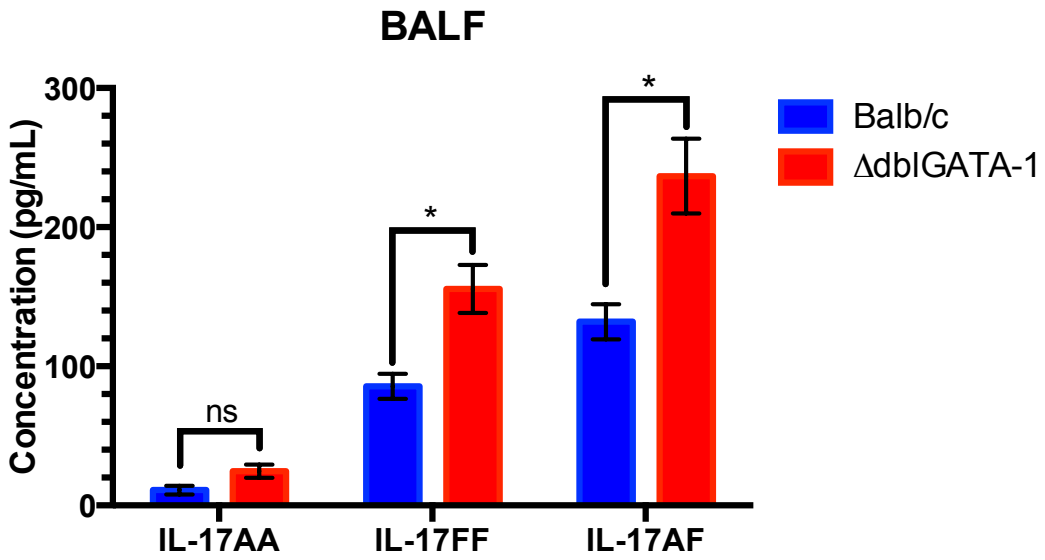

Figure 4.8: Lack of eosinophils is correlated with increased levels of IL-17FF and IL-17AF after infection with CEA10 strain of *A. fumigatus*. Increased levels of IL-17FF and IL-17AF were observed in eosinopenic mice (**red**) infected with $5x10^7$ *A. fumigatus* conidia (CEA10 strain), when compared to Balb/c (**blue**). Data were statistically analyzed using t-tests, * = $p<0.05$.

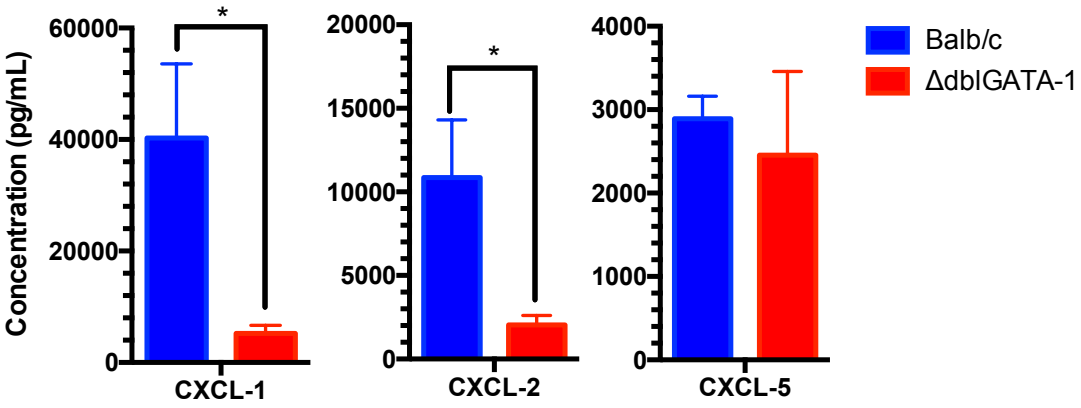

Figure 4.9: Eosinopenia correlates with decreased levels of CXCL-1 and CXCL-2 but not CXCL-5. Levels of neutrophil chemokines were assessed 60 h after challenge with the CEA10 strain of *A. fumigatus*. No statistically significant difference was observed in CXCL-5 production; however, eosinopenic mice (ΔdblGATA-1, **red**) showed lower levels of CXCL-1 and CXCL-2 compared to Balb/c (**blue**). Data were statistically analyzed using t-tests, * = $p<0.05$.

Discussion

Although only 17.5% of eosinophils were found to associate with conidia one day post-infection, and 7.8% on day three, nearly all (~96%) eosinophils were contained both IL-23p19 and IL-17AF 54 h post-infection (see Chapter III). This discrepancy suggests that direct association with *A. fumigatus* is not necessary for the production of these cytokines. In further support of this notion, co-incubation of BM-Eos with conidia or zymosan failed to elicit IL-23 or IL-17 production (see Chapter III). These findings indicate that the factor(s) eliciting IL-23 and IL-17 production by eosinophils may be host-derived. As discussed in Chapter III, several cytokines that induced IL-23 and IL-17 production from other cell-types were not capable of driving their production in BM-Eos.

Although ΔdblGATA-1 mice recruited neutrophils at the same level as Balb/c mice, the number of leukocytes ($CD45^+$ cells) that reach the lungs at day three post-infection with *A. fumigatus* was substantially decreased (**Figure 4.4A**). This was due, at least in part, to decreased recruitment of inflammatory monocytes and reduced expansion of macrophages in the lungs (**Figure 4.5A, B**). Inflammatory monocytes ($Ly6C^{Hi}$ $CCR\text{-}2^+$) are deployed from the bone marrow and recruited to sites of inflammation via several chemokines, some of which are up-regulated by IL-17 (89,111). For example, the CCR-2 ligands CCL-2, CCL-3 and CCL-7 are up-regulated by IL-17 in fibroblasts, macrophages, dendritic cells, and $CD4^+$ T cells (46,48,104,105). However, I detected no differences in CCL-2 production comparing Balb/c and ΔdblGATA-1 mice (**Figure 4.5C**). Levels of other CCR-2 ligands were not assayed. Interestingly, IL-17 itself has been previously observed to induce monocyte chemotaxis *in vitro* (112). Eosinophils may induce the

influx of inflammatory monocytes through the production of other cytokines or chemokines, as suggested by findings that BM-Eos produce CCL-4 after co-incubation with *A. fumigatus* conidia (100).

Once inflammatory monocytes arrive at the site of inflammation, they can differentiate into macrophages or dendritic cells (89). The failure of macrophages to expand in number as was observed in infected lungs by three days post-infection is most likely due to the reduced recruitment of inflammatory monocyte (**Figure 4.5A, B**). Espinosa et al. (113) have shown that inflammatory monocytes play a significant role in preventing mortality in invasive aspergillosis. They found that mortality rates were higher in the absence of CCR-2^{+} cells, a finding that was concomitant with increased hyphal growth and fungal invasion within lung parenchyma. The authors attributed the difference in mortality to enhanced neutrophil conidiocidal activity in the presence of inflammatory monocytes, and the ability of monocyte-derived dendritic cells (mo-DCs) to efficiently kill conidia (113).

Previously shown to be efficient killers *in vitro*, macrophages have recently been dismissed as essential phagocytes in response to *A. fumigatus in vivo*, in favor of neutrophils as superior killers (113,114). Mircescu et al. (115) showed that depletion of resident alveolar macrophages did not render mice susceptible to aspergillosis, while the administration of mAb against Gr-1 (RB6-8C5) does (115). Importantly, along with depleting neutrophils, the RB6-8C5 mAb depletes other myeloid cells including monocytes and eosinophils as it recognizes both Ly6G and Ly6C (**Table 3.3, Figure 3.6**)

(116). This confound was addressed by the authors by demonstrating that monocytes were also depleted in their experiments (115). Given these methodological constraints, the precise role of recruited macrophages in protecting mice from *A. fumigatus* remains unclear.

In addition to being efficient conidial killers, there is evidence that macrophages play an important role in clearing apoptotic neutrophils, thus preventing hyper-inflammation (117). In human monocyte cultures, IL-17 exposure for five days before treatment with IL-10 for an additional three days caused monocyte differentiation into alternatively activated macrophages, subtype C (M2c) (117). These cells expressed higher levels of Mer receptor tyrosine kinase (MerTK), a protein that recognizes apoptotic cells, and phagocytosed more early apoptotic neutrophils than classically activated macrophages (M1) or alternatively activated macrophages, subtype a (M2a) (117). Therefore, in addition to augmenting the expansion of macrophages in the lungs, eosinophils might also induce their differentiation into M2c by contributing to IL-17 levels in the lungs.

While the lack of eosinophils does not increase susceptibility to infection with AF293 conidia (**Figure 4.6A**), a more virulent conidial isolate (i.e., CEA10) (106) killed ΔdblGATA-1 mice at a higher rate than Balb/c mice (**Figure 4.6B**). Eosinopenic responses to infection differed when comparing CEA10 and AF293. Specifically, IL-17FF and IL-17AF levels were increased in the lungs of ΔdblGATA-1 mice infected with CEA10 (**Figure 4.8**), even though in WT mice, eosinophils produced IL-23p19 and IL-

17AF in response to this *A. fumigatus* strain (**Figure 4.7**). Additionally, IL-17 levels in eosinopenic mice had an inverse correlation with CXCL-1 and CXCL-2 levels in CEA10 infection (**Figure 4.9**). The levels of these same chemokines were unchanged when Balb/c and ΔdblGATA-1 mice infected with AF293 conidia were compared (**Figure 4.4B**). Taken together, these data highlight the versatility of eosinophil function and how these cells can differentially modulate the immune response to distinctive isolates of the same pathogen species.

CHAPTER V: Discussion

This dissertation explores how eosinophils drive incongruent fates in the host depending on the chronicity of antigen exposure. Our findings indicate that an acute exposure to *A. fumigatus* drives eosinophils to protect mice from succumbing to infection (**Figure 4.6B**). In contrast, after repeated exposure to sensitized antigens, eosinophil-derived IL-23 and IL-17 (**Figure 3.8**) may contribute to AHR, mucus hypersecretion, and lung neutrophilia, ultimately leading to obstructive airway disease (e.g., asthma, ABPA) (**Figure 5.1**) (118).

Re-thinking eosinophil function beyond the T_H1/T_H2 paradigm. Since their discovery, eosinophils have been largely associated with parasitic (i.e., helminth) infections and allergic inflammatory disorders such as asthma and atopic dermatitis (37,119). This is partly due to the fact that eosinophils are largely absent from the peripheral blood of healthy individuals, and their presence in this compartment becomes clinically relevant in disease states (37).

In studying eosinophil function in such disease processes, these granulocytes have been inextricably associated with T_H2 responses. For example, IL-5, a cytokine produced by T_H2 $CD4^+$ T cells, is directly involved in eosinophil differentiation and recruitment (37,120). Eosinophil recruitment is also regulated by other canonical T_H2 cytokines, such as IL-4 and IL-13, which activate STAT-6 to up-regulate eotaxin expression (37,120). Reciprocally, eosinophils initiate a T_H2 response by skewing dendritic cells with cytokines such as IL-4, acting as APCs themselves, recruiting effector T_H2 cells to the site of inflammation, and activating memory T_H2 cells (37,38).

Although less attention has been focused on the relationship between eosinophils and T_H1 responses, interferon (IFN)-γ ranks third in abundance of cytokines stored in the granules of circulating eosinophils (121). Pre-formed IL-12 and IL-10 are also stored within these granules, and have been shown to reciprocally induce each other's release. That is, treatment of circulating eosinophils with IL-12 induces IL-10 release and vice versa (121).

Eosinophils seem to defy categorization within the current classification of immune cells due to the diverse set of immune-modulating factors stored in their granules (**Figure 5.2**), and the assorted functions attributed to their release (reviewed in (120)). That eosinophils would deploy cytokines related to T_H17 development and function as described in Chapter III should therefore not be surprising. Nevertheless, to strengthen the evidence maintained in Chapter III, transcription of *Il17a*, *Il17f* and *Il23p19* should be assessed within eosinophils using a fluorescent reporter mouse line for each gene.

Future work should also determine the factors that elicit IL-23 and IL-17 production from eosinophils. An *in vitro* system for studying this phenomenon would be best suited for unraveling the molecular mechanisms associated with the production of each cytokine, as well as determining how their production might be related. As already discussed in Chapter III, some factors have already been tested using freshly differentiated BM-Eos, however, this method yielded no viable results.

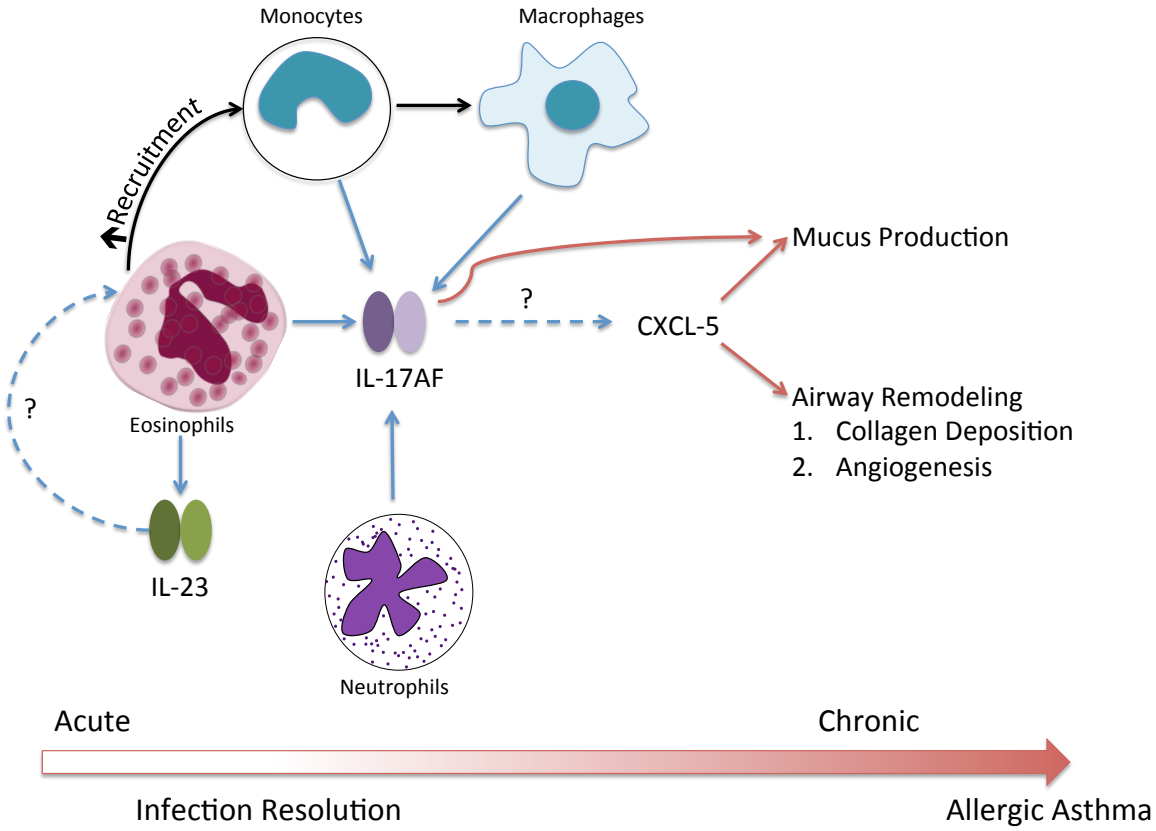

Figure 5.1: Eosinophils as drivers of the IL-23/IL-17 axis in acute aspergillosis and asthma. Eosinophils produce IL-23, which might act as an autocrine signal to induce IL-17AF production. Eosinophils also augment inflammatory monocyte recruitment and the expansion of macrophages. IL-17AF, which is produced by other myeloid, cells types including inflammatory monocytes, macrophages and neutrophils might be driving CXCL-5 expression. IL-17 and CXCL-5 have been previously shown to increase mucus production by the airway epithelia. Airway remodeling through increased collagen deposition and angiogenesis is also mediated by CXCR-2 ligands. If self-limited, this cascade of events might help in clearing *A. fumigatus* conidia from the airways, however, in the context of atopy, where these events become chronic, it might drive asthma pathogenesis.

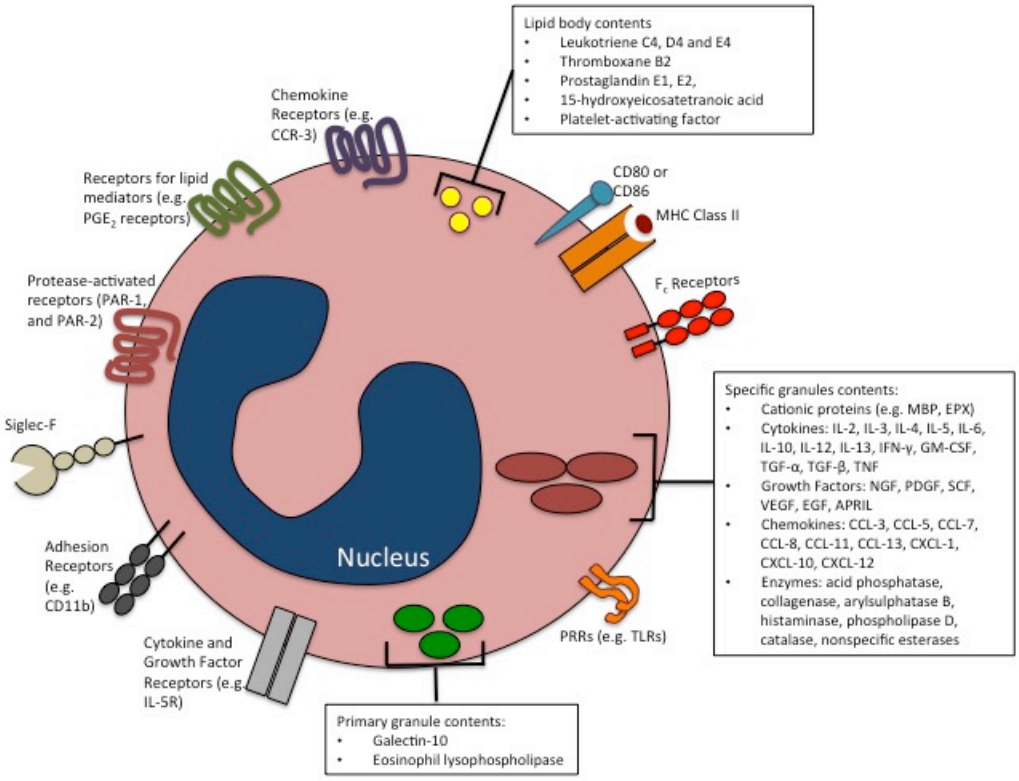

Figure 5.2: The eosinophil armamentarium. Eosinophils are equipped with a variety of immune mediators including cytokines, chemokines, enzymes, lipid signaling molecules, and growth factors as well as a diverse set of receptors that can activate release of distinctive pre-formed factors. Figure adapted from Rosenberg et al. (122). APRIL, a proliferation-inducing ligand; EGF, epidermal growth factor; EPX, eosinophil peroxidase; MBP, major basic protein; NGF, nerve growth factor; PDGF, platelet-derived growth factor; PRRs, pattern recognition receptors; SCF, stem cell factor; TLRs, toll-like receptors; VEGF, vascular endothelial growth factor.

Eosinophils and IL-17 in asthma. The convergence between IL-17 and eosinophils found in our models of allergic asthma point to a novel mechanism by which eosinophils contribute to the pathogenesis of asthma that may be independent of T_H2 cells and cytokines. If this phenotype holds up in humans, it could be of use in better stratifying asthma types, as heterogeneity in this disease has prevented the success of some targeted asthma therapies (95,119).

Although asthma is unified by a hallmark symptom of episodic shortness of breath accompanied by wheezing due to AHR, only recently has asthma been recognized to be driven by several different etiologies (35,95). These etiologies have severe consequences in therapeutic outcome, with as many as 10% of patients failing to respond to standard corticosteroid treatment (35,123). Stratification of asthma based on the predominant cellular infiltrate found in induced sputum has indicated four distinct types of asthma: eosinophilic, neutrophilic, mixed granulocytic and paucigranulocytic (124). It would be interesting to assess the presence of IL-23^+ IL-17^+ eosinophils in each of these types, as even in neutrophilic and paucigranulocytic asthma a small number of eosinophils are present (124).

To specifically assess the contribution of eosinophil-derived IL-23 and IL-17 in asthma pathogenesis, mixed bone marrow chimeras can be constructed where lethally irradiated mice are transplanted with a mixture of bone marrow cells from ΔdblGATA-1 and IL-23p$19^{-/-}$ or ΔdblGATA-1 and IL-$17A^{-/-}$ mice. Successful engraftment of bone marrow cells will produce mice that are either deficient in IL-17A- or IL-23p19-

producing eosinophils. After sensitization and challenge, parameters such as AHR, mucus hypersecretion and airway remodeling can be tested and compared with irradiated animals receiving ΔdblGATA-1 and WT bone marrow cells.

Eosinophils in pulmonary aspergillosis. In asthma, eosinophils act as drivers of inflammation and tissue remodeling (37,38,119), however, in our mouse model of acute aspergillosis, they protect against mortality (**Figure 5.1**). It is still unknown how eosinophils achieve this, nevertheless, I have found that eosinophils are able to kill *A. fumigatus* conidia (**Figure 4.3**), and modulate the types of myeloid cells that are recruited to the lungs after infection (**Figure 4.5**). Out of these two factors, the latter may play a bigger role in protecting mice from succumbing to infection. In fact, it has already been reported that depletion of inflammatory monocytes renders mice vulnerable to *A. fumigatus* infection (113). The defects in inflammatory monocyte recruitment and expansion of macrophages seen in the absence of eosinophils might decrease the phagocytic capacity of ΔdblGATA-1 mice (**Figure 4.5**), which may explain the increased mortality in this group. Alternatively activated type C macrophages (M2c) may also help attenuate hyperinflammation by clearing the lungs of apoptotic neutrophils as discussed in Chapter IV. Determining whether lower levels of $MerTK^{+}$ macrophages (M2c) are present in ΔdblGATA-1 mice would be a good start in addressing the latter hypothesis.

Disparate host responses to different strains of A. fumigatus. It is important to note that the experiments describing the decreased number of inflammatory monocytes and macrophages depicted in **Figure 4.5** were performed with the AF293 strain of *A. fumigatus.* Infection with this strain did not kill either Balb/c or ΔdblGATA-1 mice (**Figure 4.6A**). Only CEA10 infection rendered mice susceptible to infection (**Figure 4.6B**). This strain clearly elicits a different inflammatory response from ΔdblGATA-1 mice than the AF293 strain, at least when concerning IL-17FF, IL-17AF, CXCL-1 and CXCL-2 (**Figure 4.8-4.9**). Unlike the WT murine lungs, human peripheral blood mononuclear cells (PBMCs) produce more IL-17AA after co-incubation with CEA10 than AF293 conidia (106). Interestingly, AF293 elicited a cytokine profile from PBMCs that was similar to that seen in *A. nidulans,* a species that is less pathogenic than *A. fumigatus* (106).

As levels of CXCL-1 and CXCL-2 were decreased in ΔdblGATA-1 mice infected with the CEA10 strain raises the question of whether ΔdblGATA-1 mice suffer from low levels of neutrophils after infection (**Figure 4.9**), something that is not seen in AF293 infection (**Figure 4.4**). If so, it would explain the discrepancy in mortality caused by the two strains of *A. fumigatus,* as neutropenia is a known risk factor in invasive aspergillosis (10). However, in C57Bl/6 mice, Rizzetto et al. (106) have shown that pulmonary infection with $2x10^7$ CEA10 conidia was highly lethal, even though as many as 91% of BALF cells were identified as neutrophils. In comparison, infection with the same inoculum of AF293 conidia yielded 100% survival and lower proportions of neutrophils in BALF (34%) (106). Therefore, it may be that while too little of a neutrophilic response

renders mice susceptible to invasive aspergillosis, a zealous one might also be detrimental. It remains to be established how Balb/c and ΔdblGATA-1 mice respond to the CEA10 strain in terms of a neutrophil response.

It is unknown what makes the CEA10 strain so much more lethal than the AF293 strain in mice. Both strains were isolated from patients who suffered from invasive aspergillosis, and about 98% of their genomes align with high confidence (125). The 2% difference in the genomes of CEA10 and AF293 may be a factor that accounts for the difference in virulence. The CEA10 genome is 1.4% larger than that of AF293, and harbors 218 unique genes (125). Some of these genes are involved in cell envelope biogenesis, which may translate into differences in cell wall composition between the two strains (126). As such, CEA10 conidia may be recognized by different PRRs than those used to recognize the AF293 conidia (41), which may account for the discrepancies in the composition of cellular infiltrates seen by Rizzetto et al. (106).

Differences in virulence between multiple strains of *A. fumigatus* is a well documented phenomenon (106,127). It is unknown what makes some *A. fumigatus* strains more virulent than others. Presumably the answer lies as much on a particular host's intrinsic factors as on isolate-specific traits (14). This is exemplified above in the discrepancy between the 100% mortality rate observed in C57Bl/6 mice infected with CEA10 by Rizzetto et al. (106), and the 27% mortality rate reported here in Balb/c mice infected with the same strain (**Figure 4.6B**). As well as the reported differential host response to other distinct *A. fumigatus* strains (106,127). Ultimately, *A. fumigatus'*

capacity to cause disease lies in the complex interaction between a host and the pathogen.

Conclusion. The involvement of eosinophils in the acute immune response to *A. fumigatus* reveals a novel aspect of this specific host-pathogen interaction. Deployment of IL-23 and IL-17 by eosinophils in this interaction bridges the primary and the allergic response to *A. fumigatus* in an unexpected way. Further investigation into this link may broaden the understanding of how sensitization in allergic asthma is achieved, particularly as I have shown that production of IL-23 and IL-17 by eosinophils in asthma is not confined to mold antigens. That is, the same phenomenon was observed in OVA sensitized and challenged mice (**Figure 3.8-3.10**). As eosinophils are found in secondary lymphoid organs and can act as APCs (37), their role in skewing the adaptive immune response by potentially promoting either a T_H2 or T_H17 response could bring light to the factors underlying the heterogeneous etiology of asthma.

BIBLIOGRAPHY

1. Krijgsheld P, Bleichrodt R, van Veluw GJ, Wang F, Müller WH, Dijksterhuis J, et al. Development in *Aspergillus*. Studies in Mycology. 2013 Mar;74:1–29.

2. Ao J, Hao Z, Zhu H, Wen L, Yang R. Environmental Investigations and Molecular Typing of *Aspergillus* in a Chinese Hospital. Mycopathologia. 2014 Jan 18;177(1-2):51–7.

3. Hao Z, Ao J, Hao F, Yang R, Zhu H, Zang J. Environment surveillance of filamentous fungi in two tertiary hospitals in China. Chinese Medical Journal. 2011 Jun 30;124:1970–5.

4. Bennett JW. An Overview of the Genus *Aspergillus*. In: Machida M, Gomi K, editors. Aspergillus: Molecular Biology and Genomics; 2010. pp. 1–19.

5. Latge JP. *Aspergillus fumigatus* and Aspergillosis. Clinical Microbiology Reviews. 1999 Apr 26;12:310–50.

6. Hedayati MT, Pasqualotto AC, Warn PA, Bowyer P, Denning DW. *Aspergillus flavus*: human pathogen, allergen and mycotoxin producer. Microbiology. 2007 Jun 1;153(6):1677–92.

7. Kwon-Chung KJ, Sugui JA. *Aspergillus fumigatus*—What Makes the Species a Ubiquitous Human Fungal Pathogen? Heitman J, editor. PLoS Pathog. 2013 Dec 5;9(12):e1003743.

8. Samson RA, Visagie CM, Houbraken J, Hong SB, Hubka V, Klaassen CHW, et al. Phylogeny, identification and nomenclature of the genus *Aspergillus*. Studies in Mycology. Elsevier Ltd; 2014 Jun 1;78(C):141–73.

9. Timberlake WE. Molecular Genetics of *Aspergillus* Development. Annual Review of Genetics. 1990 Jul 31;24:5–36.

10. Park SJ, Mehrad B. Innate Immunity to *Aspergillus* Species. Clinical Microbiology Reviews. 2009 Oct 12;22(4):535–51.

11. Klich MA. Identification of clinically relevant aspergilli. Med Myco. 2006 Jan;44(s1):127–31.

12. Pfaller MA, Diekema DJ. Epidemiology of Invasive Mycoses in North America. Critical Reviews in Microbiology. 2010 Feb;36(1):1–53.

13. Knutsen AP, Bush RK, Demain JG, Denning DW, Dixit A, Fairs A, et al. Fungi and allergic lower respiratory tract diseases. Journal of Allergy and Clinical

Immunology. Elsevier Ltd; 2012 Feb 1;129(2):280–91.

14. Casadevall A, Pirofski L-A. Host-Pathogen Interactions: The Attributes of Virulence. The Journal of Infectious Diseases. 2001 Jul 9;184:337–44.

15. Vinh DC. Insights into human antifungal immunity from primary immunodeficiencies. The Lancet Infectious Diseases. Elsevier Ltd; 2011 Sep 22;11(10):780–92.

16. Balloy V, Chignard M. The innate immune response to *Aspergillus fumigatus*. Microbes and Infection. Elsevier Masson SAS; 2009 Oct 1;11(12):919–27.

17. Holding KJ, Dworkin MS, Wan PCT, Hanson DL, Klevens RM, Jones JL, et al. Aspergillosis among People Infected with Human Immunodeficiency Virus: Incidence and Survival. Clinical Infectious Diseases. 2000 Nov 9;31:1253–7.

18. Ghosh S, Hoselton SA, Dorsam GP, Schuh JM. Eosinophils in fungus-associated allergic pulmonary disease. Frontiers in Pharmacology. 2013 Feb 25;4:1–18.

19. Denning DW. The link between fungi and severe asthma: a summary of the evidence. Eur Respir J. 2006 Mar 1;27(3):615–26.

20. Fairs A, Agbetile J, Hargadon B, Bourne M, Monteiro WR, Brightling CE, et al. IgE Sensitization to *Aspergillus fumigatus* Is Associated with Reduced Lung Function in Asthma. American Journal of Respiratory and Critical Care Medicine. 2010 Dec;182(11):1362–8.

21. Gibson PG, Wark PAB, Simpson JL, Meldrum C, Meldrum S, Saltos N, et al. Induced sputum IL-8 gene expression, neutrophil influx and MMP-9 in allergic bronchopulmonary aspergillosis. Eur Respir J. 2003 Apr 1;21(4):582–8.

22. Chapman RW, Phillips JE, Hipkin RW, Curran AK, Lundell D, Fine JS. CXCR2 antagonists for the treatment of pulmonary disease. Pharmacology & Therapeutics. Elsevier Inc; 2009 Jan 1;121(1):55–68.

23. Wilson RH, Whitehead GS, Nakano H, Free ME, Kolls JK, Cook DN. Allergic Sensitization through the Airway Primes Th17-dependent Neutrophilia and Airway Hyperresponsiveness. American Journal of Respiratory and Critical Care Medicine. 2009 Oct 15;180(8):720–30.

24. Schuh JM, Blease K, Hogaboam CM. CXCR2 Is Necessary for the Development and Persistence of Chronic Fungal Asthma in Mice. The Journal of Immunology. 2002 Feb 1;168(3):1447–56.

25. Mehrad B, Strieter RM, Moore TA, Tsai WC, Lira SA, Standiford TJ. CXC

Chemokine Receptor-2 Ligands Are Necessary Components of Neutrophil-Mediated Host Defense in Invasive Pulmonary Aspergillosis. The Journal of Immunology. 1999 Nov 9;163:6086–94.

26. Zenobia C, Hajishengallis G. Basic biology and role of interleukin-17 in immunity and in. Periondotology 2000. 2015 Jul 20;69:142–59.

27. Iwakura Y, Ishigame H, Saijo S, Nakae S. Functional Specialization of Interleukin-17 Family Members. Immunity. Elsevier Inc; 2011 Feb 25;34(2):149–62.

28. Lambrecht BN, Hammad H. The immunology of asthma. Nature Immunology. 2014 Dec 18;16(1):45–56.

29. Iwakura Y. The IL-23/IL-17 axis in inflammation. J Clin Invest. 2006 May 1;116(5):1218–22.

30. Werner JL, Metz AE, Horn D, Schoeb TR, Hewitt MM, Schwiebert LM, et al. Requisite Role for the Dectin-1 -Glucan Receptor in Pulmonary Defense against *Aspergillus fumigatus*. The Journal of Immunology. 2009 Apr 15;182(8):4938–46.

31. Murdock BJ, Falkowski NR, Shreiner AB, Sadighi Akha AA, McDonald RA, White ES, et al. Interleukin-17 Drives Pulmonary Eosinophilia following Repeated Exposure to *Aspergillus fumigatus* Conidia. Infection and Immunity. 2012 Mar 16;80(4):1424–36.

32. Morita H, Arae K, Unno H, Toyama S, Motomura K, Matsuda A, et al. IL-25 and IL-33 Contribute to Development of Eosinophilic Airway Inflammation in Epicutaneously Antigen-Sensitized Mice. Ryffel B, editor. PLoS ONE. 2015 Jul 31;10(7):e0134226.

33. Mueller C, Keeler A, Braag S, Menz T, Tang Q, Flotte TR. Modulation of Exaggerated-IgE Allergic Responses by Gene Transfer-mediated Antagonism of IL-13 and IL-17e. Molecular Therapy. Nature Publishing Group; 2009 Nov 13;18(3):511–8.

34. Van Dyken SJ, Mohapatra A, Nussbaum JC, Molofsky AB, Thornton EE, Ziegler SF, et al. Chitin Activates Parallel Immune Modules that Direct Distinct Inflammatory Responses via Innate Lymphoid Type 2 and gd T Cells. Immunity. Elsevier Inc; 2014 Mar 20;40(3):414–24.

35. Skloot GS. Asthma phenotypes and endotypes. Current Opinion in Pulmonary Medicine. 2016 Jan;22(1):3–9.

36. Martin RA, Hodgkins SR, Dixon AE, Poynter ME. Aligning mouse models of asthma to human endotypes of disease. Respirology. 2014 May 9;19(6):823–33.

37. Travers J, Rothenberg ME. Eosinophils in mucosal immune responses. Mucosal Immunology. Nature Publishing Group; 2015 Mar 25;8(3):464–75.

38. Spencer LA, Weller PF. Eosinophils and Th2 immunity: contemporary insights. Immunol Cell Biol. 2010 Jan 12;88(3):250–6.

39. Jacobsen EA, Lee NA, Lee JJ. Re-defining the unique roles for eosinophils in allergic respiratory inflammation. Clin Exp Allergy. 2014 Aug 21;44(9):1119–36.

40. Lee JJ, Jacobsen EA, McGarry MP, Schleimer RP, Lee NA. Eosinophils in health and disease: the LIAR hypothesis. Clin Exp Allergy. 2010 Mar 11;40(4):563–75.

41. O'Dea EM, Amarsaikhan N, Li H, Downey J, Steele E, Van Dyken SJ, et al. Eosinophils Are Recruited in Response to Chitin Exposure and Enhance Th2-Mediated Immune Pathology in *Aspergillus fumigatus* Infection. Infection and Immunity. 2014 Jul 9;82(8):3199–205.

42. Baddley JW. Clinical risk factors for invasive aspergillosis. Med Myco. 2011 Apr;49(S1):S7–S12.

43. Korn T, Bettelli E, Oukka M, Kuchroo VK. IL-17 and Th17 Cells. Annu Rev Immunol. 2009 Apr;27(1):485–517.

44. Gaffen SL. Structure and signalling in the IL‐17 receptor family. Nat Rev Immunol. Nature Publishing Group; 2009 Jul 3;:1–13.

45. Witowski J, Ksiazek K, J rres A. Interleukin-17: a mediator of inflammatory responses. Cellular and Molecular Life Sciences (CMLS). 2004 Mar 1;61(5):567–79.

46. Jin W, Dong C. IL-17 cytokines in immunity and inflammation. Emerging Microbes and Infections. 2013;2:1–5.

47. Livak KJ, Schmittgen TD. Analysis of Relative Gene Expression Data Using Real-Time Quantitative PCR and the 2−ΔΔCT Method. Methods. 2001 Dec;25(4):402–8.

48. Ishigame H, Kakuta S, Nagai T, Kadoki M, Nambu A, Komiyama Y, et al. Differential Roles of Interleukin-17A and -17F in Host Defense against Mucoepithelial Bacterial Infection and Allergic Responses. Immunity. Elsevier

Inc; 2009 Jan 16;30(1):108–19.

49. Terashima A, Watarai H, Inoue S, Sekine E, Nakagawa R, Hase K, et al. A novel subset of mouse NKT cells bearing the IL-17 receptor B responds to IL-25 and contributes to airway hyperreactivity. Journal of Experimental Medicine. 2008 Nov 3;205(12):2727–33.

50. Wu Q, Martin RJ, Rino JG, Breed R, Torres RM, Chu HW. IL-23-dependent IL-17 production is essential in neutrophil recruitment and activity in mouse lung defense against respiratory *Mycoplasma* pneumoniae infection. Microbes and Infection. 2007 Jan;9(1):78–86.

51. Hufford MM, Kim TS, Sun J, Braciale TJ. Antiviral CD8+ T cell effector activities in situ are regulated by target cell type. Journal of Experimental Medicine. 2011 Jan 17;208(1):167–80.

52. Wiesner DL, Specht CA, Lee CK, Smith KD, Mukaremera L, Lee ST, et al. Chitin Recognition via Chitotriosidase Promotes Pathologic Type-2 Helper T Cell Responses to Cryptococcal Infection. Sil A, editor. PLoS Pathog. 2015 Mar 12;11(3):e1004701.

53. Onishi RM, Gaffen SL. Interleukin-17 and its target genes: mechanisms of interleukin-17 function in disease. Immunology. 2010 Mar;129(3):311–21.

54. Cua DJ, Tato CM. Innate IL-17-producing cells: the sentinels of the immune system. Nat Rev Immunol. Nature Publishing Group; 2010 Jun 18;:1–12.

55. Lamoreaux L, Roederer M, Koup R. Intracellular cytokine optimization and standard operating procedure. Nat Protoc. 2006 Nov;1(3):1507–16.

56. Yang XO, Chang SH, Park H, Nurieva R, Shah B, Acero L, et al. Regulation of inflammatory responses by IL-17F. Journal of Experimental Medicine. 2008 May 12;205(5):1063–75.

57. Adamik J, Henkel M, Ray A, Auron PE, Duerr R, Barrie A. The IL17A and IL17F loci have divergent histone modifications and are differentially regulated by prostaglandin E2 in Th17 cells. Cytokine. Elsevier Ltd; 2013 Oct 1;64(1):404–12.

58. Brieland JK, Jackson C, Menzel F, Loebenberg D, Cacciapuoti A, Halpern J, et al. Cytokine Networking in Lungs of Immunocompetent Mice in Response to Inhaled *Aspergillus fumigatus*. Infection and Immunity. 2001 Mar 1;69(3):1554–60.

59. Lo H, Lai T, Li C, Wu W. TNF-α induces CXCL1 chemokine expression and

release in human vascular endothelial cells in vitro via two distinct signaling pathways. Nature Publishing Group. Nature Publishing Group; 2014 Feb 3;35(3):339–50.

60. Shieh J, Tsai Y, Tsou C, Wu W. CXCL1 Regulation in Human Pulmonary Epithelial Cells by Tumor Necrosis Factor. Cell Physiol Biochem. 2014;34(4):1373–84.

61. Xavier AM, Isowa N, Cai L, Dziak E, Opas M, McRitchie DI, et al. Tumor Necrosis Factor-alpha Mediates Lipopolysaccharide-Induced Macrophage Inflammatory Protein-2 Release from Alveolar Epithelial Cells. American Journal of Respiratory Cell Molecular Biology. 1999 Nov 28;21:510–20.

62. Bonnett CR, Cornish EJ, Harmsen AG, Burritt JB. Early Neutrophil Recruitment and Aggregation in the Murine Lung Inhibit Germination of A*spergillus fumigatus* Conidia. Infection and Immunity. 2006 Nov 20;74(12):6528–39.

63. Conti HR, Gaffen SL. IL-17-Mediated Immunity to the Opportunistic Fungal Pathogen Candida albicans. The Journal of Immunology. 2015 Jul 17;195(3):780–8.

64. Conti HR, Shen F, Nayyar N, Stocum E, Sun JN, Lindemann MJ, et al. Th17 cells and IL-17 receptor signaling are essential for mucosal host defense against oral candidiasis. Journal of Experimental Medicine. 2009 Feb 16;206(2):299–311.

65. Puel A, Cypowyj S, Marodi L, Abel L, Picard C, Casanova JL. Inborn errors of human IL-17 immunity underlie chronic mucocutaneous candidiasis. Current Opinion in Allergy and Clinical Immunology. 2012 Jan 7;12:616–22.

66. Underhill DM, Pearlman E. Immune Interactions with Pathogenic and Commensal Fungi: A Two-Way Street. Immunity. Elsevier Inc; 2015 Nov 17;43(5):845–58.

67. Freeman AF, Holland SM. The Hyper-IgE Syndromes. Immunology and Allergy Clinics of North America. 2008 May;28(2):277–91.

68. Cho ML, Kang JW, Moon YM, Nam HJ, Jhun JY, Heo SB, et al. STAT3 and NF-kB Signal Pathway Is Required for IL-23-Mediated IL-17 Production in Spontaneous Arthritis Animal Model IL-1 Receptor Antagonist-Deficient Mice. The Journal of Immunology. 2006 Apr 18;176(9):5652–61.

69. Zelante T, De Luca A, Bonifazi P, Montagnoli C, Bozza S, Moretti S, et al. IL-23 and the Th17 pathway promote inflammation and impair antifungal immune resistance. European Journal of Immunology. 2007 Oct;37(10):2595–706.

70. Cenci E, Mencacci A, Del Sero G, Bacci A, Montagnoli C, Fe d'Ostiani C, et al. Interleukin-4 Causes Susceptibility to Invasive Pulmonary Aspergillosis through Suppression of Protective Type I Responses. Journal of Infectious Diseases. 1999 Nov 11;180:1957–68.

71. Mansour MK, Tam JM, Vyas JM. The cell biology of the innate immune response to *Aspergillus fumigatus*. Annals of the New York Academy of Sciences. 2012 Dec 11;1273(1):78–84.

72. Cohen NR, Tatituri RVV, Rivera A, Watts GFM, Kim EY, Chiba A, et al. Innate Recognition of Cell Wall Beta-Glucans Drives Invariant Natural Killer T Cell Responses against Fungi. Cell Host and Microbe. Elsevier Inc; 2011 Nov 17;10(5):437–50.

73. Roilides E, Tsaparidou S, Kadiltsoglou I, Sein T, Walsh TJ. Interleukin-12 Enhances Antifungal Activity of Human Mononuclear Phagocytes against *Aspergillus fumigatus*: Implications for a Gamma Interferon-Indepedent Pathway. Infection and Immunity. 1999 Jun 10;67:3047–50.

74. Levitz SM, Selsted ME, Ganz T, Lehrer RI, Diamond RD. In vitro Killing of Spores and Hyphae of *Aspergillus fumigatus* and *Rhizopus oryzae* by Rabbit Neutrophil Cationic Peptides and Bronchoalveolar Macrophages. The Journal of Infectious Diseases. 1986 Sep 24;154:483–9.

75. Osherov N. *Aspergillus fumigatus* and Aspergillosis. Latge JP, Steinbach WJ, editors. ASM Press; 2009.

76. Bernink JH, Krabbendam L, Germar K, de Jong E, Gronke K, Kofoed-Nielsen M, et al. Interleukin-12 and -23 Control Plasticity of CD127. Immunity. Elsevier Inc; 2015 Jul 13;:1–16.

77. Taylor PR, Roy S, Leal SM, Sun Y, Howell SJ, Cobb BA, et al. Activation of neutrophils by autocrine IL-17A–IL-17RC interactions during fungal infection is regulated by IL-6, IL-23, RORγt and dectin-2. Nature Immunology. 2013 Dec 22;15(2):143–51.

78. Song C, Luo L, Lei Z, Li B, Liang Z, Liu G, et al. IL-17-Producing Alveolar Macrophages Mediate Allergic Lung Inflammation Related to Asthma. The Journal of Immunology. 2008 Oct 20;181(9):6117–24.

79. Zhu X, Mulcahy LA, Mohammed RA, Lee AH, Franks HA, Kilpatrick L, et al. IL-17 expression by breast-cancer-associated macrophages: IL-17 promotes invasiveness of breast cancer cell lines. Breast Cancer Res. 2008;10(6):R95.

80. Starnes T, Robertson MJ, Sledge G, Kelich S, Nakshatri H, Broxmeyer HE, et al.

Cutting Edge: IL-17F, a Novel Cytokine Selectively Expressed in Activated T Cells and Monocytes, Regulates Angiogenesis and Endothelial Cell Cytokine Production. The Journal of Immunology. 2001 Oct 15;167(8):4137–40.

81. Molet S, Hamid Q, Davoineb F, Nutku E, Tahaa R, Pagé N, et al. IL-17 is increased in asthmatic airways and induces human bronchial fibroblasts to produce cytokines. Journal of Allergy and Clinical Immunology. 2001 Sep;108(3):430–8.

82. Shimura E, Shibui A, Narushima S, Nambu A, Yamaguchi S, Akitsu A, et al. Potential role of myeloid cell/eosinophil-derived IL-17 in LPS-induced endotoxin shock. Biochemical and Biophysical Research Communications. Elsevier Inc; 2014 Oct 10;453(1):1–6.

83. Herzenberg LA, Tung J, Moore WA, Herzenberg LA, Parks DR. Interpreting flow cytometry data: a guide for the perplexed. Nature Immunology. 2006 Jul 5;7:681–5.

84. Dyer KD, Moser JM, Czapiga M, Siegel SJ, Percopo CM, Rosenberg HF. Functionally Competent Eosinophils Differentiated Ex Vivo in High Purity from Normal Mouse Bone Marrow. The Journal of Immunology. 2008 Sep 3;181(6):4004–9.

85. Kitami S, Tanaka H, Kawato T, Tanabe N, Katono-Tani T, Zhang F, et al. IL-17A suppresses the expression of bone resorption-related proteinases and osteoclast differentiation via IL-17RA or IL-17RC receptors in RAW264.7 cells. Biochimie. Elsevier Masson SAS; 2010 Apr 1;92(4):398–404.

86. Lee JJ, Jacobsen EA, Ochkur SI, McGarry MP, Condjella RM, Doyle AD, et al. Human versus mouse eosinophils: ‘‘That which we call an eosinophil, by any other name would stain as red’’. Journal of Allergy and Clinical Immunology. Elsevier Ltd; 2012 Sep 1;130(3):572–84.

87. Stevens WW, Kim TS, Pujanauski LM, Hao X, Braciale TJ. Detection and quantitation of eosinophils in the murine respiratory tract by flow cytometry. Journal of Immunological Methods. 2007 Oct;327(1-2):63–74.

88. Yu C. Targeted Deletion of a High-Affinity GATA-binding Site in the GATA-1 Promoter Leads to Selective Loss of the Eosinophil Lineage In Vivo. Journal of Experimental Medicine. 2002 Jun 3;195(11):1387–95.

89. Gordon S, Taylor PR. Monocyte and macrophage heterogeneity. Nat Rev Immunol. 2005 Dec;5(12):953–64.

90. Chesné J, Braza F, Mahay G, Brouard S, Aronica M, Magnan A. IL-17 in Severe

Asthma. Where Do We Stand? American Journal of Respiratory and Critical Care Medicine. 2014 Nov 15;190(10):1094–101.

91. Nials AT, Uddin S. Mouse models of allergic asthma: acute and chronic allergen challenge. Disease Models and Mechanisms. 2008 Nov 1;1(4-5):213–20.

92. Griseri T, Arnold IC, Pearson C, Krausgruber T, Schiering C, Franchini F, et al. Granulocyte Macrophage Colony-Stimulating Factor-Activated Eosinophils Promote Interleukin- 23 Driven Chronic Colitis. Immunity. The Authors; 2015 Jul 21;43(1):187–99.

93. Mosser DM, Edwards JP. Exploring the full spectrum of macrophage activation. Nat Rev Immunol. Nature Publishing Group; 2008 Dec 1;8(12):958–69.

94. Chesné J, Braza F, Chadeuf G, Mahay G, Cheminant M-A, Loy J, et al. Prime role of IL-17A in neutrophilia and airway smooth muscle contraction in a house dust mite-induced allergic asthma model. Journal of Allergy and Clinical Immunology. American Academy of Allergy, Asthma & Immunology; 2015 Jun 1;135(6):1643–5.

95. Aujla SJ, Alcorn JF. Th17 cells in asthma and inflammation. Biochimica et Biophysica Acta. Elsevier B.V; 2011 Nov 1;1810(11):1066–79.

96. Shimizu S, Kouzaki H, Ogawa T, Takezawa K, Tojima I, Shimizu T. Eosinophil-epithelial cell interactions stimulate the production of MUC5AC mucin and profibrotic cytokines involved in airway tissue remodeling. American Journal of Rhinology & allergy. 2014 Mar;28(2):103–9.

97. Ono N, Kusunoki T, Ikeda K. Relationships between IL-17A and macrophages or MUC5AC in eosinophilic chronic rhinosinusitis and proposed pathological significance. Allergy & Rhinology. 2012 Sep 18;3(2):50–4.

98. Tang W, Smith SG, Beaudin S, Dua B, Howie K, Gauvreau G, et al. IL-25 and IL-25 receptor expression on eosinophils from subjects with allergic asthma. Int Arch Allergy Immunol. 2014;163(1):5–10.

99. Spencer LA, Bonjour K, Melo RC, Weller PF. Eosinophil secretion of granule-derived cytokines. Frontiers in Immunology. 2014 Oct 27;5:1–9.

100. Lilly LM, Scopel M, Nelson MP, Burg AR, Dunaway CW, Steele C. Eosinophil Deficiency Compromises Lung Defense against *Aspergillus fumigatus*. Infection and Immunity. 2014 Feb 18;82(3):1315–25.

101. Shepardson KM, Jhingran A, Caffrey A, Obar JJ, Suratt BT, Berwin BL, et al. Myeloid Derived Hypoxia Inducible Factor 1-alpha Is Required for Protection

against Pulmonary *Aspergillus fumigatus* Infection. Gaffen S, editor. PLoS Pathog. 2014 Sep 25;10(9):e1004378.

102. Jhingran A, Mar KB, Kumasaka DK, Knoblaugh SE, Ngo LY, Segal BH, et al. Tracing Conidial Fate and Measuring Host Cell Antifungal Activity Using a Reporter of Microbial Viability in the Lung. Cell Reports. The Authors; 2012 Dec 27;2(6):1762–73.

103. Mantovani A, Sica A, Sozzani S, Allavena P, Vecchi A, Locati M. The chemokine system in diverse forms of macrophage activation and polarization. Trends in Immunology. 2004 Dec;25(12):677–86.

104. Erbel C, Akhavanpoor M, Okuyucu D, Wangler S, Dietz A, Zhao L, et al. IL-17A Influences Essential Functions of the Monocyte/Macrophage Lineage and Is Involved in Advanced Murine and Human Atherosclerosis. The Journal of Immunology. 2014 Sep 24;:1–12.

105. Sutton CE, Lalor SJ, Sweeney CM, Brereton CF, Lavelle EC, Mills KHG. Interleukin-1 and IL-23 Induce Innate IL-17 Production from gammadelta T Cells, Amplifying Th17 Responses and Autoimmunity. Immunity. Elsevier Ltd; 2009 Aug 21;31(2):331–41.

106. Rizzetto L, Giovannini G, Bromley M, Bowyer P, Romani L, Cavalieri D. Strain Dependent Variation of Immune Responses to *A. fumigatus*: Definition of Pathogenic Species. Schlievert PM, editor. PLoS ONE. 2013 Feb 18;8(2):e56651.

107. Scharf DH, Heinekamp T, Remme N, Hortschansky P, Brakhage AA, Hertweck C. Biosynthesis and function of gliotoxin in *Aspergillus fumigatus*. Appl Microbiol Biotechnol. 2011 Nov 18;93(2):467–72.

108. Wiederhold NP, Najvar LK, Vallor AC, Kirkpatrick WR, Bocanegra R, Molina D, et al. Assessment of Serum (1->3)- beta-D-Glucan Concentration as a Measure of Disease Burden in a Murine Model of Invasive Pulmonary Aspergillosis. Antimicrobial Agents and Chemotherapy. 2008 Feb 25;52(3):1176–8.

109. Fuller KK, Chen S, Loros JJ, Dunlap JC. Development of the CRISPR/Cas9 System for Targeted Gene Disruption in *Aspergillus fumigatus*. Eukaryotic Cell. 2015 Oct 26;14(11):1073–80.

110. Pasqualotto AC. Differences in pathogenicity and clinical syndromes due to *Aspergillus fumigatus* and *Aspergillus flavus*. Med Myco. 2009 Jan;47(s1):S261–70.

111. Shi C, Pamer EG. Monocyte recruitment during infectionand inflammation. Nat Rev Immunol. Nature Publishing Group; 2011 Oct 10;11(11):762–74.

112. Shahrara S, Pickens SR, Dorfleutner A, Pope RM. IL-17 Induces Monocyte Migration in Rheumatoid Arthritis. The Journal of Immunology. 2009 Mar 15;182(6):3884–91.

113. Espinosa V, Jhingran A, Dutta O, Kasahara S, Donnelly R, Du P, et al. Inflammatory Monocytes Orchestrate Innate Antifungal Immunity in the Lung. Sheppard DC, editor. PLoS Pathog. 2014 Feb 20;10(2):e1003940.

114. Swamydas M, Break TJ, Lionakis MS. Mononuclear phagocyte-mediated antifungal immunity: the role of chemotactic receptors and ligands. Cellular and Molecular Life Sciences. Springer Basel; 2015 Apr 16;:1–19.

115. Mircescu MM, Lipuma L, van Rooijen N, Pamer EG, Hohl TM. Essential Role for Neutrophils but not Alveolar Macrophages at Early Time Points following Aspergillus fumigatusInfection. Journal of Infectious Diseases. 2009 Aug 15;200(4):647–56.

116. Daley JM, Thomay AA, Connolly MD, Reichner JS, Albina JE. Use of Ly6G-specific monoclonal antibody to deplete neutrophils in mice. Journal of Leukocyte Biology. 2007 Sep 17;83(1):64–70.

117. Zizzo G, Cohen PL. IL-17 Stimulates Differentiation of Human Anti-Inflammatory Macrophages and Phagocytosis of Apoptotic Neutrophils in Response to IL-10 and Glucocorticoids. The Journal of Immunology. 2013 May 3;190(10):5237–46.

118. Kawaguchi M, Adachi M, Oda N, Kokubu F, Huang S-K. IL-17 cytokine family. Journal of Allergy and Clinical Immunology. 2004 Dec;114(6):1265–73.

119. Furuta GT, Atkins FD, Lee NA, Lee JJ. Changing roles of eosinophils in health and disease. Annals of Allergy, Asthma & Immunology. American College of Allergy, Asthma & Immunology; 2014 Jul 1;113(1):3–8.

120. Rothenberg ME, Hogan SP. The Eosinophil. Annu Rev Immunol. 2006 Apr;24(1):147–74.

121. Spencer LA, Szela CT, Perez SAC, Kirchhoffer CL, Neves JS, Radke AL, et al. Human eosinophils constitutively express multiple Th1, Th2, and immunoregulatory cytokines that are secreted rapidly and differentially. Journal of Leukocyte Biology. 2008 Oct 23;85(1):117–23.

122. Rosenberg HF, Dyer KD, Foster PS. Eosinophils: changing perspectives in

health and disease. Nat Rev Immunol. Nature Publishing Group; 2012 Nov 16;13(1):9–22.

123. Pakhale S, Sunita Mulpuru, Matthew Boyd. Optimal Management of Severe/Refractory Asthma. CCRPM. 2011 Aug;5:37–47.

124. Simpson JL, Scott R, Boyle M, Gibson PG. Inflammatory subtypes in asthma: Assessment and identification using induced sputum. Respirology. 2006 Jan 9;11:54–61.

125. Fedorova ND, Khaldi N, Joardar VS, Maiti R, Amedeo P, Anderson MJ, et al. Genomic Islands in the Pathogenic Filamentous Fungus *Aspergillus fumigatus*. Richardson PM, editor. PLoS Genetics. 2008 Apr 11;4(4):e1000046.

126. Rokas A, Payne G, Fedorova ND, Baker SE, Machida M, Yu J, et al. What can comparative genomics tell us about species concepts in the genus? Studies in Mycology. CBS-KNAW Fungal Biodiversity Centre; 2007 Jan 11;59:11–7.

127. Amarsaikhan N, O'Dea EM, Tsoggerel A, Owegi H, Gillenwater J, Templeton SP. Isolate-Dependent Growth, Virulence, and Cell Wall Composition in the Human Pathogen Aspergillus fumigatus. Cramer RA, editor. PLoS ONE. 2014 Jun 19;9(6):e100430.